USING *ASPERGILLUS NIDULANS* TO STUDY ALPHA-1,3-GLUCAN SYNTHESIS AND THE RESISTANCE MECHANISM AGAINST CELL WALL TARGETING DRUGS

A Thesis Submitted to the College of

Graduate Studies and Research

In Partial Fulfillment of the Requirements

For the Degree of Doctor of Philosophy

In the Department of Biology

University of Saskatchewan

Saskatoon

By

XIAOXIAO HE

Permission to Use

In presenting this thesis in partial fulfilment of the requirements for a Postgraduate degree from the University of Saskatchewan, I agree that the Libraries of this University may make it freely available for inspection. I further agree that permission for copying of this thesis in any manner, in whole or in part, for scholarly purposes may be granted by the professor or professors who supervised my thesis work or, in their absence, by the Head of the Department or the Dean of the College in which my thesis work was done. It is understood that any copying or publication or use of this thesis or parts thereof for financial gain shall not be allowed without my written permission. It is also understood that due recognition shall be given to me and to the University of Saskatchewan in any scholarly use which may be made of any material in my thesis.

Requests for permission to copy or to make other use of material in this thesis in whole or part should be addressed to:

Head of the Department of Biology

University of Saskatchewan

Saskatoon, Saskatchewan, S7N5E2

ABSTRACT

Systemic fungal infection is a life-threatening problem. Anti-fungal drugs are the most effective clinical strategy to cure such infections. However, most current anti-fungal drugs either have high toxicity or have a narrow spectrum of effect. Meanwhile, anti-fungal drugs are losing their clinical efficacy due to emerging drug resistance. To protect us from these deadly pathogenic fungi, scientists need to study new drug targets and to solve problems related to drug resistance.

The cell wall is essential for fungal cell survival and is absent from animal cells, so it is a promising reservoir for screening safe and effective drug targets. Alpha-1,3-glucan is one of the major cell wall carbohydrates and is important for the virulence of several pathogenic fungi. In this thesis, molecular biology and microscopy techniques were used to investigate the function and the synthesis process of α-1,3-glucan in the model fungus *A. nidulans*.

My results showed that α-1,3-glucan comprises about 15% of *A. nidulans* cell wall dry weight, but also that α-1,3-glucan does not have an important role in cell wall formation and cell morphology. Deletion of α-1,3-glucan only affects conidial adhesion and cell sensitivity to calcofluor white. In contast, elevated α-1,3-glucan content can cause severe phenotypic defects.

To study the α-1,3-glucan synthesis process, I systematically characterized four proteins, including two α-1,3-glucan synthases (AgsA and AgsB) and two amylase-like proteins (AmyD and AmyG). Results showed AgsA and AgsB are both functional synthases. AgsB is the major

synthase due to its constant expression. AgsA mainly functions in conidiation stages. AmyG is a cytoplasmic protein that is critical for α-1,3-glucan synthesis, likely being required for an earlier step in the synthesis process. In contrast to the other three proteins, AmyD has a repressive effect on α-1,3-glucan accumulation. These results shed light on therapeutic strategies that might be developed against α-1,3-glucan.

I also developed a strategy to investigate drug resistance mutations. The tractability of *A. nidulans* and the power of next generation sequencing enabled an easy approach to isolate single mutation strains and to identify the causal mutations from a genome scale efficiently. I suggest this strategy has applications to study the drug resistance mechanisms of current anti-fungal drugs and even possibly future ones.

ACKNOWLEDGMENTS

First of all, I would like to thank Dr. Kaminskyj for giving me an opportunity to start a Ph.D. in her lab. Dr. Kaminskyj is a great mentor, who is always ready to help me out of my troubles. It is hard to describe her influence on me, because there are some many of them in every aspect. The most important gift that I learned from her is working in science is a happiness. The experience in her lab assures me to continue a career in the field of science.

I also owe a great many thanks to my advisors Dr. Andrés, Dr. Carvalho, Dr. Sanders and Dr. Wei, especially for their constructive criticism, which pointed out the weakness of my work.

I would also like to thank every member in Dr. Kaminskyj's lab and many students from the Biology Department. They are great friends and invaluable source of advice.

My Ph.D. study was supported by a Graduate Teaching Fellowship from Biology Department, University of Saskatchewan.

Last but most importantly, I want to thank my parents and my wife for their support in this period, which helps me to go through the rough times.

TABLE OF CONTENTS

LIST OF TABLES

LIST OF FIGURES

LIST OF ABBREVIATIONS

Abbreviation	Full name
β-glucan	β-1,3-glucan
actA(p)	*actinA* promoter
ags	alpha-1,3-glucan synthesis gene
alcA(p)	alcohol dehydrogenase I promoter
BLAST	basic local alignment search tool
Casp	caspofungin
cDNA	complementary DNA
CFW	calcofluor White
chs	chitin synthesis gene
CM	complete medium
CR	congo red
CWI	cell wall intergrity pathway
fks	beta-glucan synthesis gene
Gal*f*	galactofuranose
gDNA	genomic DNA
GFP	green fluorescent protein
GPI	glycophosphatidylinositol
H2A(p)	*hitsone 2A* promoter
HOG	high osmolarity glycerol

L10	galactofuranose antibody
MM	minimal medium containing
MOPC 104E	alpha-1,3-glucan antibody
NGS	next generation sequencing
nkuA	homolog of human KU70
PCR	polymerase chain reaction
PKC	protein kinase C
pyrG	orotidine 5'-monophosphate decarboxylase
pyroA	pyridoxine biosynthesis gene
qRT-PCR	quantitative real time polymerase chain reaction
SNP	single nucleotide polymorphism
SEM	scanning electron microscopy
TEM	transmission electron microscopy
ugmA	UDP-galactopyranose mutase gene

CHAPTER 1

GENERAL INTRODUCTION

1.1. Fungi are Important for Human Lives

Fungi are a diverse group of organisms, which are classified as a distinct kingdom, the Mycota, in the domain, Eukarya. Evolutionary analysis showed fungi and animals may share a common ancestor about a billion years ago (Taylor and Berbee, 2010), so fungi can be seen as the 'distant relatives' of animals. Although fungi and animals have distinct appearances, they do share common characteristics. For example, both fungi and animals are heterotrophic eukaryotic organisms, which mean they need to absorb organic food from the environment and digest them for energy. To do this, the cells use certain enzymes to release the nutrients from the environment (e.g. amylase to hydrolyze starch). Therefore, some metabolic pathways at the cellular level are similar between fungi and animals.

Fungi have two main morphologies: yeast form and filamentous form (Harris, 2011). The yeast fungi are unicellular, and they reproduce by budding or fission. The filamentous fungi are multicellular, and they reproduce by generating conidia. The filamentous fungi have cell differentiation during asexul life cycle and therefore are more complex in respect to morphology. However, recent evidence suggested filamentous form is actually the morphology of ancestral fungi (Harris, 2011). This tentative statement is still debatable, but there is no doubt that the yeast and filamentous fungi have a common mechanism of cell growth based on secretory vesicles. As filamentous fungi have more complex growth controls, I will use filamentous fungi

as examples to explain the fungal growth. Filamentous fungi are composed of long tubular cells called hyphae that exhibited tip localized growth (Kaminskyj and Health, 1996). The polarity of hyphal growth is determined by a protein complex called the polarisome (Harris and Momany, 2003). Then vesicles that contain cell wall-synthesizing enzymes, membrane proteins and membrane lipids are transported to the apical regions of hyphae, where they are integrated into the cell membrane (Read, 2011). A special fungal organelle complex called the Spitzenkörper is the vesicle supply center and directly decides the growth rate of the hyphal tips (Bartnicki-Garcia, 2002). Cytoskeletal filaments actin and microtubulin, and cell turgor pressure are all involved in hyphal tip growth regulation (Bartnicki-Garcia, 2002; Harris and Momany, 2003). The yeast fungi have similar growth mechanism as that of filamentous fungi. The yeast cells need the polarisome to regulate growth polarity and need vesicles to provide growth materials. The Spitzenkörper is not present in yeast cells (Harris and Momany, 2003; Crampin et al. 2005).

In nature, fungi can live in soil, in water and on/in plants. Most times you may not notice their presence. But fungi do have a wide distribution on this planet, even in Antarctica (Fubino et al., 2013). These small organisms have irreplaceable roles in nature. Firstly many fungi are decomposers that recycle the nutrients on the planet (Barr and Aust, 1994; Hattenschwiler et al., 2011; Lunghini et al., 2012). For example, leaf litter is difficult to decompose especially for plant parts with high lignin content. Some fungi, such as white-rot and brown-rot fungi, can digest such materials efficiently (Barr and Aust, 1994, Osono, 2006). Secondly some fungal species form symbiotic relationships with plant partners. These symbiotic systems sometimes are essential for both sides to survive in stressful terrestrial environments (Rodriguez and Redman,

2008; Lee et al., 2013). Not only in plants, fungi are also symbiotic with some animals. Rumen fungi are members of microbial consortia that are essential for herbivores (such as cattle and sheep) to digest plant materials (Bauchop, 1989; Gordon and Philips, 1998). Otherwise these animals would get essentially no carloric value from the food they ate.

Besides their natural roles, some fungi are also important in industry, especially for fermentation. These fungi are used commercially in production of alcoholic beverages, bread and many biochemicals (e.g. citric acid) (Bennett, 1998; Nevalaine and Peterson, 2014; Sohier et al., 2014). Therefore, it is valid to say that nowadays humans could not live on this planet without the help from fungi.

1.2. Fungi can be Human Pathogens

Although fungi have many positive impacts on our lives, they can also be dangerous, because they may infect humans. Some fungi can cause superficial infection on our skin and nails. These infections usually can be cured by topical therapies (Hawkins and Smidt, 2014). However, without proper diagnosis and treatment, even superficial fungal infection can lead to chronic problems.

Some other fungi can cause even more dangerous infections—systemic infections. This section will focus on the most common human systemic fungal pathogens. These pathogenic fungi include *Aspergillus fumigatus*, *Candida albicans*, *Histoplasma capsulatum* and *Cryptococcus neoformans* (Antinori, 2014; Davis et al., 2014; Hebecker et al., 2014; Perfect, 2014). *A. fumigatus*, *H. capsulatum* and *C. neoformans* all have worldwide distributions, and *C.*

albicans is a commensal microorganism of human gut flora, so we cannot avoid contacting these pathogens. Thanks to our strong immune system, systemic fungal infection mostly happens to the individuals with compromised immune system, such as HIV, cancer and transplant patients (Lilic, 2012; Davis et al., 2014; Hebecker et al., 2014; Perfect, 2014). However, recent reports have pointed out that the infection of healthy individuals is rising (Brown et al., 2012). The mortality rate caused by systemic infection ranges from 30% to 50% (Netea and Brown, 2012) or higher. So we should be aware that fungal infection has become as heavy a burden on human health as other pathogens (bacteria, viruses or parasites) (Netea and Brown, 2012).

The above mentioned pathogenic fungi are in different morphologies during pathogenesis. This requires them to use different mechanisms to fulfill the infection. *Aspergillus* and *Candida* are in filamentous form during pathogenesis. The cells of these two fungi can germinate in human body, and then their hyphae can penetrate into a tissue and invade an organ locally (Mavor et al., 2005; Dagenais and Keller, 2009), which causes physical damage to the body. Later, fragments of hyphae may disseminate through our circulation system to infect other parts of the body (Mavor et al., 2005; Dagenais and Keller, 2009). For *Histoplasma* and *Cryptococcus*, the invading fungal cells are in yeast form during pathogenesis. When these yeast fungal cells are present in our bodies, our innate immune system can recognize them and kill them. Phagocytes are the most common 'killers' for this job. However, instead of being killed, some fungi can survive in phagocytes, and even proliferate within the immune cells (Qin et al. 2011). Eventually, these pathogens escape from phagocytes and spread the infection in human body (Qin et al. 2011).

1.3. Fungal Cell Wall is an Essential Structure

Fungi need cell walls to survive in nature, which is a major distinction between fungi and animals. The cell wall is about 30% of the fungal biomass (Gastebois et al., 2009), and cell wall related genes are predicted to include as many as one third of the fungal genome (de Groot et al., 2009). Thus cell wall is a very complex three-dimensional structure. Even with decades of effort to characterize individual components, many details about cell wall biosynthesis, composition, and maintenance are still poorly understood.

In general, fungal cell walls are mostly (80-90%) carbohydrate supplemented with proteins (Latgé, 2010). The major carbohydrate components of the fungal cell wall are chitin and glucans, unlike the cell walls of plants, which contain cellulose (Cosgrove, 2005). Among the fungal cell wall components, β-glucan is most extensively studied. Beta-glucan has been shown to be essential for some fungal species, including species of *Aspergillus* and *Candida* (Douglas et al., 1997; Firon et al., 2002). Beta-glucan is made from β-glucose subunits connected by 1,3-glycosidic linkages, and is supposed to be the core of the cell wall of *A. fumigatus* (Fig.1-1) (Latgé, 2007). Beta-glucan covalently binds to other polysaccharides via its side branches, especially to chitin.

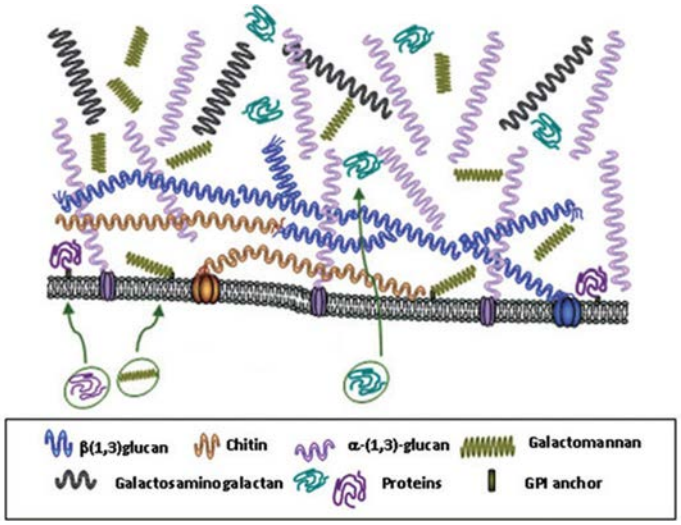

Fig.1-1 Speculative cell wall structure of *Aspergillus* species (Modified from Latgé, 2010)

Chitin is another important cell wall component and it is also considered as part of the core structure of the *A. fumigatus* cell wall (Latgé, 2007). Chitin synthesis and regulation are well studied in *S. cerevisiae*. Among the three chitin synthases in *S. cerevisiae*, Chs3p is the major one. It is responsible for the synthesis of most chitin component in cell wall, especially at the budding sites (Shaw et al., 1991; Ziman et al., 1996). The Chs3p needs to bind to an activator (Chs4p) to function (Ono et al., 2000). In *C. albicans*, elevated chitin content can rescue cells experimentally challenged by echinocandins (Walker et al., 2008), which block β-glucan synthesis. This shows chitin can partially compensate for the lack of β-glucan to stabilize the *Candida* cell wall. In *Aspergillus* species, usually more chitin synthases are found (e.g. eight chitin synthases predicted in *A. nidulans*). This redundancy makes it harder to study chitin function in the *Aspergillus* cell wall. However, double deletion of CsmA and CsmB, two of the major chitin synthases, is lethal for *A. nidulans*, revealing the critical role of chitin in the cell wall (Takeshita et al., 2006).

Galactomannan is another major wall carbohydrate. It is composed of a linear core of α-mannans with short side chains of β-1,5-galactofuranose (Gastebois et al., 2009). This mannan-Gal*f* core structure usually binds to wall proteins or the branches of β-glucan in the cell wall (Engel et al., 2012). Studies have shown galactomannan is important for the wild type cell wall formation in *A. nidulans* and some other fungi (El-Ganiny et al., 2008; Engel et al., 2012).

Apart from these carbohydrate components, the cell wall proteins may also play crucial roles in the cell wall formation. Some of the wall proteins are shown to be involved in cell-cell interaction, such as adhesion, biofilm formation and mating (Nather and Munro, 2008). But there are still many other proteins without clear functions yet. Some of them should have roles in cell wall composition. One of the hypotheses is these proteins should be involved in the modification of cell wall carbohydrates. The carbohydrate components need to be linked together to form a solid but flexible armor outside the cell membrane (Latgé, 2007). However, the linkages between carbohydrate components in fungal cell wall are still largely unknown. Right now we know most of the carbohydrate fibrils are generated individually and then are deposited to the cell wall (Latgé, 2007). The linking steps between fibrils should happen in the cell wall and the wall proteins are expected to fulfill these jobs (Latgé, 2007). Understanding the cross-linking between carbohydrates during wall maturation is one of the future challenges for the cell wall study.

Cell wall is considered to be a dynamic structure. The dynamics are controlled by cell wall integrity (CWI) signaling pathways. Three different pathways have been reported in different fungi (Levin, 2005): the protein kinase C (PKC) cell wall integrity pathway, the high osmolarity glycerol response (HOG) pathway, and the Ca^{2+}–calcineurin pathway. CWI pathways regulate

wall component synthesis throughout the cell cycle and respond with repair activity when wall integrity is challenged by anti-fungal agents or environmental stresses (Garcia-Rodriguez et al., 2000; Teepe et al., 2007; Fuchs and Mylonakis, 2009; Walker et al., 2010). Therefore, fungal cell walls as well as CWI pathways are essential for fungi to survive in nature.

1.4. Alpha-1,3-glucan is a Major Wall Component and is Important for Fungal Pathogenesis

Among the wall carbohydrate components, α-1,3-glucan is thought to be a major one due to the biomass analysis in *A. fumigatus* (Latgé, 2010). Alpha-1,3-glucan is a long chain (more than 200 units) of α-glucose joined by 1,3-glycosidic linkage; and it is thought to lack side branches (Grün et al., 2005; Choma et al., 2013). Some (about 10% of total units) 1,4-glycosidic linked α-glucoses are also found at the reducing end of α-1,3-glucan (Grün et al., 2005). Compared to β-glucan and chitin, until recently α-1,3-glucan has attracted relatively little research attention. Early studies showed α-1,3-glucan was essential for the morphology of *S. pombe* (Hochstenbach et al., 1998), because lack of α-1,3-glucan affected cell wall strength during cytokinesis (Cortés et al., 2012). In contrast, α-1,3-glucan is not essential in *Paracoccidioides brasiliensis* (Pereira et al., 2000), *C. neoformans* (Reese and Doering, 2003), *H. capsulatum* (Rappeleye et al. 2004), and *Aspergillus* species (Damveld et al., 2005; Henry et al. 2012; Yoshimi et al., 2013). However, α-1,3-glucan synthase was still highly expressed by *A. nidulans*, especially when the cell was challenged by echinocandins (Fujioka et al., 2007) that target β-glucan synthase FksA, by Calcofluor White (CFW) that inhibits chitin crystallization (Elorza et al., 1983), and by genetic

manipulations to reduce galactofuranose (Gal*f*) content (Damveld et al, 2008; Alam et al., 2012). In addition, Fujioka et al. (2007) showed that the expression of α-1,3-glucan synthase was controlled by PKC signaling pathway. Thus, there is considerable reason to suspect that the expression level of α-1,3-glucan is related to cell wall composition, cell function and perhaps also to anti-fungal drug sensitivity.

Recent evidence has pointed out that α-1,3-glucan has important roles for fungal virulence. In *C. neoformans*, loss of α-1,3-glucan led to loss of the capsule, which is an essential structure for virulence of this species (Reese et al., 2007). In *H. capsulatum* and *Magnaporthe oryzae*, α-1,3-glucan was shown to be the outside layer of cell wall, which suppresses host immune response to facilitate a successful infection (Rappleye et al. 2007; Fujikawa et al., 2012). In *A. fumigatus*, loss of α-1,3-glucan caused remodeling of cell wall architecture, which led to avirulence (Beauvais et al., 2013). Although the role of α-1,3-glucan in the cell wall remains controversial, the fact is clear that α-1,3-glucan is important for full virulence of these pathogenic fungi. Therefore α-1,3-glucan can be claimed as a virulence factor. Now developing antimicrobial drug that target virulence factors is a new trend in drug development (Clatworthy et al. 2007; Allen et al., 2014). Unlike previous drug targets, which were usually essential cell elements, virulence factors are non-essential for cell survival but essential for pathogenesis. Therefore, antivirulence drug are not expected to kill the pathogen directly but should be able to inhibit their pathogenesis. In addition, antivirulence drugs have been hypothesized to generate less selection force for drug resistance (Clatworthy et al. 2007), so antivirulence drug could be relatively ‘evolution-proof’. Although this hypothesis is being challenged by recent evidence

(Allen et al., 2014), there is no doubt that virulence factors can be useful drug targets for future antimicrobial drug development.

Alpha-1,3-glucan is synthesized by α-1,3-glucan synthase. So far, all characterized α-1,3-glucan synthases share a common multi-domain structure (Fig.1-2) (Hochstenbach et al., 1998; Pereira et al., 2000; Rappeleye et al. 2004; Damveld et al., 2005; Henry et al. 2012; Yoshimi et al., 2013). At least three functional domains are present. They are the α-amylase domain, α-1,3-glucan synthesis domain and transmembrane domain in order from N-terminal to C-terminal. Based on data from *S. pombe*, Grün and colleagues (2005) presented a protein model for α-1,3-glucan synthase (Fig.1-2). According to this model, the α-1,3-glucan synthesis domain synthesizes the α-1,3-glucan polymer in cytoplasm and then transports the new polymer through transmembrane domain to the cell wall. The α-amylase domain, which localizes on the cell wall side, completes the synthesis process by joining different polymers. However, much more data are needed to verify this model, especially from *in vitro* enzymatic studies.

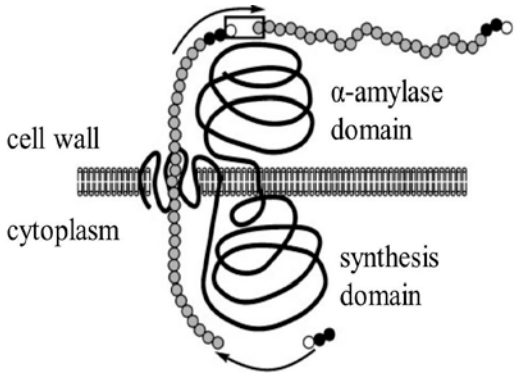

Fig. 1-2 A speculative model of α-1,3-glucan synthesis by α-1,3-glucan synthase (modified from Grün et al., 2005)

The black and white circles are the putative primer structures, which are α-1,4-glycosidic linked α-glucose. The grey circles are the main chain of α-1,3-glucan. The primer structure presents at the reducing end of a α-1,3-glucan.

Other evidence showed that α-1,3-glucan synthesis requires more than just α-1,3-glucan

synthase (Grün et al., 2005), because the synthase needs a primer to initiate the process. This primer structure is believed to be a α-1,4-glucan at the reducing end (Grün et al., 2005). The only evidence from *H. capsulatum* suggested a α-amylase-like protein may synthesize this primer (Marion et al., 2006). The homologue of this protein is found in *A. nidulans*. In addition, the post-synthesis modification process of α-1,3-glucan is totally unknown. Alpha-1,3-glucan has been shown to have no branches (Grün et al., 2005; Choma et al., 2013), but it has to cross-link with other wall components or the cell membrane to be stable in the wall. These questions need to be resolved for a better understanding of α-1,3-glucan.

1.5. Current Anti-fungal Drugs are Losing Their Efficacy due to Emerging Drug Resistance

Since the 1950s, scientists have made great progress to treat systemic fungal infections. Currrently, the three main classes of anti-fungal drugs are the polyenes, azoles and echinocandins. Polyenes directly bind ergosterol, which is the major sterol in fungal cell membrane, to form a drug-lipid complex. This complex functions as a channel to release ions from cytoplasm and in turn kill the fungal cell (Ostrosky-Zeichner et al., 2010). Azoles interfere with the biosynthetic enzymes in the ergosterol synthesis pathway (Chen and Sorrell, 2007). When the ergosterol cannot be synthesized, an alternative toxic sterol will accumulate in fungal cell and exert stress on the cell membrane (Lupetti et al., 2002). Although such kinds of drugs have a wide spectrum for fungal infection, the high similarity between ergosterol in fungal cells and cholesterol in mammalian cells make polyenes and azoles toxic to human cells and limit their usage

(Carrillo-Muñoz et al, 2006; Cowen, 2008). The only clinically used drugs that target fungal cell wall structures are the echinocandins, which specifically inhibit β-glucan synthase. As human cells do not have cell walls, reports on toxicity of echinocandins are rare, but echinocandins have a narrow spectrum of activity (Denning, 2003).

Due to the high metabolic similarity between fungal and animal cells, discovering new safe and effective drug targets is extremely difficult. However, this is still not the worst news. What worries us more is: all existing anti-fungal drugs are now challenged by emerging drug resistance and so are losing clinical efficacy (Cowen, 2008). For azoles, fungi are reported to gain the resistance in several ways. Genetic mutations in gene that encodes the drug target are the most common way. In *C. albicans,* at least three distinct "hot-spot" mutation regions have been identified in *erg11,* which encodes the target of azoles (Marichal et al., 1999). In addition, fungi can also up-regulate the drug transporter (efflux) or activate the stress response pathways to gain drug resistance (Cowen, 2008; Shapiro et al., 2011). Echinocandins are facing the similar problem as azoles, because they also specifically target an enzyme. Hot mutation sites within *fks1*, which encodes the target of the echinocandins, are identified from many clinically resistant strains (Walker et al, 2010). Increasing cell wall chitin content also leads to higher resistance to echinocandins in *C. albicans* (Walker et al, 2008). Even polyenes, developed in 1950's and considered as a durable drug, are now experiencing difficulties in the clinic, although the resistance mechanisms are not well understood (Kanafani and Perfect, 2008). Therefore, it is inevitable that more fungi will become resistant to the existing anti-fungal drugs.

1.6. *Aspergillus nidulans* is a Tractable Model System for Cell and Evolutionary Biology

There are more than 200 species in the genus *Aspergillus*, all of which are filamentous fungi. Most *Aspergillus* species function ecologically as decomposers, but some of them also have additional roles. For example, *A. niger* and *A.oryzae* are industrially used for biochemical production (Schuster et al., 2002; Bechman et al., 2012); *A. fumigatus* is a deadly pathogen for humans and animals (Dagenais and Keller, 2009), whereas *A. flavus* could be pathogen for both plants and animals (Vandecasteele et al., 2002; Hedayati et al., 2009). My study model—*A.nidulans*, is mainly considered as a tractable research model. Although it is a bio-safety level 2 organism in Canada, reports of *A. nidulans* infections are rare (Lucas et al., 1999).

A. nidulans can be easily cultured on defined medium and the phenotypes are easy to observe under the microscope. It has a simple cell differentiation program and a short life cycle. Molecular techniques are also well established for this organism. In addition, *A. nidulans* genome has been sequenced and the data are publicly available (AspGD: www.aspgd.org; Broad Institute: www.broadinstitute.org). In the past 70 years, *A. nidulans* has been used in many fields of biological research. Its most prominent contribution is in cell biology. For example, some initial studies of tubulin were done in this organism (Sheir-Neiss et al., 1978; Morris et al., 1979). It was also one of the early systems for studying nuclear migration and mitosis (Morris, 1975).

A. nidulans has well defined asexual and sexual life cycles. Its asexual life starts from a uninucleate spore, called a conidium. After germination, the hyphae, which are multinucleate, grow on and in the medium and then aerial conidiophores form from mature regions of the

colony (Fig.1-3). When a conidiophore matures, hundreds of conidia will be generated on each conidiophore to finish the asexual life cycle (Todd et al., 2007) (Fig.1-3). Under suitable temperature, a wild type *A. nidulans* can go through the asexual life cycle in about 2 days. During the whole asexual life cycle *A. nidulans* genome is haploid. A haploid genome has only one copy of each gene, so every gene will exhibit their effects. This feature makes *A. nidulans* convenient to dissect the roles of genes through the isolation and analysis of mutations.

The *A. nidulans* sexual life cycle is much more complex. It requires the fusion of two individual hyphae, formation of a dikaryotic cell and nuclear fusion to form a diploid nucleus. Then a closed sexual fruiting body (cleistothecium) will form around the fused hyphae and covered with some Hülle cells. The ascus is the cell in which meiosis occurs, and this cell is developed inside of cleistothecium (Todd et al., 2007). After meiosis, four sexual spores (ascospores) will form in each ascus (Todd et al., 2007). Then after another round of mitosis, a mature ascus with eight ascospores is eventually produced (Todd et al., 2007). The formation of ascus is repeated in a cleistothecium. In the end, a large number of (usually more than 10,000) ascospores are produced in each cleistothecium, and they are all the progeny of one pair of parental nuclei. For wild type strains, a sexual life cycle usually takes 3-4 weeks. In a lab condition, the asexual and sexual life cycles of *A. nidulans* can be precisely controlled.

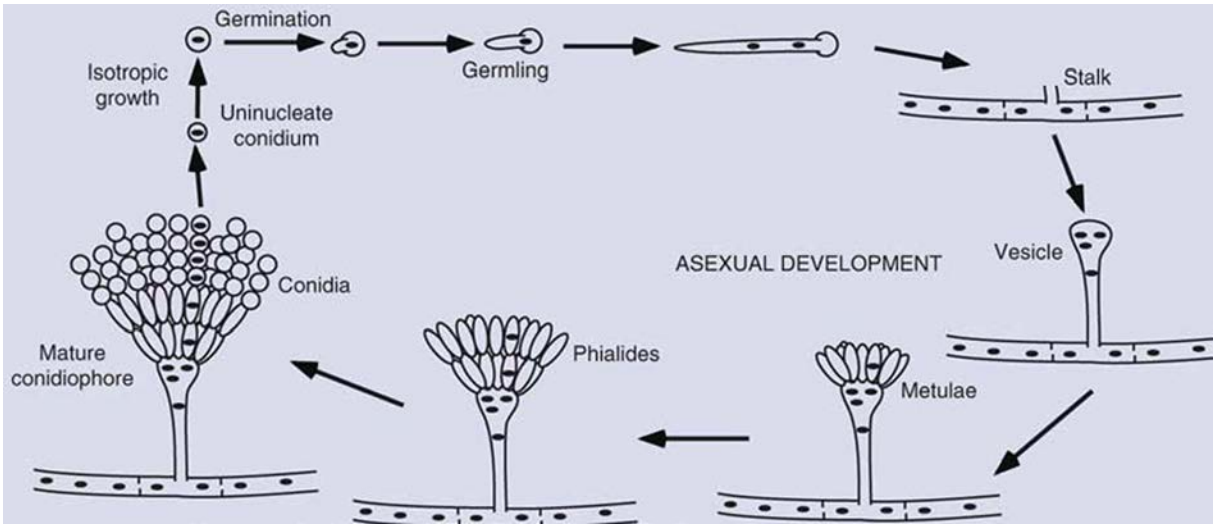

Fig. 1-3 Asexual life cycle of *A. nidulans* (modified from Todd et al., 2007)

Recently, *A. nidulans* has also drawn the attention of evolutionary biologists (Schoustra et al., 2009). Schoustra and colleagues found *A. nidulans* has strong adaptive ability in a detrimental environment (Schoustra et al., 2006). They showed the typical length of *A. nidulans* adaptive walk against a certain stress is only one to three mutations (Schoustra et al., 2009). In addition, the mutants with beneficial mutations can be readily detected and isolated from pure medium. All together, they proposed *A. nidulans* as a promising model for the study of evolution.

1.7. Summary

Systemic fungal infection is a growing problem in the last several decades, especially for developed countries. This kind of infection is difficult to treat by surgery. Therefore, anti-fungal drugs are the only hope for effective treatment. However, most anti-fungal drugs that target ergosterol in fungal cell membrane are toxic to humans because of the chemical similarity between ergosterol and cholesterol. The newest class of anti-fungal drug, echinocandins, is not

toxic to humans, but it has a narrow spectrum. Meanwhile, all anti-fungal drugs are losing their efficacy due to emerging drug resistance. Therefore, substantial work is urgently needed to protect us from these deadly pathogens. I suggest the work in the following two directions will be extremely helpful: 1) studying the metabolism of potential drug targets; 2) identifying drug resistance mutations.

Scientists have spent lots of effort to search for new anti-fungal drug targets. Recently, α-1,3-glucan has been shown to act as a virulence factor in several pathogenic fungi (Reese et al., 2007; Rappleye et al. 2007; Fujikawa et al., 2012; Beauvais et al., 2013) making it a potential drug target. Considering a α-1,3-glucan synthase homolog is not present in human cells, the drug targeting it should have minimal side effects for humans. However, we still have very little knowledge about the synthesis process of α-1,3-glucan in fungi, which hinders the development of drugs. *A. nidulans* provides a good model for such study. Firstly, *A. nidulans* is a tractable research model for cell biology and it has a substantial amount of α-1,3-glucan in its cell wall. Secondly, *A. nidulans* only has two α-1,3-glucan synthases making it easier to study the synthesis and the function of α-1,3-glucan. I believe studying α-1,3-glucan synthesis in *A. nidulans* will provide insights about the metabolism of this wall component, and in turn facilitate the development of anti-fungal drugs.

On the other hand, we also need to avoid losing the current anti-fungal drug due to emerging drug resistance. Identifying resistance mutations and understanding the resistance mechanisms are the key steps. *A. nidulans* can also be a useful model for such study. As Schoustra et al. (2006) showed, *A. nidulans* with beneficial mutations that compensate for a particular stress will grow

faster than the parental strain on the medium with the stress. Because of the phenotypic change, such mutants can be readily detected and isolated. With the advances of next generation sequencing technique, whole genome sequencing can greatly facilitate the identification of individual mutations, especially for the organisms with a small genome size such as *A. nidulans* (about 30Mb). Thus, the use of *A. nidulans* as a platform to induce and isolate drug resistance mutations can be an invaluable strategy in understanding the molecular response to anti-fungal drugs.

1.8. Research Outline and Hypotheses

This thesis contains six chapters. Chapter 1 is a general introduction for fungi and their cell walls. In chapter 2, I characterize two α-1,3-glucan synthases (AgsA and AgsB) and two amylase-like proteins (AmyD and AmyG) in *A.nidulans*. This is my initial study on α-1,3-glucan synthesis. In this chapter, I establish methods to detect α-1,3-glucan content in cell wall and point out the roles of these four proteins in α-1,3-glucan synthesis. Chapter 3 and 4 are the extended studies based on the result from chapter 2. In chapter 3, I further study the role of α-1,3-glucan and α-1,3-glucan synthases using overexpression analysis. Then in chapter 4, I examine the α-1,3-glucan degradation process in order to understand the mechanism of AmyD. Results from chapters 2, 3 and 4 provide new insights for α-1,3-glucan metabolism in *A. nidulans*. These data could be useful in future drug development against this cell wall component. Chapter 5 describes a strategy to quickly identify drug resistance mutations. I suggest this strategy could be helpful to solve the emerging drug resistance. Chapter 6 is a general discussion and conclusion. I discuss

the role of α-1,3-glucan in the cell wall of *A.nidulans*, the regulation of α-1,3-glucan synthesis, and how a lab-based experimental approach can help us to predict the mutations involved in clinical drug resistance.

My thesis is based on following objectives and hypotheses:

Objective 1: Exploring the roles of α-1,3-glucan synthesis related enzymes in *A. nidulans*.

Hypothesis 1: Deletion of any α-1,3-glucan synthesis related enzymes [α-1,3-glucan synthases (AgsA and AgsB) and amylase-like proteins (AmyD and AmyG)] will substantially reduce α-1,3-glucan content in the cell wall of *A. nidulans*.

Objective 2: Exploring the roles of α-1,3-glucan in α-1,3-glucan synthases overexpression strains.

Hypothesis 2: Extra α-1,3-glucan in cell wall will reduce conidiation rate but increase condial adhesion in liquid medium.

Objective 3: Exploring the role of AmyD in α-1,3-glucan degradation process.

Hypothesis 3: AmyD and α-1,3-glucanase works synergistically to degrade α-1,3-glucan from the cell wall.

Objective 4: Using *A. nidulans* as a model to indentify drug resistance mutations.

Hypothesis 4: The first arising accelerated growth sectors are due to the first beneficial mutations and such mutations can be identified by next generation sequencing.

CHAPTER 2

CHARACTERIZATION OF *ASPERGILLUS NIDULANS* ALPHA-1,3-GLUCAN SYNTHESIS: ROLES FOR TWO SYNTHASES AND TWO AMYLASES

This is my initial study on α-1,3-glucan synthesis in *A. nidulans*. In this chapter, I characterized the roles of four candidate proteins in α-1,3-glucan synthesis. They are two α-1,3-glucan synthases and two amylase-like proteins. Studies from several fungi have shown the α-1,3-glucan synthases are the enzymes that respond for α-1,3-glucan synthesis. Based on sequence analysis, two α-1,3-glucan synthases (AgsA and AgsB) are found in *A. nidulans*. Results from previous studies also suggest, α-1,3-glucan synthases are not the only enzymes involved in the α-1,3-glucan synthesis process. Some amylase-like proteins may contribute to the α-1,3-glucan synthesis. I found two amylase-like proteins (AmyD and AmyG) encoding genes are clustered with one of the α-1,3-glucan synthase (AgsB) genes in *A. nidulans* genome. Gene cluster grouped by genes involved in the same metabolic pathway is common in fungal genomes. Thus, these two α-1,3-glucan synthases and two amylase-like proteins are all chosen as the candidates in the initial work. When I started the work, none of these proteins have been studied in *A. nidulans*.

My role in this research: designed the study along with S Kaminskyj who funded it. I wrote thefirst draft; and contributed to the final revised draft. S Li provided technical assistance during the project. The results from this chapter have been published as “Characterization of *Aspergillus nidulans* α-1,3-glucan synthesis: roles for two synthases and two amylases” by He X., Li S. and Kaminskyj S.G.W. in Molecular Microbiology 2014: 91(3):579-95.

Characterization of *Aspergillus nidulans* α-1,3-glucan synthesis: roles for two synthases and two amylases.

Xiaoxiao He*, Shengnan Li, Susan G. W. Kaminskyj

Department of Biology, University of Saskatchewan, 112 Science Place, Saskatoon, SK S7N 5E2, Canada

*Author for correspondence

Tel: +1 306 966 2765; email: sean.he@usask.ca or seanhe630@hotmail.com

Key words: Alpha-1,3-glucan, cell wall, drug sensitivity, cell adhesion, alpha-1,3-glucan synthase, alpha-amylase,

2.1. Abstract

Cell wall is essential for fungal survival and growth. Fungal walls are ~90 % carbohydrate, mostly types not found in humans, making them promising targets for anti-fungal drug development. Echinocandins, which inhibit the essential β-glucan synthase, are already clinically available. In contrast, α-1,3-glucan, another abundant fungal cell wall component has attracted relatively little research attention because it is not essential for most fungi. *Aspergillus nidulans* has two α-1,3-glucan synthases (AgsA and AgsB) and two α-amylases (AmyD and AmyG), all of which affect α-1,3-glucan synthesis. Gene deletion showed that AgsB was the major synthase. In addition, AmyG promoted α-1,3-glucan synthesis whereas AmyD had a repressive effect. The lack of α-1,3-glucan had no phenotypic impact on solid medium, but reduced conidial adhesion during germination in shaken liquid. Moreover, α-1,3-glucan level correlated with resistance to Calcofluor White. Intriguingly, overexpression of *agsA* could compensate for the loss of *agsB* at the α-1,3-glucan level, but not for phenotypic defects. Thus, products of AgsA and AgsB have different roles in the cell wall, consistent with *agsA* being mainly expressed at conidiation. These results suggest that α-1,3-glucan contributes to drug sensitivity and conidia adhesion in *A. nidulans*, and is differentially regulated by two synthases and two amylases.

2.2. Introduction

Alpha-1,3-glucan is a major component of the walls of nearly all filamentous fungi as well as many yeasts (Latgé, 2010). Compared with β-glucan and chitin, α-1,3-glucan has attracted relatively little research effort, likely because α-1,3-glucan synthases are only essential in *Schizosaccharomyces pombe* (Hochstenbach et al., 1998) when examined by gene deletion. Alpha-1,3-glucan is not essential in *Paracoccidioides brasiliensis* (Pereira et al., 2000), *Cryptococcus neoformans* (Reese and Doering, 2003), *Histoplasma capsulatum* (Rappeleye et al. 2004), and *Aspergillus* species (Damveld et al., 2005; Henry et al. 2012; Yoshimi et al., 2013). However, substantial evidence has shown that α-1,3-glucan can contribute to cell morphology (Hochstenbach et al., 1998; Reese and Doering, 2003; Cortés et al., 2012), cell wall integrity (Fujioka et al., 2007), and even virulence for some pathogenic fungi (Rappleye et al. 2007; Reese et al., 2007; Fujikawa et al., 2012).

In *A. nidulans*, α-1,3-glucan synthesis is significantly up-regulated when the cell is challenged by echinocandins that target β-glucan synthase FksA (Fujioka et al., 2007), by Calcofluor White (CFW) that inhibits chitin crystallization (Elorza et al 1983), and by genetic manipulations to reduce galactofuranose (Gal*f*) content (Damveld et al, 2008; El-Ganiny et al., 2008; Alam et al., 2012). Fujioka et al. (2007) showed that alpha-1,3-glucan synthesis was regulated by the protein kinase C (PKC) pathway. The PKC pathway is thought to be central cell wall integrity regulation in all fungi, responding to cell wall stress (Levin, 2005; Teepe et al., 2007; Fuchs and Mylonakis, 2009; Kovács et al., 2013). Thus, there is considerable reason to

suspect that the expression level of α-1,3-glucan is related to cell morphology, cell wall composition, and perhaps also to anti-fungal drug sensitivity.

A gene cluster composed of one α-1,3-glucan synthase and two α-amylases is conserved in all *Aspergillus* species studied except *A. fumigatus*, and has been suggested to increase α-1,3-glucan synthesis efficiency (Nakamura et al., 2006; de Groot et al., 2009). Yoshimi et al. (2013) recently described *A. nidulans* AgsA (ANID 5885) and AgsB (ANID3307) as α-1,3-glucan synthases. AgsB is part of this conserved gene cluster [*agsB*←→*amyG*, *amyD*], and it is the major α-1,3-glucan synthase in *A. nidulans* (Yoshimi et al., 2013). However the *agsB*Δ strain does not show any growth or conidiation defect when grown on agar medium. The major phenotype is that conidial adhesion during germination in shaken liquid culture is substantially reduced, so that many small colonies are formed rather than a few large ones (Yoshimi et al., 2013).

There is still limited knowledge about the relationship between α-1,3-glucan synthases and the overall α-1,3-glucan synthesis process. Some studies have suggested that the α-amylase-like proteins are involved in α-1,3-glucan synthesis, perhaps functioning in the initiation step (Grün et al., 2005; Marion et al., 2006; van der Kaaij et al., 2007; Yuan et al., 2008). Alpha-amylase belongs to glycoside hydrolase (GH) family 13. Based on sequence similarity, GHs can be classified into more than 100 families (Henrissat et al., 1995; Henrissat and Bairoch, 1996; see also www.cazy.org/Glycoside-Hydrolases.html). As well as α-amylases, GH 13 contains transglycosidases, isomerases and other enzymes (MacGregor et al., 2001), all of which act on α-glycoside linkages.

The *A. nidulans* gene cluster α-amylases are AmyD (ANID3308) and AmyG (ANID3309). These genes are not up-regulated by carbon starvation (Nakamura et al., 2006) suggesting they likely do not play a role in glucose catabolism. In addition, the homologue of AmyD in *A. niger* has been shown to have very low starch hydrolysis ability, consistent with a function such as transglycosylation (van der Kaaij et al., 2007), perhaps as a glucanotransferase. The homologue of AmyG in *H. capsulatum* (AMY1) has been shown to be crucial for α-1,3-glucan synthesis (Marion et al., 2006; Camacho et al., 2012). This evidence strongly suggests AmyD and AmyG may participate in α-1,3-glucan synthesis but not in glucose catabolism. Considering the fact that ~10 % of α-1,4-glucosidic linkage was found in α-1,3-glucan (Grün et al. 2005; Choma et al., 2013), the amylases are suspected to have a role in these α-1,4-linkages, possibly serving to package a primer structure to nucleate efficient α-1,3-glucan synthesis (Grün et al., 2005; Marion et al., 2006; van der Kaaij et al., 2007). Metabolic pathways encoded by clustered genes have been described in *Aspergillus* (e. g. Keller et al., 1997).

In this study, we characterized two *A. nidulans* α-1,3-glucan synthase genes and two α-amylase genes by deletion and overexpression. Our results confirmed that AgsB is the major synthase and also revealed that *agsA* is mainly expressed during conidiation. In addition, we found the two α-amylases have different effects in α-1,3-glucan synthesis, and that the polymers produced by AgsA and AgsB have different roles in the cell wall. These results suggest future questions regarding the synthesis and function of α-1,3-glucan in fungal cell wall.

2.3. Materials and Methods

2.3.1. Strains, Plasmids and Media

All strains in this study were constructed in *A. nidulans* A1149. The A1149 strain was also the wild type control for all assays in this paper. Strains used in this study are listed in Table 1. Primers and plasmids are listed in Table S2-1. Strategies for gene deletion and confirmation methods were described by Szewczyk et al. (2006) and El-Ganiny et al. (2008). Briefly, a targeted replacement construct was constructed by fusion PCR including 1 kb upstream, a selectable marker, and 1 kb downstream (details see Fig. S2-1A). This construct was transformed to A1149 protoplasts. *A. fumigatus pyrG* and *pyroA* were used as selectable markers (details for each strain see Fig. S2-1B). Strategies for promoter exchange and GFP-tagging were previously described in Alam et al. (2012), except that in this study the actin promoter *actA*(p) was used as a high expression constitutive promoter. This had been amplified previously from A1149 genomic DNA. For promoter exchange, the transformation construct was 1 kb upstream of the target, the selectable marker, *actA*(p) and 1 kb downstream of the target gene (Fig. S2-1A). For GFP-tagging, the transformation construct was 1 kb of target gene at the 3' end (lacking the stop codon), *gfp*, a selective marker and 1 kb downstream of target gene (Fig. S2-1A). Again, details for each construction see Fig. S2-1B.

All strains were grown on complete medium (CM: 1 % glucose, 0.2 % peptone, 0.1 % yeast extract, 0.1 % casamino acids, 50 mL 20 x nitrate salts, 1 mL trace elements, 1 mL vitamin solution, pH 6.5) or minimal medium (MM: 1 % glucose, 50 mL 20 x nitrate salts, 1 mL trace

elements, 0.001 % thiamine, pH 6.5) supplemented with nutrition solution as required. Trace elements, vitamin solution, nitrate salt and all nutrition stocks are described in Kaminskyj (2001). For transformation medium, 1 M sucrose was added to MM as osmoticum. All strains were grown at 30ºC, unless mentioned specifically.

2.3.2. Microscopy Studies

For transmission electron microscopy (TEM), A1149 and [*agsA*Δ, *agsB*Δ] strains were grown on dialysis tubing overlying CM for 2 d at 30 ºC. TEM protocol was followed Kaminskyj, (2000). Briefly, samples were fixed in 2% glutaraldehyde in 50 mM phosphate buffer for 1 h and post-fixation in 1% OsO4 in 50 mM phosphate buffer for 1 h. Then samples were dehydrated in a graded ethanol series (20%, 40%, 60%, 80% and 100%) for 10 min in each concentration, and transfer to acetone in the end for 1 h. Samples were embedded in Eponate 12 resin. Then, 75 nm sections were made and stained by uranyl acetate for 20 min, followed by lead citrate for 2 min. Sections were rinsed with H_2O between and after each staining solution for 30 s. TEM images were taken by a Philips CM10 model.

For immunogold-TEM, strains were grown in shaken liquid medium (CM) for 16 h at 30 ºC. TEM protocol was adapted from Skepper and Powell (2008). Briefly, samples were fixed in 4% formaldehyde in PIPES for 1 h at 4 ºC and were rinsed four times in 0.1M PIPES buffer over a period of 20 min and twice in H_2O. Then all samples were incubated in 2% aqueous uranyl acetate for 30 min at room temperature and then three times rinse in H_2O. All cells dehydrated in three changes of 70% ethanol, three changes of 95% ethanol and three changes of 100% ethanol,

all for 5 min each. Then cells were imbedded in a 50:50 mixture of 100% LR white and 100% ethanol overnight, and in two daily changes of 100% LR white. At last, samples were placed in a gelatin capsule and incubated at 55 ºC for 24 h. Then 70 - 90 nm sections were made and placed on nickel grids. For antibody staining, grids were blocked by 1% BSA 30 min, and then stained by 1:20 diluted MOPC 104E (Sigma) and 1:100 diluted 12-nm gold label goat anti mouse IgG + IgM (Jackson Immunoresearch) 1 h respectively at room temperature, 30 s rinse by H_2O was needed after each antibody. In the end, all grids were post stained by uranyl acetate and lead citrate as described above. TEM images were taken by a Philips CM10 model. A mouse IgM (Sigma: M5909) and L10 (IgM, anti-galactofuranose) were used as negative and positive control.

For scanning electron microscopy (SEM), A1149 and [*agsA*Δ, *agsB*Δ] strains were grown on dialysis tubing overlying CM for 2 d at 30 ºC. Isolated colonies were fixed at 100 % relative humidity over 4 % aqueous glutaraldehyde for 1 h, frozen to -80 ºC in pre-chilled acetone for 1 h, then transfer to -20 ºC, 4 ºC and room temperature for 1 h respectively. Samples were dried by critical point dryer and then gold sputter coated. SEM images were taken by a JEOL JSM-6010 LV model and conditions for each image were shown under the image.

For antibody staining, primary antibody MOPC 104E and secondary antibody TRITC-conjugated goat-anti-mouse (Sigma) were used at 1:20 and 1:50 respectively. Antibody staining procedures followed El-Ganiny et al. (2008). Briefly, conidia were grown on dialysis tubing overnight at 30 ºC. Dialysis tubing was cut into 1 cm x 1 cm squares. Fungal cells were fixed in 6 % formaldehyde in P+BS buffer (50 mM PIPES, 2 mM EGTA, 2 mM $MgSO_4$, 137 mM NaCl, 268 µM KCl, pH 6.8) for 30min. Fixed samples were washed in P+BS for 3 x

5 min. Membranes were permeabilized by 3 x freeze (-80 ºC) and thaw (Shi et al 2004), then nonspecific binding was blocked with freshly made 5 % non-fat milk in P+BS buffer for 20 min. Primary antibody was diluted in 0.5 % non-fat milk in P+BS then cells were stained for 60 min. Samples were washed 3 x 5 min in P+BS buffer. Secondary antibody was diluted in 0.5 % non-fat milk in P+BS, and cells were stained for 60 min. Excess secondary antibody was removed by washing in P+BS buffer 3 x 5min. Samples were examined using a Zeiss META501 confocal epifluorescence microscope at 63 x, N.A. 1.2 objective lens. Confocal imaging used 543 nm excitation, with emission controlled by BP 560-615 nm filter.

For GFP signal, conidia were grown on dialysis tubing at 30 ºC. Then samples were examined using a Zeiss META501 confocal epifluorescence microscope at 63 x or 25 x objective lens. Confocal imaging used 488 nm excitation with emission controlled by BP 505-530 nm filter.

2.3.3. Quantification of Conidiation

1.5 mL CM or MM agar were added to 24-well plate and seeded with 10^5 conidia after solidification. Plates were incubated for 4 d, then 1 mL ultrapure water was used to collect conidia from each well. Conidia were quantified by hemocytometer.

2.3.4. Alpha-1,3-glucan Quantification

This method was adopted from Momany et al. (2004) and Marion et al. (2006). Briefly, 10^7 conidia were grown at 30 ºC in 100 mL liquid CM, shaken at 150 r.p.m. for 24 h. Colonies were

collected by filtration and washed with 0.5 M NaCl. Cells were frozen at -80 ºC for 2-4 h, then broken in disruption buffer (DB: 20 mM Tris, 50 mM EDTA, pH 8.0) using a Virsonic Ultrasonic Cell Disrupter until hyphal ghosts formed. Cell walls were separated by centrifugation at 3500 x *g* for 10 min. The pellet containing the cell wall fraction was washed in DB with stirring for 4 h at 4 ºC followed by a wash with sterile ultrapure water under the same conditions, pelleted again, and lyophilized. Dry cell wall samples were weighed, then suspended in 1 M NaOH at 0.5 mg mL^{-1}. Alkaline extraction was performed overnight at 37 ºC. Then 0.5 mL alkaline-soluble fraction (containing α-1,3-glucan) was used for the following process. The alkali was neutralized by acetic acid until pH to 5.5. Alpha-1,3-glucan was collected by centrifugation 12000 x *g* for 10min, and then washed twice in ultrapure water. Finally, α-1,3-glucan was hydrolyzed by 0.5 mL 3 M H_2SO_4, at 100 ºC for 1 h. Glucose content (mainly from α-1,3-glucan in the alkali-soluble fraction) was quantified by anthrone assay (Ashwell, 1957). All experiments were repeated three times with duplicates each time.

2.3.5. RT-PCR and qPCR

For the CFW treatment test, 10^7 conidia were inoculated in liquid CM and incubated at 30 ºC with shaking at 150 r.p.m. for 13 h, then CFW was added into medium at final concentration of 50 μg mL^{-1} and keep growing for another 1 h. Control groups were grown for 14h with equal amount of ultrapure water added in the last hour. In the end, colonies were collected by filtration and frozen in liquid nitrogen immediately, then lyophilized.

For time-course expression study, 10^7 conidia were inoculated in liquid CM and incubated at 30 ºC with or without shaking at 150 r.p.m., then colonies were collected at 14 h and 24 h for both groups. In static condition, only the colonies grown on the liquid surface were collected. Then colonies were frozen in liquid nitrogen immediately and lyophilized.

For the overexpression study, 10^7 conidia were inoculated in liquid CM and incubated at 30 ºC with shaking at 150 r.p.m. for 16 h. Colonies were collected by filtration, immediately frozen in liquid nitrogen, then lyophilized.

Total RNA was extracted using an RNeasy plant kit (Qiagen) following manufacturer's instructions. RNA concentration was measured using a Nanodrop®, then diluted to 500 ng μL^{-1}. Genomic DNA elimination and reverse transcription used a QuaniTect reverse transcription kit (Qiagen) following the manufacturer instructions.

Quantitative real time PCR (qPCR) was performed in 96-well optical plates in an iQ5 real-time PCR detection system (Bio-Rad). Gene expression was assayed in total volume of 20 µL per reaction containing cDNA at an appropriate dilution and SYBR green fluorescein (Qiagen). A no-template control was used for each pair of primers. Histone was used as a reference gene (Fujioka et al., 2007). Primers for qPCR are listed in Table S2-1.

The qPCR amplification used the following conditions: 95 ºC /15 min for one cycle, 95 ºC /15 s, 55 ºC /40 s and 72 ºC /30 s for 40 cycles and final extension cycle of 72 ºC /2 min. Melting curve analysis was done using the following cycle: 15 s at 65 ºC with an increase of 0.5 ºC each cycle to 95 ºC. The relative expression was normalized to histone and calculated using

the ΔΔCt method (Livak and Schmittgen, 2001). Three independent experiments with triplicates were performed for each reaction.

2.3.6. Conidia Adhesion Test

For shaken liquid colonies, 2 x 10^7 freshly harvested conidia of each strain were grown in 20 mL liquid CM in a sterile GelSlick-coated 50 mL glass Erlenmeyer flask, at 150 r.p.m. and 30 ºC for 14 h. Then 3 mL medium was poured to Petri dishes and pictures were taken by flat-bed scanning. For conidia clusters, 2 x 10^7 of freshly harvested conidia of each strain were grown in 20 mL liquid CM in a sterile GelSlick-coated 50 mL glass Erlenmeyer flask, 150 r.p.m., at 37 ºC for 6 h. We examined 20 µL of liquid medium plus germlings using transmitted light microscopy (10 x objective lens) with images collected using a Dino-eye CCD.

2.3.7. Drug Sensitivity Test

Calcofluor White (American Cyanamid Company) was prepared as a stock at 10 mg mL^{-1} in 25 mM KOH (Hill et al., 2006). Congo Red (British Drug Houses Ltd.) was prepared as a stock as 10 mg mL^{-1} in ultrapure water. Caspofungin was a kind gift from Merck, and prepared as a stock at 20 mg mL^{-1} in ultrapure water. All stock solutions were sterilized by filtration. For testing, each stock solution was added to CM agar cooled to 55~60 ºC. Then, 10^5 conidia of each strain were inoculated on plate on the same day. Plates were incubated for 72 h at 30 ºC.

2.4. Results

2.4.1. Genes in the Conserved Alpha-1,3-glucan Cluster can be Differentially Regulated

In *A. nidulans*, the conserved α-1,3-glucan gene cluster consists of the α-1,3-glucan synthase AgsB, and the α-amylases, AmyD and AmyG. The *agsB* and *amyD-amyG* coding regions are on opposite strands of chromosome VI, so they could potentially share upstream regulatory elements (Fig. 2-1A), whereas *agsA* is on chromosome I. Alpha-1,3-glucan synthases *agsA* and *agsB* are each ~8 kb in length, and each is predicted to encode a multiple domain protein. These domains are: an α-amylase domain, a starch synthase catalytic domain, a glycosyl transferase domain and a 12-transmembrane domain (Fig. 2-1B). The amino acid sequence identity between AgsA and AgsB is ~67 %. AgsA and AgsB hydropathy analysis predicted an extracellular domain, a single membrane-span, an intracellular domain and a multiple-transmembrane domain, which was very similar to that of the essential α-1,3-glucan synthase in *S. pombe* (Hochstenbach et al., 1998) (Fig. 2-1C).

Fujioka et al. (2007) showed that *agsB* was up-regulated when *A. nidulans* was challenged by micafungin. Following this idea, we used CFW to treat *A. nidulans* cells and to test whether the genes in the cluster were coordinately regulated. In response to 50μg mL^{-1} CFW, the expression of all three genes in this cluster was increased, but to different extents: *amyG* > *agsB* > *amyD* (Fig. 2-2A). The expression of *agsA* was assessed in the same experiment, showing a limited increase (Fig. 2-2A). We concluded that the genes in this cluster could share a regulatory

element(s), which was different from that of *agsA*. However, the different regulation of the three genes in the cluster also argues that they have distinct roles in α-1,3-glucan synthesis.

To test this notion, we performed a time-course expression study for all of our candidate genes. We compared two growth conditions (shaken liquid and static liquid) and two time points (14 h and 24 h after inoculation). In shaken liquid, *A. nidulans* was restricted to only the growth of vegetative mycelia. However in static liquid, the colonies grown on the liquid surface underwent asexual development and conidiated within 24 h. So the combination of these two growth conditions and time points gave us a comprehensive view of the expression profile for each gene. In shaken cultures, the only notable change in gene expression was for *amyD*, which showed a 5.9-fold increase at 24 h (Fig. 2-2B). In static culture, there was an even greater increase (10.3-fold) for *amyD* expression at 24 h, plus a dramatic increase (69-fold) for *agsA* expression (Fig. 2-2C). In contrast, *agsB* and *amyG* had relatively constant expression levels at 14 h and 24 h in both culture conditions. Collectively, our results showed that the genes in this cluster were not always co-regulated.

2.4.2. AgsA and AgsB are the Only α-1,3-glucan Synthases in *Aspergillus nidulans*

In order to confirm the roles of *agsA* and *agsB*, we replaced each of them by a nutrition marker (strategy see Fig. S2-1). The constructed strains were confirmed by PCR (Fig. S2-2; primers and plasmids are listed in Table S2-1). The *agsA*Δ, *agsB*Δ, and [*agsA*Δ, *agsB*Δ] deletion strains each had a wild type phenotype on solid medium (Fig. 2-3A on CM; Fig. S2-3 on MM), consistent with reports by Yoshimi et al. (2013). In contrast, when grown in shaken liquid, the

*agsB*Δ and [*agsA*Δ, *agsB*Δ] strains formed many tiny colonies, compared to a few large colonies as for wild type and *agsA*Δ strains (Fig. 2-3C). Fontaine et al. (2010) had reported that α-1,3-glucan is responsible for aggregation of germinating conidia in *A. fumigatus*, so we also monitored earlier and later stages of germination in shaken liquid. After 6 h growth at 37 ºC, and unlike wild type, the *agsB*Δ and [*agsA*Δ, *agsB*Δ] strains lacked the large discrete conidia colonies that are characteristic of wild type strains (Fig. S2-3), however small clusters of conidia were visible when examined by light microscopy (Fig. S2-3). This suggested that wall α-1,3-glucan was important for conidial adhesion during germination in liquid but was likely not solely responsible for the interaction.

To have a closer view, we also examined the ultrastructure of [*agsA*Δ, *agsB*Δ] strain by TEM and SEM. Although no significant difference was found for cell wall thickness (Fig. 2-4A), multiple (3 or 4) phialides were seen on most metulae in the double deletion strain (Fig.2-4B). In addition, wild type hyphae had smoother cell walls than deletion strains (Fig. 2-4D), but this was not seen for conidia (Fig. 2-4C). Together, these data suggested α-1,3-glucan does not have an important role in *A. nidulans* cell wall construction, but may affect formation of extracellular matrix.

Alpha-1,3-glucan is also considered to be important in the sexual life of *A. nidulans* (Wei et. al., 2001). We performed a mating experiment between [*agsA*Δ, *agsB*Δ] and a wild type strain (AXM20). No difference was found in mating process in respect to the formation of cleistothecia and the number of ascospores in each cleistothecium (*data not shown*). We also mated a green [*agsA*Δ, *agsB*Δ] strain (original strain) and a white [*agsA*Δ, *agsB*Δ] strain obtained from last

mating experiment. Again, there was no difference in cleistothecial or ascospore formation compared to a wild type::wild type mating. We conclude that α-1,3-glucan does not affect the sexual cycle of *A. nidulans*.

In order to confirm the changes of wall α-1,3-glucan content in deletion strains, we used two methods: an anthrone reducing-sugar analysis of alkali-extracted walls for overall quantification (Marion et al., 2006; Camacho et al., 2012), and an α-1,3-glucan immunolocalization for distribution. Compared to wild type (defined as 100 % in Table 2-2) the α-1,3-glucan content of the *agsA*Δ strain (94.3 %) was marginally reduced and that of the *agsB*Δ strain (3.1 %) was substantially reduced. The α-1,3-glucan content of the [*agsA*Δ, *agsB*Δ] strain was even lower, only 1.2 % remained. A low level of glucose was also seen in the Yoshimi et al. (2013) [*agsA*Δ, *agsB*Δ] double deletion strain.

Our anthrone quantification results were consistent with immunolocalization used to stain vegetative colonies grown on dialysis tubing (Fig. 2-5). Unlike wild type hyphae, no α-1,3-glucan signal was detected in the [*agsA*Δ, *agsB*Δ] strain confirming a loss of immunodetectable wall α-1,3-glucan. And this is consistent with the conclusion in Yoshimi et al (2013) that *agsA* and *agsB* are the only two α-1,3-glucan synthases in *A. nidulans*.

Antibody staining was also performed on the *agsA*Δ and *agsB*Δ strains. We found these two synthases are not equally important for α-1,3-glucan synthesis. A clear α-1,3-glucan signal was observed in the *agsA*Δ strain (Fig. 2-5), but only trace amounts of α-1,3-glucan were detected in the *agsB*Δ strain (Fig. 2-5). Therefore AgsB is the major α-1,3-glucan synthase in *A. nidulans*.

Unexpectedly, α-1,3-glucan immunolocalization showed that the growing wild type tips lacked substantial immunolocalizable α-1,3-glucan, whereas basal regions showed more or much more prominent α-1,3-glucan content (Fig. 2-5). Similar longitudinal distributions of α-1,3-glucan were also seen for the *agsA*Δ and *amyD*Δ strains. As expected, the *agsB*Δ, [*agsA*Δ, *agsB*Δ] and *amyG*Δ lacked visible immunolocalizable α-1,3-glucan.

2.4.3. AmyD and AmyG Have Distinct Roles in α-1,3-glucan Synthesis

In the *A. nidulans* genome, *amyD* and *amyG* are adjacent but divergently transcribed from *agsB.* Both are predicted to encode α-amylase like proteins. Similarly, the homologue of AmyG in *H. capsulatum*, Amy1 has been characterized and shown to be crucial for α-1,3-glucan synthesis. Amy1 is anticipated to synthesize the primer structure of α-1,3-glucan (Marion et al., 2006). Although the majority of α-1,3-glucan in *H. capsulatum* is 1,3-linked (Grün et al., 2005; Choma et al., 2013), there is evidence that a 1,4-linked oligomer forms a primer structure (Grün et al., 2005; Marion et al., 2006; van der Kaaij et al., 2007). Enzymatic study and genomic analysis suggested AmyD may also have a role in α-1,3-glucan synthesis (van der Kaaij et al., 2007; de Groot et al., 2009).

We created *amyD*Δ and *amyG*Δ strains to assess their roles in *A. nidulans* α-1,3-glucan synthesis. As with the *agsA*Δ and *agsB*Δ deletions, neither the *amyD*Δ nor *amyG*Δ strain showed a phenotypic change compared to wild type when grown on solid medium (Fig. 2-3A). The *amyG*Δ strain, but not *amyD*Δ, formed many tiny colonies in shaken liquid (Fig. 2-3C). This was comparable to the *agsB*Δ strain, and indicated that AmyG but not AmyD was critical for

α-1,3-glucan synthesis. Anthrone analysis showed that *amyG*Δ walls had low (12.7 %) α-1,3-glucan content (Table 2-2), consistent with AmyG having an important role in α-1,3-glucan synthesis. In contrast, the α-1,3-glucan content of the *amyD*Δ strain walls was 1.5-fold higher than wild type (Table 2-2). To test whether the accumulation of α-1,3-glucan in the *amyD*Δ strain was due to AgsB and AmyG, we constructed a cluster deletion [*agsB*Δ, *amyD*Δ, *amyG*Δ] strain. The triple knockout had almost no α-1,3-glucan (2.9 %) (Table 2-2) and its colony phenotype in shaken liquid resembled the *agsB*Δ and *amyG*Δ strains (Fig. 2-3C). Together, these results indicated that the roles of AmyD and AmyG in α-1,3-glucan synthesis differ, and that both are important. The function(s) of AmyD and AmyG require further study.

2.4.4. Overexpression of *agsB, amyD* and *amyG* Further Suggest Their Roles in α-1,3-glucan Synthesis

For overexpression studies, we used the *A. nidulans* actin promoter, *actA*(p) to provide strong constitutive expression that was not affected by medium glucose. Promoter exchange methods and strain confirmation are shown in Fig. S2-1 and S2-2. The qPCR results reported in Table 2-3 are with respect to the native expression for each gene (*agsB* > *amyD* > *amyG* >> *agsA*) in vegetative growth (16 h in shaken liquid culture). The native level of gene expression was lower than when driven by *actA*(p).

We constructed an *actA*(p)-*agsB* strain to study the effect of increased AgsB on cell wall α-1,3-glucan. Anthrone and qPCR analysis showed comparable increases in cell wall α-1,3-glucan (Table 2-2) and *agsB* mRNA (Table 2-3) confirming our strategy. This strain

showed a moderate (30 % or 40 % depending on growth medium) reduction in conidiation (Table S2-2), but no change in growth rate or conidial adhesion (Fig. 2-3B and D). Then we used *actA*(p) to overexpress *amyD* and *amyG*, in order to compare the relative effect of overexpression with that of gene deletion. The *actA*(p)-*amyD* construct up-regulated *amyD* but led to a reduction for wall α-1,3-glucan (Table 2-2 and 2-3). Consistent with this, the *actA*(p)-*amyD* strain had fragmented colonies in shaken liquid and lacked discrete conidia clusters (Fig. 2-3D and S2-3), both of which were correlated with the loss of α-1,3-glucan. The *actA*(p)-*amyG* construct up-regulated *amyG* 18-fold at mRNA level (Table 2-3), but it only led to slightly higher cell wall α-1,3-glucan (Table 2-2).

Our overexpression study further suggested the roles of these three gene products in α-1,3-glucan synthesis process. AgsB is the limiting step, because it can positively regulate the amount of α-1,3-glucan. Although AmyG is critical for synthesis, it cannot overproduce α-1,3-glucan without the help of other proteins. Therefore, we conclude AmyG does not directly synthesize α-1,3-glucan and the abundance of AmyG is more than sufficient at its normal expression level. AmyD can negatively regulate wall α-1,3-glucan, so it clearly has a repressive role for α-1,3-glucan synthesis.

2.4.5. Wall α-1,3-glucan Mediates Sensitivity to Calcofluor White, but not Caspofungin or Congo Red

Recent evidence showed that reduced wall α-1,3-glucan correlated with CFW hypersensitivity in *A. niger* (Damveld et al., 2005) and *H. capsulatum* (Marion et al., 2006). To

assess the effect of our gene manipulations on drug sensitivity, we added anti-fungal agents into solid medium and inoculated equivalent numbers of conidia on these plates to test their growth ability. The *agsB*Δ, [*agsA*Δ, *agsB*Δ], and *amyG*Δ strains were CFW hypersensitive, barely able to germinate on 30 μg mL^{-1} CFW within 3 d (Fig. 2-6A). Notably, these cells were inhibited but not killed, since they were viable when transferred to CFW-free medium after 3 d (*data not shown*). Higher wall α-1,3-glucan in the *actA*(p)-*agsB* strain (Table 2-2) did not confer resistance to CFW (Fig. 2-6B).

Alam and Kaminskyj (2012) showed that α-1,3-glucan and β-glucan content of *A. nidulans* cell walls were coordinately regulated with galactofuranose (Gal*f*) content. Reduction or loss of Gal*f* by manipulation of UgmA function was correlated with increased α-1,3-glucan and decreased β-glucan, as well as with increased sensitivity to Caspofungin. In this study, we found that Caspofungin sensitivity was not affected by altered α-1,3-glucan content (Fig. 2-6) suggesting that α-1,3-glucan and β-glucan synthesis were independent. Yoshimi et al. (2013) reported that *agsB*Δ and [*agsA*Δ, *agsB*Δ] strains were hypersensitive compared to wild type to 20 – 80 μg mL^{-1} Congo Red (CR). We tested for a growth response up to 200 μg mL^{-1} CR, but saw no difference in any of our strains compared to wild type (Fig. 2-6). Therefore in our experiment, α-1,3-glucan had a role in the drug sensitivity to CFW but not CR or Caspofungin.

2.4.6. AgsA Mainly Functions at Conidiation, and It Cannot Compensate for the Loss of AgsB

The *agsA* sequence has been shown to have a very low expression level in vegetative colonies (Fujioka et al., 2007; Futagami et al., 2011), even in the absence of *agsB* (Yoshimi et al., 2013). *Aspergillus nidulans* does not form conidia when grown in submerged liquid culture as is typical for qPCR analysis samples. Our time-course study showed that *agsA* expression increased in the 24 h static culture group only (Fig. 2-2C). This strongly suggested the expression of *agsA* was related to conidiation, which had not been reported previously. To test this, we used the *agsA* promoter to drive GFP expression [*agsA*(p)-GFP] in order to visualize when and where *agsA* was expressed. The GFP signal was seen in foot cells, conidiophores, metulae, phialides and conidia, but not significantly in hyphae (Fig. 2-7A). So *agsA* appeared to have a high expression during conidiation.

Encouraged by this finding, we wondered if overexpression of *agsA* could compensate for the loss of *agsB*. We used *actA*(p) to overexpress *agsA* in an *agsB*Δ background [*actA*(p)-*agsA*; *agsB*Δ]. The expression level of *agsA* was substantially up-regulated (123-fold, Table 2-3). Anthrone analysis showed that the α-1,3-glucan level of the [*actA*(p)-*agsA*; *agsB*Δ] strain had recovered from the *agsB*Δ strain levels to more than double the wild type levels (3.1 % to 228 %) (Table 2-2). This suggested that AgsA is a fully functional α-1,3-glucan synthase. Intriguingly, the [*actA*(p)-*agsA*; *agsB*Δ] strain still produced tiny fragmented colonies in shaken liquid medium (Fig. 2-3D), comparable to the *agsB*Δ strain. In addition, it was still more sensitive to

CFW than the wild type strain, but better than *agsB*Δ (Fig. 2-6B). So overexpression of *agsA* could only partially compensate for the loss of *agsB.*

2.4.7. Functions of Both AgsA and AgsB are Dependent on AmyG

Combining our previous results that AgsB is the main synthase in vegetative growth and AmyG was crucial for wild type α-1,3-glucan synthesis in hyphae, it appeared that AgsB function was AmyG-dependent. The fact that AgsA could not fully compensate the loss of AgsB raised the question: was AgsA also AmyG-dependent? To test this, we constructed [*actA*(p)-*agsA*; *amyG*Δ] strain. If AgsA was AmyG-dependent, this strain should have low α-1,3-glucan content, similar to *amyG*Δ. If not, the α-1,3-glucan content should be similar to that of [*actA*(p)-*agsA*; *agsB*Δ]. The result showed a low α-1,3-glucan content (19.0 %) in the [*actA*(p)-*agsA*; *amyG*Δ] strain (Table 2-2), and this strain behaved as *amyG*Δ strain in shaken liquid (Fig. 2-3D) and on CFW (Fig. S2-5). All these results were consistent with both AgsA and AgsB being AmyG-dependent.

2.4.8. AgsB-GFP is Concentrated at Growing Hyphal Tips

AgsA and AgsB are predicted to have an N-terminal signal peptide (by SignalP 4.1 server) and C-terminal multiple-transmembrane domains (Fig. 2-1C). Some experiments have proven their localization on cell membrane (Hochstenbach et al., 1998; Beauvais et al., 2005; Cortés et al., 2012). However, no fluorescence-tagging information was yet available for Ags in a filamentous fungal species. We tagged the C-terminal of AgsB with GFP to visualize the

localization of this protein. AgsB-GFP fluorescence was mostly concentrated on the membrane of growing tips (Fig. 2-7B), consistent with recent result from *S. pombe* (Cortés et al., 2012). However, C-terminal GFP-tagging killed the function of AgsB (based on fragmentation in shaken liquid culture, Fig. S2-6), indicating that the C-terminal was essential for AgsB function, which was also seen in *S. pombe* Ags1 (Cortés et al., 2012). As expected for an N-terminal GFP-tagged strain (GFP-AgsB; *data not shown*) AgsB function was maintained, however, GFP-AgsB fluorescence had an even cytoplasmic distribution, consistent with having the GFP tag being removed with the signal peptide. So the C-terminal tagging strain (AgsB-GFP) revealed the most likely localization (Fig. 2-7B). In addition, since AmyG is also crucial for α-1,3-glucan synthesis in *A. nidulans*, we also C-terminal tagged AmyG with GFP. The AmyG-GFP was a functional strain (Fig. S2-6) and the signal evenly distributed in the cytoplasm of the hyphae and conidia (Fig. 2-6C), suggesting there was no obvious co-localization between AgsB and AmyG.

2.4.9. Alpha-1,3-glucan can be Immunolocalized Throughout the *A. nidulans* cell wall

To further explore the difference of AgsA-α-1,3-glucan and AgsB-α-1,3-glucan, we wondered if these two cell wall components could have different localization within the cell wall. We used immunogold-TEM to assess this. MOPC 104E was used to detect α-1,3-glucan. A purified mouse immunoglobulin (IgM: no target in fungal cell) and L10 (anti-galactofuranose) were used for negative and positive control. In wild type strains, α-1,3-glucan was mostly seen at the outer layer of the cell wall, but also at the inner layer (Fig.2-8). This showed α-1,3-glucan

presented throughout the *A. nidulans* cell wall without a noticeable pattern. In [*actA*(p)-*agsA*, *agsB*Δ] (only AgsA-α-1,3-glucan) and *agsA*Δ (only AgsB-α-1,3-glucan), similar patterns of α-1,3-glucan distribution were also found (Fig. 2-8). Although slightly more gold particles near the cell membrane were presented in [*actA*(p)-*agsA*, *agsB*Δ] strain, we did not think this revealed an essentially different distribution, especially considering α-1,3-glucan is a polymer (a long chain) instead of a single molecule. In addition, we found much more binding gold particle on wild type strain cell wall when using L10 (Fig. S2-8). However, galactofuranose is a less abundant component compared with α-1,3-glucan. So the number of gold particles was more affected by antibody affinity, than the abundance of particular cell wall components.

2.5. Discussion

We have presented a systematic investigation of four genes likely to be involved in *A. nidulans* α-1,3-glucan synthesis. These include α-1,3-glucan synthases AgsA and AgsB, and α-amylases AmyD and AmyG. All except AgsA are part of a conserved cluster in most *Aspergillus* species. Another protein, UGP1 (*A. nidulans* GalF; UTP-glucose-1-phosphate uridylyltransferase that synthesizes UDP-glucose monomers) has also been shown to be involved in α-1,3-glucan synthesis in *H. capsulatum* (Marion et al., 2006), consistent with a requirement for UDP-glucose. The *A. nidulans* UGP1 homologue (GalF) is essential (Alam and Kaminskyj, *unpublished data*). Since GalF function is upstream of the genes in this study and likely is not specific to this pathway, we considered it to be not directly relevant.

2.5.1. AgsA and AgsB Have Distinct Expression Profiles and Different Roles in *A. nidulans* Cell Walls

Previous studies have noted that *agsA* has a very low expression level compared to *agsB* (Fujioka et al., 2007; Futagami et al., 2011; Yoshimi et al., 2013). However, those studies did not consider the expression time-course of *agsA*. Using qPCR and GFP tagging, we found that *agsA* had a low expression at most life stages, but a high expression during conidiation. Since *agsB* also expressed at conidiation (Fig.S2-5), this raised the question: do *A. nidulans* conidia need extra α-1,3-glucan compared to vegetative hyphae, or, are the products of AgsA and AgsB are somehow different?

We overexpressed *agsA* in an *agsB*Δ background to see if it could compensate. Based on α-1,3-glucan quantification with the anthrone assay, overexpression of *agsA* more than compensated for the loss of *agsB,* so a full phenotype compensation of the *agsB*Δ defect was expected. Instead, only a slight recovery was seen for phenotypic defects in shaken liquid or on CFW-containing plates. Therefore the products of AgsA and AgsB appear to have different roles in *A. nidulans* cell walls. Despite this difference, we also showed that both synthases appear to be AmyG dependent. Combining the results that substantial amounts of AgsA-α-1,3-glucan and AgsB-α-1,3-glucan were both present in conidia but only the loss of AgsB reduced conidial adhesion, we concluded that AgsB-α-1,3-glucan was responsible for the conidia adhesion interaction. In addition, AgsB-α-1,3-glucan is also responsible for drug sensitivity. The biological function of AgsA-α-1,3-glucan is still unknown.

Distinct roles for AgsA-α-1,3-glucan and AgsB-α-1,3-glucan could relate to differences in wall localization or polymer-linkage. No side branches were found for α-1,3-glucan in *S. pombe* (Grün et al. 2005) and *A. wentii* (Choma et al., 2013), suggesting that different localization is more likely. Information from other fungal species did not show a consistent localization for α-1,3-glucan. In *H. capsulatum* (Rappleye et al., 2007) and *M. oryzae* (Fujikawa et al., 2012) α-1,3-glucan is suggested to be part of the outside wall layer. In *S. pombe* α-1,3-glucan is thought to be in the inner wall layer, as it appears to be deposited early in protoplast wall regeneration (Osumi, 2012). *S. pombe* α-1,3-glucan is also critical to secondary septum formation for cell separation (Cortes et al., 2012). In *A. fumigatus* two separate layers of α-1,3-glucan have been localized using immunogold transmission electron microscopy of hyphae grown in submerged

culture (Beauvais et al., 2007). Immunogold-TEM showed that α-1,3-glucan was found throughout the cell wall (Fig. 2-8), and no distinguishable distribution was seen for strains engineered to have only AgsA-α-1,3-glucan compared to only AgsB-α-1,3-glucan (Fig.2-8). Immunolocalization does not explain how the products of AgsA and AgsB are different. In addition, as we were not able to show the localization of AgsA and AgsB in a functional format, the difference between AgsA and AgsB needs further exploration.

Our other TEM and SEM results showed that α-1,3-glucan depletion did not significantly change the *A. nidulans* hyphal wall thickness. There was a minor difference in cell morphology (Fig. 2-4) suggesting α-1,3-glucan does not have an obvious role in hyphal cell wall construction in *A. nidulans*. But it is still too early to say α-1,3-glucan is dispensable (Henry et. al., 2012) because evidence has shown it is involved in host-pathogen recognition process (Rappleye et al. 2007; Fujikawa et al., 2012). We are planning to use functionalized AFM to examine α-1,3-glucan to study cell wall morphology, as per (Paul et al., 2011). These studies should lead to a better overall understanding of the function of α-1,3-glucan.

2.5.2. There is a Delay for α-1,3-glucan Deposition at the Tips

Immunofluorescence with the MOPC 104E monoclonal antibody showed that α-1,3-glucan was not detectable at hyphal tips (Fig. 2-5). This was unexpected, especially as AgsB-GFP was most abundant at growing tips (Fig. 2-7B and Cortés et al., 2012). Alpha-1,3-glucan is composed of glucose monomers that are later assembled into extended polymers of >100 subunits (Grün et al., 2005; Choma et al., 2013). To our knowledge the time-course for *in vitro* α-1,3-glucan

synthesis has not been estimated, however, the immunofluorescence distribution suggests it is delayed with respect to chitin and beta-glucan. In addition, the MOPC 104E antibody has a relatively low affinity at least for immunofluorescence (Hogan and Klein, 1994; Klein et al., 1997; Fujikawa et al. 2009; Wang, et al. 2009). Since α-1,3-glucan localization is first visualized in subapical regions, we expect that near-apical α-1,3-glucan is below the immunofluorescence detection threshold rather than being absent. Because our most definitive localizations were in cross-sections or glancing sections, we cannot be sure of where these were taken with respect to the hyphal tip. In addition, we have successfully stained the tips by using the same isotype antibody (L10 against galactofuranose; Alam et. al., 2012). So it is less likely we cannot reach α-1,3-glucan at those positions. However, the possibility that other materials blocked α-1,3-glucan from being detected at the tips still cannot be ruled out.

2.5.3. The AgsB C-terminal is Essential for Function

In our experiment, the C-terminal tagged AgsB-GFP strain had a phenotype resembling *agsB*Δ in shaken liquid (Fig. S2-6) and hypersensitivity on CFW containing medium (*data not shown*), suggesting it was unable to synthesize cell wall α-1,3-glucan. Grün et al. (2005) made the reasonable suggestion that the transmembrane domain formed a passage through the membrane to transport α-1,3-glucan from cytoplasm to cell wall right after synthesis. Hydropathy analysis (Fig. 2-1C) suggested that the AgsB C-terminal was the transmembrane domain, so it is possible that the C-terminal GFP was reducing channel function through steric hindrance. Nevertheless, we were able to find evidence of AgsB-GFP localization at the apical

cell membrane of growing hyphae. Recently, Cortes et al (2012) made thirteen separate N-terminal, C-terminal, and internal GFP-tagged constructs targeting the *S. pombe* Ags1 functional domains. Of these only one of the internal GFP-tagged strains was functional as assessed by phenotype rescue of the *ags1* deletion strain, and it revealed cell-membrane localization. So the GFP may block the transmembrane passage when it is tagged at the C-terminal.

2.5.4. AmyG is a Cytoplasmic Protein that May Not Interact Directly with AgsB

The only α-amylase that has been confirmed as a factor in α-1,3-glucan synthesis is AMY1 in *H. capsulatum* (Marion et al., 2006). Further work also showed the conserved role of this protein in *P. brasiliensis* (Camacho et al., 2012). In this study, we provided the first evidence that an α-amylase, AmyG, also has crucial function in *A. nidulans* α-1,3-glucan synthesis. Since AmyG is predicted to have neither a signal peptide nor a GPI-anchor site (de Groot et al., 2009), which is consistent with our AmyG-GFP tagging result, we conclude AmyG is a cytoplasmic protein, albeit one that is important for the synthesis of a cell wall component. Our overexpression studies revealed that the native expression level of *amyG* was only 10 % that of *agsB*, raising the question: how could AmyG efficiently serve for AgsB-mediated α-1,3-glucan synthesis?

Analysis of α-1,3-glucan showed that it contained non-reducing end α-1,4-glycosidic oligosaccharide thought to be the primer structure for α-1,3-glucan (Grün et al., 2005; Choma et al., 2013). In *S. pombe* this primer was shown to be synthesized by Ags itself (Vos et al. 2007).

In *H. capsulatum,* AMY1 (homologous to AmyG) is also suggested to be involved in synthesizing this primer (Marion et al., 2006). Hydropathy analysis of the putative Ags structure suggested that it has both extracellular and intracellular domains (Grün et al., 2005), which is also suggested by hydropathy analysis of AgsB (Fig. 2-1C). We hypothesized that AmyG synthesizes the primer structure and directly interacts with the intracellular fraction of Ags to efficiently facilitate the synthesis of α-1,3-glucan, meaning that they should co-localize. However our AmyG-GFP tagging result was inconsistent with this idea. Therefore a question remains: if AmyG is responsible for the primer structure, how is the primer delivered to Ags? In the future, protein interaction experiment (e.g. yeast two hybrid or TAP-tagging) will be needed to verify whether AmyG physically interacts with intracellular fraction of Ags. Moreover, enzymatic study will also be needed to find out the function of AmyG, and to clarify the primer structure for α-1,3-glucan synthesis.

2.5.5. AmyD Has a Repressive Effect for α-1,3-glucan; the Gene Cluster is not Properly Defined

Unlike AmyG, the AmyD sequence is predicted to have both a signal peptide and a GPI-anchor site (de Groot et al., 2009). In this study, we showed that AmyD has a clear repressive role on α-1,3-glucan synthesis: the *amyD*Δ strain had more α-1,3-glucan than wild type whereas the *actA*(p)-*amyD* strain had less. The expression of *amyD* was independently-regulated with respect to *agsB* and *amyG* (Fig. 2-2C). And the [*agsB*←→*amyG*, *amyD*] gene cluster is only found in most *Aspergillus* species, but not in other

fungi that also have α-1,3-glucan, such as *S. pombe, C. neoformans* and *H. capsulatum*. It is possible these three 'clustered' genes have roles apart from α-1,3-glucan synthesis.

Enzymatic study of AgtA, the homologue of AmyD in *A. niger*, has revealed its function as a glucanotransferase that acts on α-1,4-glycosidic bonds (van der Kaaij et al., 2007), however AgtA cannot hydrolyze α-1,3-glucan directly. In addition, three α-1,3-glucanases are found in *A. nidulans* genome (de Groot et al., 2009), which likely have roles in α-1,3-glucan degradation. Their homologue in *S. pombe*, Agn, is already shown to be able to hydrolyze α-1,3-glucan polysaccharide into α-1,3-glucan pentasaccharides (Dekker et al., 2004). Moreover, considering that *amyD* showed a high expression in the later life stage of *A. nidulans*, we hypothesize that AmyD might degrading the α-1,3-glucan primer, which is α-1,4-glycosidic linked. This primer structure may stabilize α-1,3-glucan *in vivo*. If the primer is degraded, this could lead to the degradation of α-1,3-glucan. Further experiments are needed to test this hypothesis.

2.5.6. Alpha-glucan Has Limited Ability to Mediate Drug Sensitivity

In our experiments, we found *A. nidulans* wall α-1,3-glucan content correlated with CFW sensitivity. Similar results have been shown in *A. niger* (Damveld et al., 2005) and *H. capsulatum* (Marion et al., 2006). In contrast, results in Yoshimi et al (2013) showed that α-1,3-glucan content did not correlate with sensitivity to CFW in *A. nidulans*. Yoshimi et al (2013) used low CFW concentrations (5 and 10 μg mL^{-1}) compared to our studies (30 μg mL^{-1}). Previous result in our lab showed that low concentration (≤10 μg mL^{-1}) CFW did not have inhibitory effect on wild type strain and even has beneficial effect on *ugmA*Δ strain (El-Ganiny et

al., 2008). This inconsistency is likely due to the CFW concentration used in these two assays. In addition, hypersensitivity to CR was not seen in our study but was reported in Yoshimi et al. (2013). We applied CR concentrations up to 200 μg mL^{-1} to our strains, however the growth inhibitory effect was the same at all CR concentrations (10, 50 and 100 μg mL^{-1} *data not shown*; 200 μg mL^{-1} see Fig.2-6). The difference could be related to the source of CR, which was not indicated in Yoshimi et al (2013). Based on our own results, we do not think α-1,3-glucan has the ability to regulate the sensitivity against CR.

In this study, we functionally characterized two *A. nidulans* α-1,3-glucan synthases (AgsA and AgsB) and two α-amylases (AmyD and AmyG) by deletion and overexpression. We showed that AgsB is the major α-1,3-glucan synthase at most of the life stages, whereas AgsA has a specific high expression level at conidiation. Nevertheless, loss of AgsB-α-1,3-glucan but not AgsA-α-1,3-glucan decreased conidial adhesion during germination in shaken liquid, and drug sensitivity against CFW. Intriguingly, overexpression of *agsA* in an *agsB*Δ background more than doubled α-1,3-glucan content, but only had a slight recovery effect on the *agsB*Δ phenotypic defects, indicating different roles of their products in cell wall. Immunolocalization did not show difference between these two polymers. Meanwhile, we found the gene cluster is not for efficient α-1,3-glucan synthesis. Although the crucial function of AmyG for α-1,3-glucan synthesis is proven for the first time in a filamentous fungus, AmyD clearly shows a repressive effect on α-1,3-glucan synthesis. Enzymatic studies will be needed to investigate the nature of each enzyme and in turns to reveal the synthesis process of α-1,3-glucan.

2.6. Acknowledgements

We are pleased to acknowledge support from the Natural Science and Engineering Council of Canada Discovery Grant program (SGWK), and the University of Saskatchewan (XSH). We thank Merck for the Caspofungin, and the Peta Bonham-Smith lab (Department of Biology, University of Saskatchewan) for access to qPCR, and also Robert Peace (Department of Mechanic Engineering, University of Saskatchewan) for help with SEM.

2.7. Tables

Table 2-1 Anthrone assay quantification of alpha-1,3-glucan in *Aspergillus nidulans* cell walls

Strain	Relative glucose (%) in alkaline soluble fraction (Mean ± SD)
A1149	100.0 ± 6.0
*agsA*Δ	94.3 ± 8.5
*agsB*Δ	3.1 ± 0.6
*agsA*Δ, *agsB*Δ	1.2 ± 1.0
*amyD*Δ	152.5 ± 13.5
*amyG*Δ	12.7 ± 0.9
clusterΔ	2.9±0.9
actA(p)-*agsA*	211.5±28.0
actA(p)-*agsB*	291.0 ± 25.7
actA(p)-*amyD*	56.3 ± 4.0
actA(p)-*amyG*	127.7 ± 4.2
actA(p)-*agsA, agsB*Δ	227.8 ± 17.7
actA(p)-*agsA, amyG*Δ	19.0±6.3

Results represent the average from three independent experiments with duplicates each time ± standard deviation

Table 2-2 qPCR results for overexpression strains

Strain	Relative expression of actin-promoter regulated genes compared to wild type (100 %)
actA(p)-*agsB*	179% ± 18%
actA(p)-*amyD*	230% ± 25%
actA(p)-*amyG*	1803% ± 368%
actA(p)-*agsA, agsB*Δ	12367% ± 2434%

Results represent the average of three independent qPCR tests with triplicates each time ± standard deviation

Table 2-3 *Aspergillus nidulans* strains in this study

Strains	**alias**	**Genotype**	**Origin**
A1149	A1149	*pyrG89*; *pyroA4*; *nkuA*::*argB*	FGSC
*agsA*Δ	AXH11	*AN5885*::*AfpyrG*; *pyrG89*; *pyroA4*; *nkuA*::*argB*	this study
*agsB*Δ	AXH1	*AN3307*::*AfpyrG*; *pyrG89*; *pyroA4*; *nkuA*::*argB*	this study
*agsA*Δ, *agsB*Δ	AXH21	*AN5885*::*AFpyroA*; *AN3307*::*AfpyrG*; *pyrG89*; *pyroA4*; *nkuA*::*argB*	this study
*amyD*Δ	AXH2	*AN3308*::*AfpyrG*; *pyrG89*; *pyroA4*; *nkuA*::*argB*	this study
*amyG*Δ	AXH3	*AN3309*::*AfpyrG*; *pyrG89*; *pyroA4*; *nkuA*::*argB*	this study
clusterΔ	AXH12	*AN3307, AN3308, AN3309*::*AfpyrG*; *pyrG89*; *pyroA4*; *nkuA*::*argB*	this study
actA(p)-*agsB*	AXH17	*agsB*p::*AfpyrG*:*actA*p:*agsB*; *pyrG89*; *pyroA4*; *nkuA*::*argB*	this study
actA(p)-*amyD*	AXH38	*amyD*p:: *AfpyroA*:*actA*p:*amyD*; *pyrG89*; *pyroA4*; *nkuA*::*argB*	this study
actA(p)-*amyG*	AXH36	*amyG*p::*AfpyroA*:*actA*p:amyG; *pyrG89*; *pyroA4*; *nkuA*::*argB*	this study
agsA(p)-GFP-*actA*(p)-*agsA*	AXH30	*agsA*p::*agsA*p:*gfp*:*AfpyroA*:*actA*p:*agsA*; *pyrG89*; *pyroA4*; *nkuA*::*argB*	this study
actA(p)-*agsA*, *agsB*Δ	AXH23	*agsA*p:: *agsA*p:*gfp*:*AfpyroA*:*actA*p:*agsA*; *AN3307*::*AfpyrG*; *pyrG89*; *pyroA4*; *nkuA*::*argB*	this study
actA(p)-*agsA*, *amyG*Δ	AXH41	*agsA*p:: *agsA*p:*gfp*:*AfpyroA*:*actA*p:*agsA*; *AN3309*::*AfpyrG*; *pyrG89*; *pyroA4*; *nkuA*::*argB*	this study
agsB-GFP	AXH15	*agsB*::*agsB*:*gfp*:*AfpyrG*; *pyrG89*; *pyroA4*; *nkuA*::*argB*	this study
amyG-GFP	AXH33	*amyG*p:*amyG*:: *AfpyroA*:*actA*p:*amyG*:*gfp*:*AfpyrG* ; *pyrG89*; *pyroA4*; *nkuA*::*argB*	this study
Mating strain	AXM20	*nicB; wA2*	this study

2.8. Figures

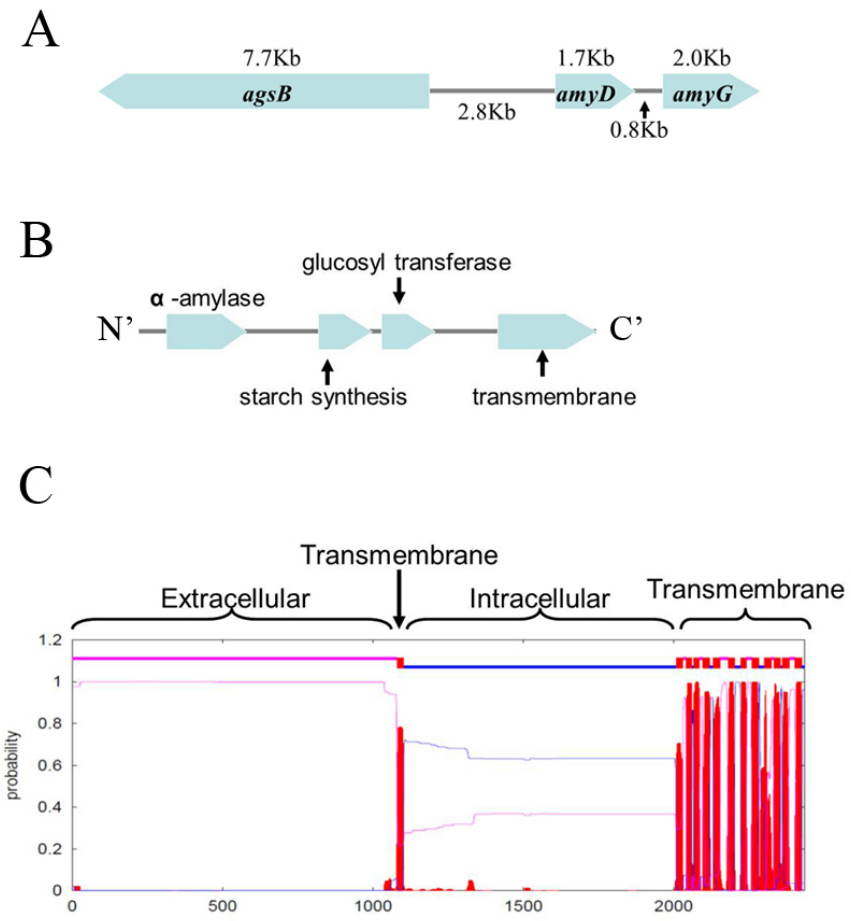

Fig. 2-1 Sequence analysis of Ags and the alpha-1,3-glucan synthase gene cluster

A. *agsB* and *amyD-amyG* are on different strands and transcribed in opposite directions

B. Domains predicted for alpha-1,3-glucan synthase are an α-amylase domain, a single transmembrane-span, a starch synthase catalytic domain, a glycosyl transferase domain and a multiple-transmembrane domain. Information was collected from Broad Institute.

C. Hydropathy prediction of AgsB revealed an extracellular fraction at the N-terminal, an intracellular fraction and a mutiple-transmembrane domain at C-terminal. AgsA had a very similar prediction result (*data not shown*). Hydropathy prediction was done by TMHMM 2.0 web-server.

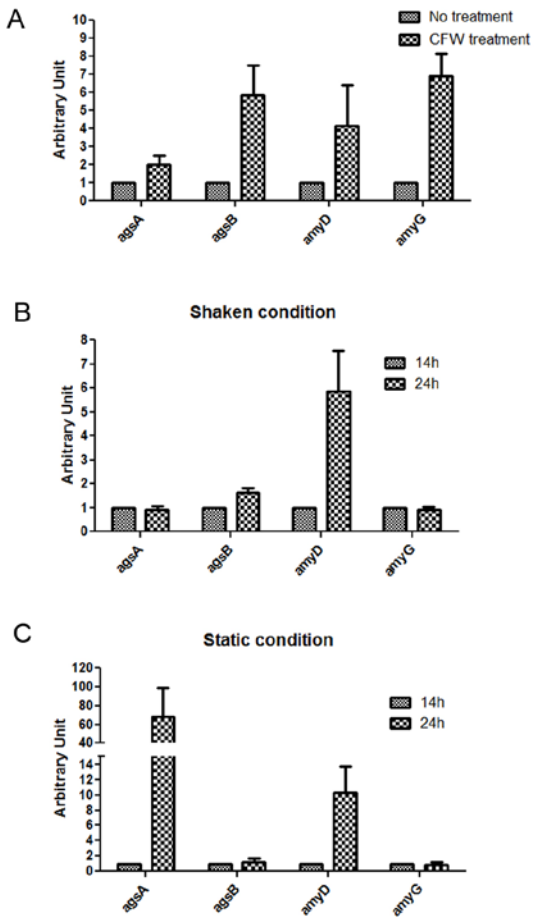

Fig. 2-2 qPCR examination of the expression of *agsA*, *agsB*, *amyD* and *amyG*

In each test $2x10^7$ spores of wild type strain were inoculated 20 mL complete medium in designed condition. Results represent the average of three independent qPCR tests with triplicates each time ± standard deviation

A. No treatment group was grown in flask at 30 °C with 150rpm for 14h; CFW treatment group was grown at the same condition except CFW was added to the medium at the last hour at a concentration of 50 μg mL^{-1}. No treatment group was used as control.

B. All groups were grown in flask at 30 °C with 150rpm for 14h or 24h as designed. 14 h group was used as control.

C. All groups were grown in petri dish at 30 °C with 150rpm for 14h or 24h as designed. Only the mycelia mat at the surface was collected for RNA extraction. 14 h group was used as control.

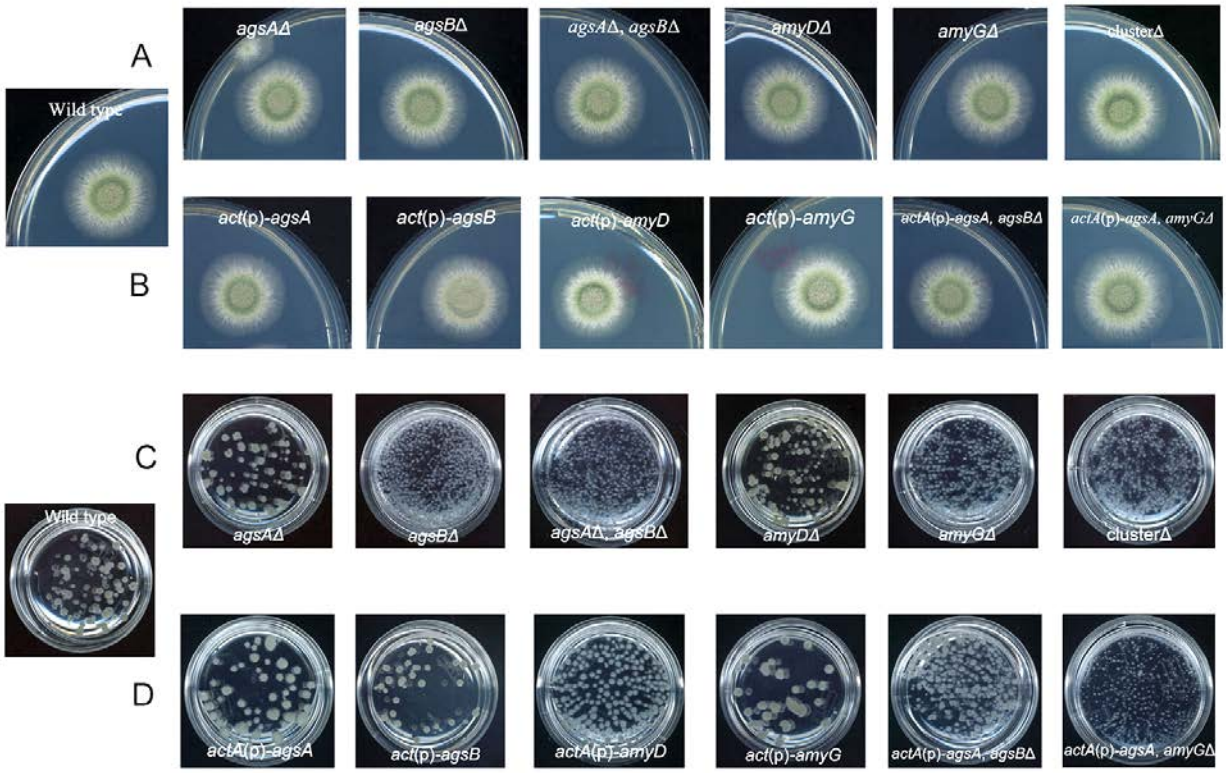

Fig. 2-3 Phenotypes of wild type and all constructed strains on solid medium and in shaken liquid medium

A. 10^5 freshly harvested conidia of each deletion strain were inoculated on the complete medium and the plates were incubated at 30 °C for 48 h. All constructed strains showed the wild type colony phenotype on solid medium.

B. 10^5 freshly harvested conidia of each overexpression strain were inoculated on the complete medium and the plates were incubated at 30 °C for 48 h. Only *actA*(p)-*agsB* showed a moderate reduction in conidiation.

C. $5x10^7$ freshly harvested conidia were inoculated in 20 mL complete medium, incubated at 30 °C, 150 r.p.m., overnight. In deletion strain group, *agsB*Δ, [*agsA*Δ, *agsB*Δ] and *amyG* Δ formed many tiny colonies compared to a few large colonies in wild type. These same deletion strains had dramatically reduced wall α-1,3-glucan.

D. $5x10^7$ freshly harvested conidia were inoculated in 20 mL complete medium, incubated at 30 °C, 150 r.p.m., overnight. In overexpression strain group, *actA*(p)-*amyD* resembled the phenotype as *agsB*Δ strain, but the colony sizes were visibly bigger. This is consistent with the anthrone result that wall α-1,3-glucan reduction is not as much as *agsB*Δ strain. The [*actA*(p)-*agsA, agsB*Δ] strain also had a similar phenotype as *agsB*Δ strain, suggesting overexpression of *agsA* cannot compensate for the loss of *agsB.*

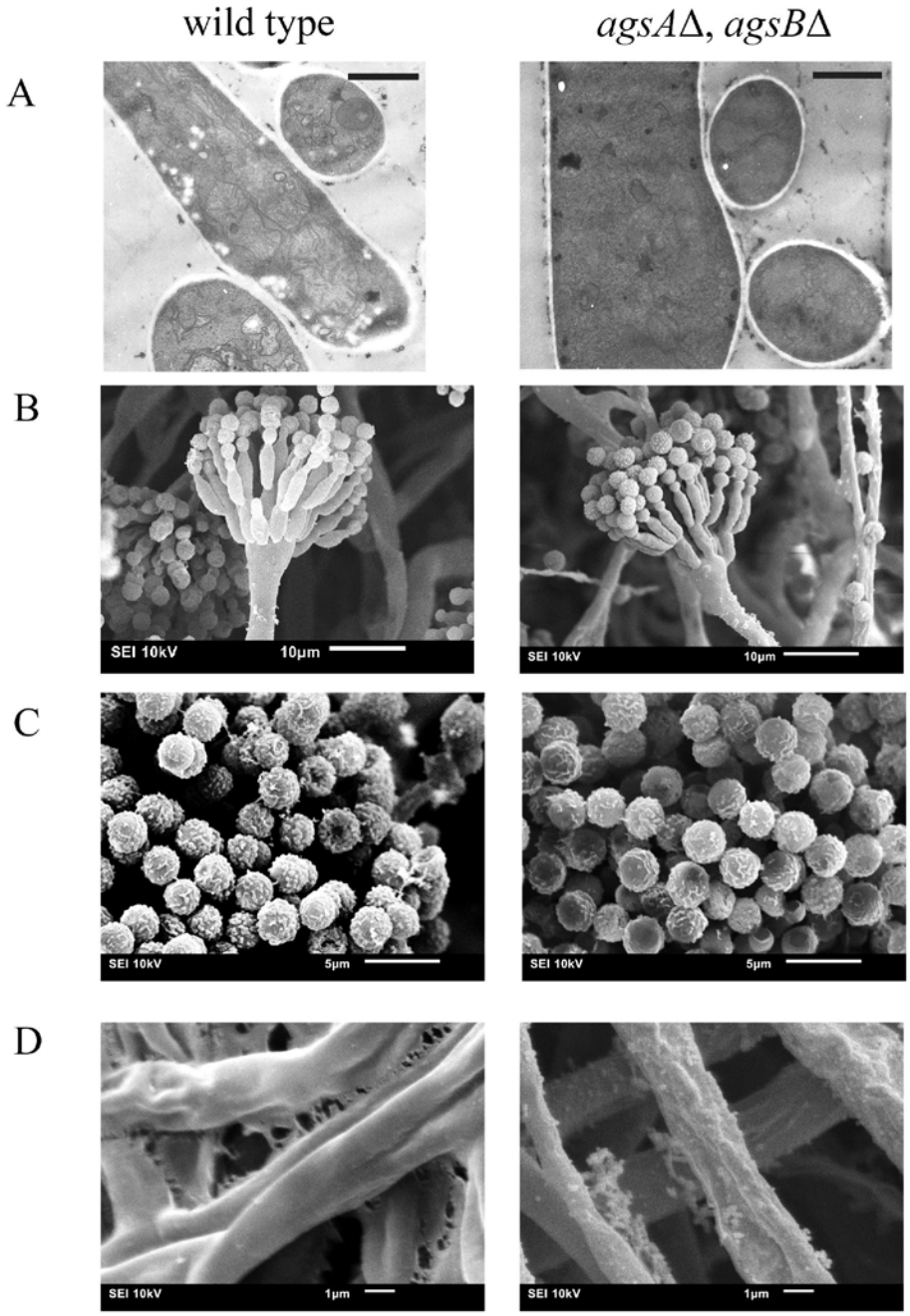

Fig. 2-4 TEM and SEM examination of the wild type strain and the [*agsA*Δ, *agsB*Δ] strain

A. Samples were grown on dialysis tubing at 30 °C for 48 h. 75nm thin sections were used for TEM imaging. Scale bar = 1μm

For SEM, samples were grown on dialysis tubing at 30 °C for 48 h. Conidiaphore, conidia and hyphae were shown in **B**, **C** and **D** respectively.

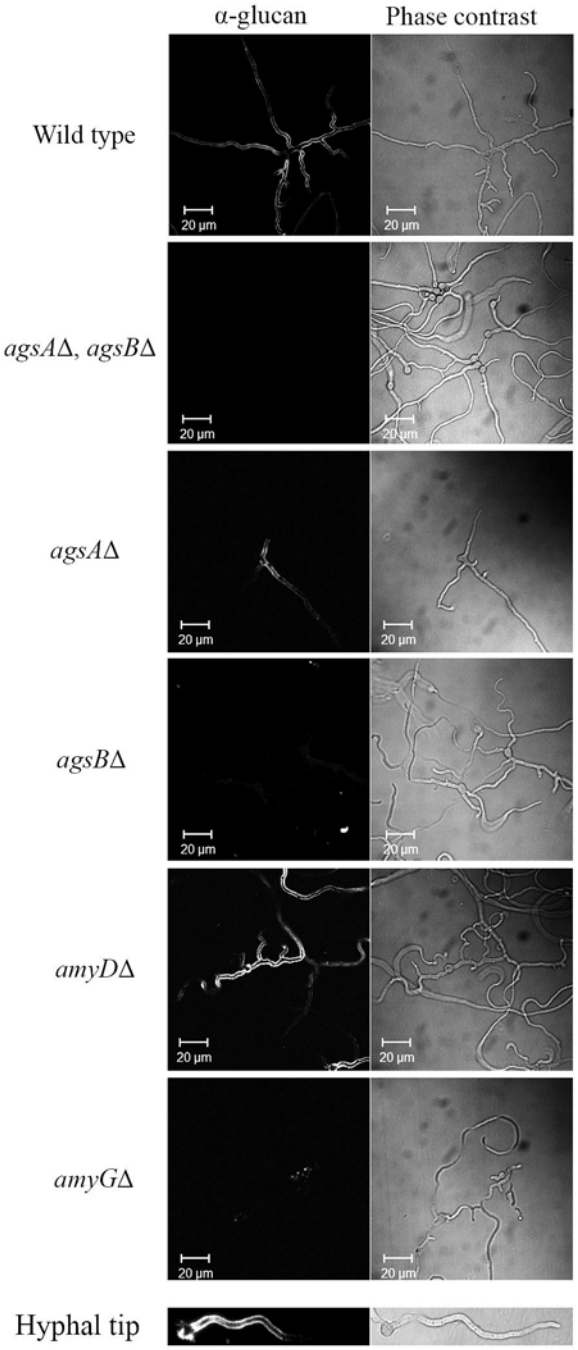

Fig. 2-5 MOPC 104E antibody immunofluorescent staining of wild type and deletion strains

Germlings grew overnight on dialysis tubing at 30ºC. Hyphal tip was from a wild type strain and was shown for the gradual decrease of antibody staining.

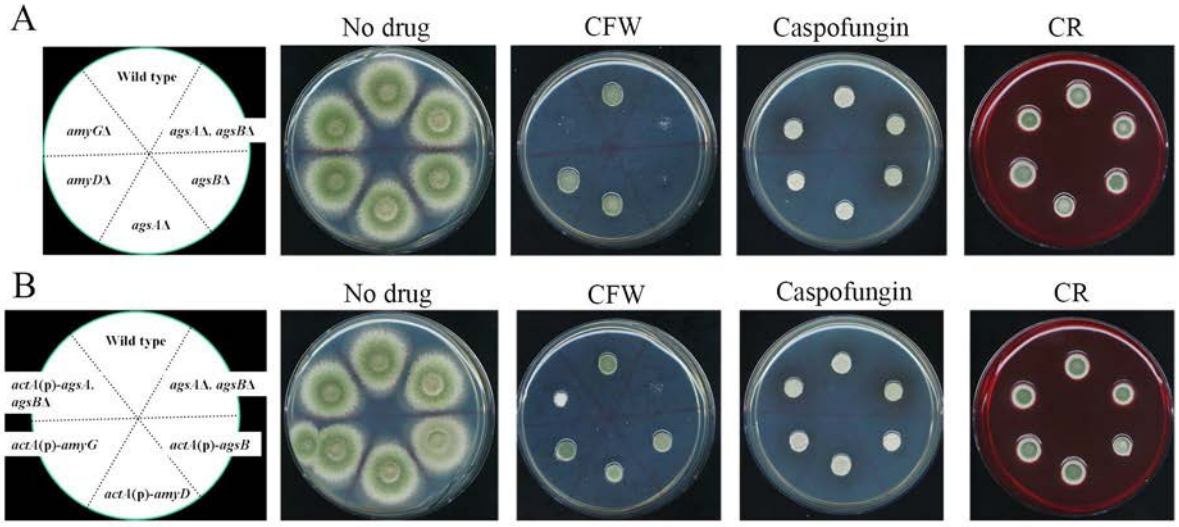

Fig. 2-6 Drug sensitivity test of constructed strains. For each strain, 10^5 conidia were inoculated on plates and incubated for 72 h at 30 ºC.

A. All deletion strains had wild type phenotype on solid medium when not challenged by anti-fungal agent. The *agsB*Δ, [*agsA*Δ, *agsB*Δ] and *amyG*Δ strains were hypersensitive to Calcofluor White (30 μg mL^{-1}), but all strains maintained comparable sensitivity against Caspofungin (10 μg mL^{-1}) and Congo Red (200 μg mL^{-1}).

B. Overexpression strains were selected to test their drug sensitivity on Calcofluor White (30 μg mL^{-1}), Caspofungin (10 μg mL^{-1}) and Congo Red (200 μg mL^{-1}). [*agsA*Δ, *agsB*Δ] was used as a negative control. Overexpression of *agsB*, *amyD* and *amyG* did not have a noticeable effect on drug sensitivity against Calcofluor White, and overexpression of *agsA* in an *agsB*Δ background [*actA*(p)-*agsA*, *agsB*Δ] can only slightly recover the hypersensitivity. All tested strains still had comparable sensitivity against Caspofungin and Congo Red.

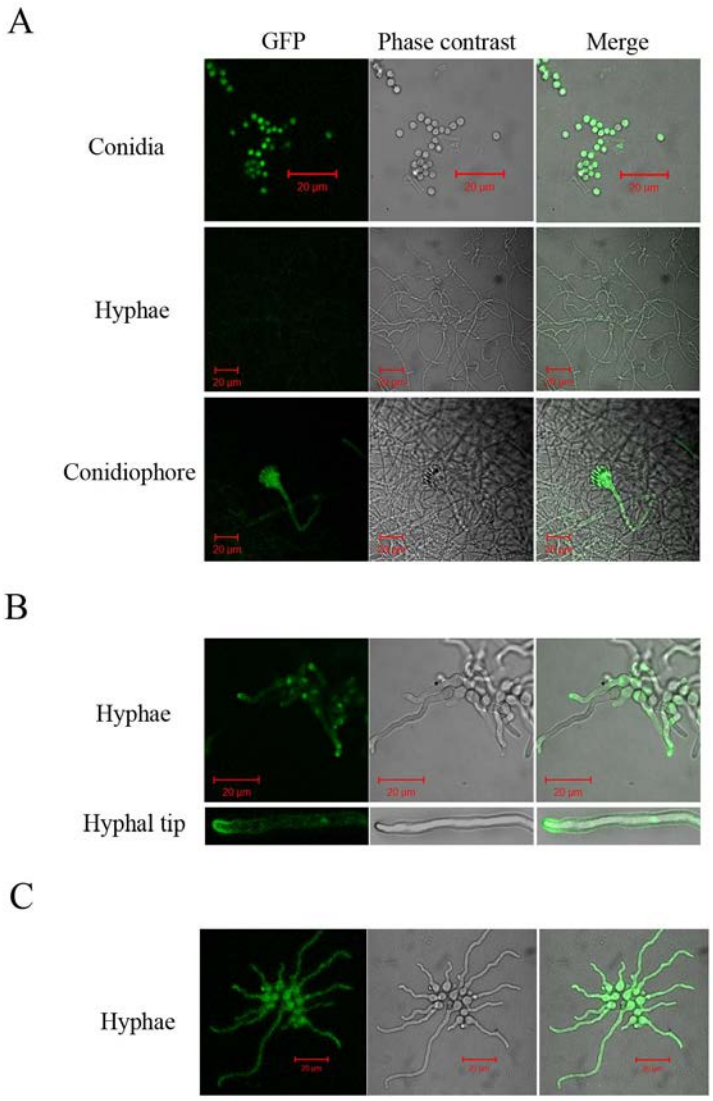

Fig. 2-7 Fluorescence examination of *agsA*(p)-GFP, AgsB-GFP and AmyG-GFP strains

A. Samples at different life stages were prepared of *agsA*(p)-GFP strain to visualize the expression profile of *agsA*. The GFP signal was seen in conidia, foot cell, conidiophores, metulae and phialides, which are all involved in conidiation, but not in vegetative hyphae. Therefore *agsA* has a specific high expression during conidiation.

B, GFP signal for the AgsB-GFP strain can be seen along the hypha, but mainly concentrated in tips (top panel). Magnified view revealed the signal is come from the membrane.

C. Signal of the AmyG-GFP strain was evenly distributed in hyphae and conidia, suggesting a cytoplasmic localization.

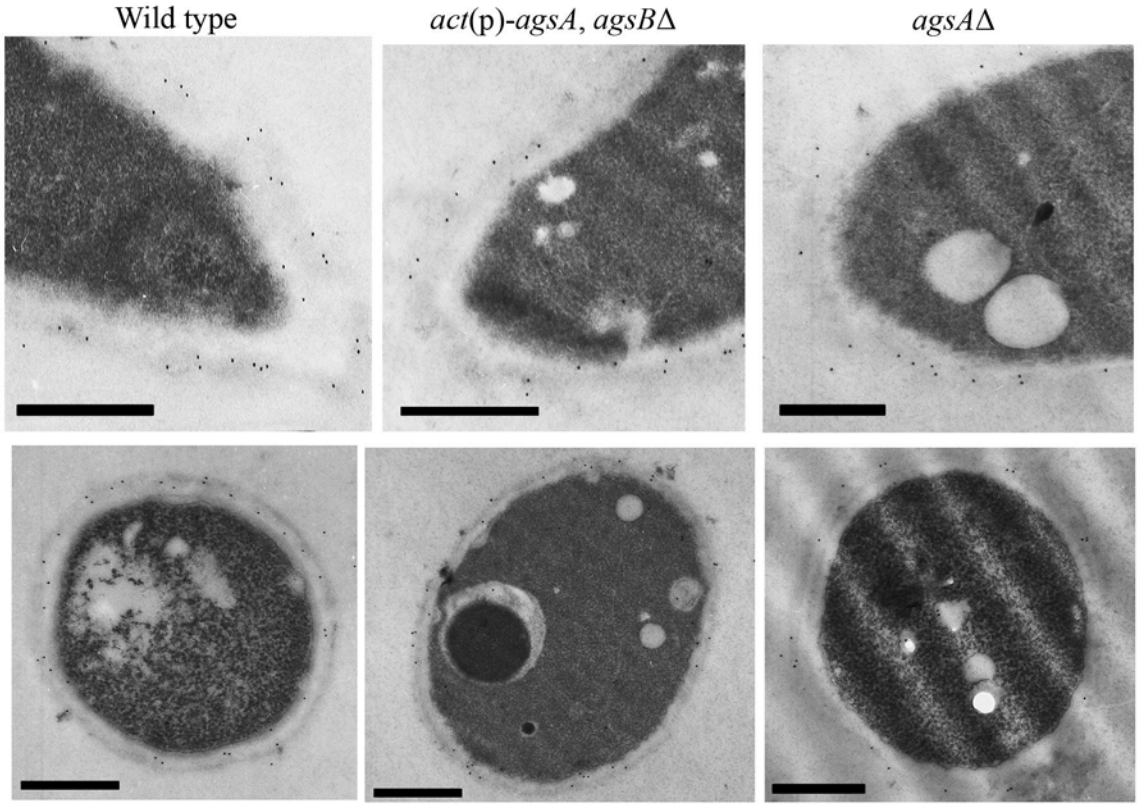

Fig. 2-8 Alpha-1,3-glucan distribution in wild type, [*actA*(p)-*agsA*, *agsB*Δ] and *agsA*Δ strains. All scale bar = 500 nm.

All samples were grown in shaken liquid medium for 16 h, fixed and then embedded in LR White. We used 70-90 nm sections for antibody (MOPC 104E followed by 12nm-gold labeled goat anti mouse) straining.

2.9. Supplemental Materials

Table S2-1 Primers and plasmids in this study

Primers	Sequence 5' to 3'	Description
Selective marker and strain confirmation		
AME1	ATGTCGTCCAAGTCGCAATT	Af*pyrG**
AME2	TCATGACTATGCCGCATACTAC	Af*pyrG**
SE231	GGACATCAGATGCTGGATTACTAAAG	Af*pyroA* with native promoter
SE232	TTACCATCCTCTCTTGGCCA	Af*pyroA* with native promoter
AME7	CAATACCGTCCAGAAGCAATAC	Af*pyrG* confirmation*
AME8	CACATCCGACTAGCACTATCC	Af*pyrG* confirmation*
AME15	ATTCCTGTCATGGCCAAAG	Af*pyroA* confirmation*
AME16	TCAACAACATCTCCGGTACC	Af*pyroA* confirmation*
Gene deletion		
SE77	CATACAAAAATCCATGGACCG	*agsB* upstream F
SE78	AATTGCGACTATGGACGACATACTAGATGAAGCGAGAACGAG	*agsB* upstream R (pyrG tail)
SE79	GAGTATGCGGCAAGTCATGAGGCTTAGCAACCGTAGTTTGG	*agsB* downstream F (pyrG tail)
SE80	CTGGATTAAACATGAGAGGGAGA	*agsB* downstream R
SE81	AGCAAACGATTTTCAGGGTC	*agsB* Fusion F
SE82	AGCAACCCAAACGCTACG	*agsB* Fusion R
SE191	TACGTTAAAGGCTCGCCC	*A.nidulans actA*(p) F
SE190	AATTGCGACTATGGACGACATGGTGTTTAGGGGTGGATTAGAA	*A.nidulans actA*(p) R (pyrG tail)
SE85	TAGACGAGGAACATTTACCGG	*agsA* upstream F
SE197	GGGCGAGCCTTTAACGTAGGTCGATTTTTCCGGATGT	*agsA* upstream R (*actA*(p) tail)
SE87	GAGTATGCGGCAAGTCATGACAACTAAAAGGCTACGCTTTGGT	*agsA* downstream F (pyrG tail)
SE88	AAGTTCACAACCCTCAAGGG	*agsA* downstream R
SE89	GGCTTGTAGACTAGGAATGGTATCT	*agsA* Fusion F
SE90	GGTCTTGGCTCTGCTCTCTTC	*agsA* Fusion R
SE242	CTTAGTAATCCAGCATCTGATGTCCGGTCGATTTTTCCGGATGT	*agsA* upstream R (pyroA tail)
SE99	TGGCCAAGAGAGGATGGTAACAACTAAAAGGCTACGCTTTGGT	*agsA* downstream F (pyroA tail)
SE103	CGGCCATTGACCATGAAC	*amyD* upstream F
SE104	AATTGCGACTATGGACGACATTGTGACGATGTCTGGACCG	*amyD* upstream R (pyrG tail)
SE105	GAGTATGCGGCAAGTCATGATTTGATCTGTTTTCATCTTTTTGC	*amyD* downstream F (pyrG tail)
SE106	GTCATAGATGTCATACCCGTTTCC	*amyD* downstream R
SE107	GTCTTCATCCGGTCCACTATC	*amyD* Fusion F
SE108	GAAGATGAGGGTGTTGTCG	*amyD* Fusion R

SE111	CGGATGTGTTGCACTAGTGTT	*amyG* upstream F
SE112	AATTGCGACTATGGACGACATGTTCTCCTGGGGGCAGAC	*amyG* upstream R (pyrG tail)
SE113	GAGTATGCGGCAAGTCATGA GAAGCCAGAGACGCAAATAGA	*amyG* downstream F (pyrG tail)
SE114	GCAAATCGACTAGGGACTAGA	*amyG* downstream R
SE115	CAGACCTGATGGAAGGAAGTG	*amyG* Fusion F
SE116	TCAGAGTCTGCTTCCGTGACTA	*amyG* Fusion R
SE134	AATTGCGACTTGGACGACATGAAGCCAGAGACGCAAATAGA	Cluster deletion (pair with SE114)
Promoter exchange and GFP tagging		
SE207	GAGTATGCGGCAAGTCATGATACGTTAAAGGCTCGCCC	*actA*(p) F (pyrG tail)
SE209	TTCTAATCCACCCCTAAACACCATGGGGAGGCTCCAGCTC	*agsB* F (*actA*(p) tail)
SE143	GATAGACCCAAAAGTATTGCCTCC	*agsB*_1210 R
SE144	AGGCAATGATCATGCATGTG	*actA*(p)-*agsB* Fusion R
SE233	CTTAGTAATCCAGCATCTGATGTCCTGTGACGATGTCTGGACCG	*amyD* upstream R (pyroA tail)
SE234	TGGCCAAGAGAGGATGGTAATACGTTAAAGGCTCGCCC	*actA*(p) F (pyroA tail)
SE208	GGTGTTTAGGGGTGGATTAGAA	*actA*(p) R
SE235	TTCTAATCCACCCCTAAACACCATGAAAATCCTCCCATCCTTG	*amyD* F (*actA*(p) tail)
SE236	CATCATTGAAGCTCGGCAC	*amyD*_1000 R
SE237	CCTTGGGTAAAGGCGTCC	*actA*(p)-*amyD* Fusion R
SE238	CTTAGTAATCCAGCATCTGATGTCCGTTCTCCTGGGGGCAGAC	*amyG* upstream R (pyroA tail)
SE239	TTCTAATCCACCCCTAAACACCATGTTGTCGCTCCTAACATGC	*amyG* F (*actA*(p) tail)
SE240	CGAGAGGAACATCATACGCC	*amyG*_1095 R
SE241	CTCCCCTATAATATAGAACCCCG	*actA*(p)-*amyG* Fusion R
SE276	ATGAGTAAAGGAGAAGAACTATTTCACTAGG	GFP F
SE277	CTTAGTAATCCAGCATCTGATGTCCCCCGCGAAGAGGGTGAAGA	GFP R (pyroA tail)
SE278	CCAGTGAAAAGTTCTTCTCCTTTACTACATGGTCGATTTTTCCGGATGT	*agsA* upstream R (GFP tail)
SE243	TTCTAATCCACCCCTAAACACCATGAGGTGGAGGCCTTTAAAC	*agsA* F (*actA*(p) tail)
SE146	ATTGGTTGGGCTGTCTTCC	*agsA*_1200 R
SE147	CACACTACACGATAAGCACTACG	*actA*(p)-*agsA* Fusion R
AME27	GGAGCTGGTGCAGGC	GFP-pyrG construct F*
AME28	TCATGACTATGCCGCATACTA	GFP-pyrG construct R*
SE148	GCCGAGAAACTAGTACGGAAT	*agsB*_6300 F
SE149	CTCCAGCGCCTGCACCAGCTCCAGGCTTCGCAAGTTGCTC	*agsB* R (GFP tail)
SE150	GTATGGAATTGCGTTCCTCTTC	*agsB*-GFP Fusion F
SE217	GTACTAGGACTAGCCAATATACGG	*amyG*_1034 F
SE218	GCCTGCACCAGCTCCGATAGCGTGGTAAATGTTCACATC	*amyG* R (GFP tail)
SE219	GCTGATCTGAGGCGGATATT	*amyG*-GFP Fusion F

qPCR		
SE244	CACCCGGACACTAGGTATCTC	Histone qPCR F#
SE245	GAATACTATCGTAACGGCCTTGG	Histone qPCR R#
SE246	ATCGGACACTAACCTTCCCTG	*agsB* qPCR F#
SE247	GACTATGGCTGACGATCAACG	*agsB* qPCR R#
SE248	GCTTTCCAAATCCCACAGTTGG	*agsA* qPCR F#
SE249	GTGAAGCAGATATGCATCCGTG	*agsA* qPCR R#
SE153	GGATGGAGATGACCCTGCTA	*amyD* qPCR F
SE154	TGCGCATCATGGTAGTCATT	*amyD* qPCR R
SE155	CGCAATCAGGACAAATGATG	*amyG* qPCR F
SE156	ATTCGGATGCTTAACGTTGG	*amyG* qPCR R

#, Fujioka et al. (2007)

*, Alam et al. (2012)

Table S2-2 Conidiation of wild type and *actA*(p)-*agsB*

Medium	**CM**		**MM**	
Strains	Wild type	*actA*(p)-*agsB*	Wild type	*actA*(p)-*agsB*
Conidiation	100% ± 16%	60% ± 7%	100% ± 9%	73% ± 6%

10^5 conidia were grown on 1.5mL medium in 24-well plate at 30 °C for 4 d. 1 mL ddH_2O was used to collect conidia from each well. Conidia were quantified by hemocytometer. Results represent the average of three independent quantification tests with triplicates each time ± standard deviation

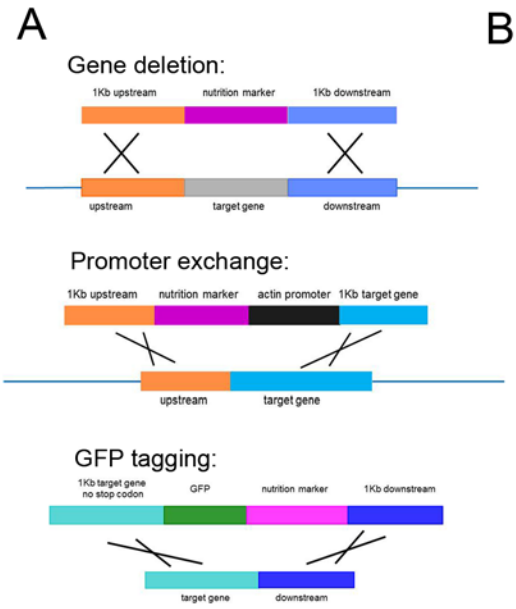

B

PCR construct of each strain and primer used in each reaction:

agsBΔ:	
1Kb agsB upstream + AfpyrG + 1Kb agsB downstream (SE77+SE78) (AME1+AME2) (SE79+SE80)	Fusion PCR: SE81+SE82
agsAΔ:	
1Kb agsA upstream + actA(p)+ AfpyrG + 1Kb agsB downstream (SE85+SE197) (SE190+SE191) (AME1+AME2) (SE87+SE88)	Fusion PCR: SE89+SE90
agsAΔ, agsBΔ:	
1Kb agsB upstream + AfpyrG + 1Kb agsB downstream (SE77+SE78) (AME1+AME2) (SE79+SE80)	Fusion PCR: SE81+SE82
1Kb agsA upstream + AfpyroA + 1Kb agsA downstream (SE85+SE242) (SE231+SE232) (Sep99+SE88)	Fusion PCR: SE89+SE90
amyDΔ:	
1Kb amyD upstream + AfpyrG + 1Kb amyD downstream (SE103+SE104) (AME1+AME2) (SE105+SE106)	Fusion PCR: SE107+SE108
amyGΔ:	
1Kb amyG upstream + AfpyrG + 1Kb amyG downstream (SE111+SE112) (AME1+AME2) (SE113+SE114)	Fusion PCR: SE115+SE116
cluster Δ	
1Kb amyG downstream + actA(p)+ AfpyrG + 1Kb agsB downstream (SE114+SE134) (SE190+SE191) (AME1+AME2) (SE79+SE80)	*Fusion PCR: SE82+SE116*
actA(p)-*agsB*:	
1Kb agsB upstream + AfpyrG + actA(p) + 1Kb agsB (SE77+SE78) (AME1+AME2) (SE207+SE208) (SE209+SE143)	Fusion PCR: SE81+SE144
actA(p)-*amyD*:	
1Kb amyD upstream + AfpyroA + actA(p) + 1Kb amyD (SE103+SE233) (SE231+SE232) (SE207+SE208) (SE235+SE236)	Fusion PCR: SE107+SE237
actA(p)-*amyG*:	
1Kb amyG upstream + AfpyroA + actA(p) + 1Kb amyG (SE111+SE238) (SE231+SE232) (SE207+SE208) (SE240+SE241)	Fusion PCR: SE115+SE242
agsA(p)-GFP- *actA*(p)-*agsA*:	
1Kb agsA upstream + GFP + AfpyroA + actA(p)+ 1Kb agsA (SE85+SE278) (SE276+SE277) (SE231+SE232) (E207+SE208)(SE243+SE146)	Fusion PCR: SE89+SE147
actA(p)-*agsA*, *agsBΔ*:	
1Kb agsB upstream + AfpyrG + 1Kb agsB downstream (SE77+SE78) (AME1+AME2) (SE79+SE80)	Fusion PCR: SE81+SE82
1Kb agsA upstream + GFP + AfpyroA + actA(p)+ 1Kb agsA (SE85+SE278) (SE276+SE277) (SE231+SE232) (E207+SE208)(SE243+SE146)	Fusion PCR: SE89+SE147
actA(p)-agsA, amyGΔ:	
1Kb amyG upstream + AfpyrG + 1Kb amyG downstream (SE111+SE112) (AME1+AME2) (SE113+SE114)	*Fusion PCR: SE115+SE116*
1Kb agsA upstream + GFP + AfpyroA + actA(p)+ 1Kb agsA (SE85+SE278) (SE276+SE277) (SE231+SE232) (E207+SE208)(SE243+SE146)	*Fusion PCR: SE89+SE147*
agsB-GFP:	
1Kb agsB + GFP-AfpyrG + 1Kb agsB downstream (SE148+SE149)(AME27+AME28) (SE79+SE80)	Fusion PCR: SE150+SE82
amyG-GFP:	
1Kb amyG upstream + AfpyroA + actA(p) + 1Kb amyG (SE111+SE238) (SE231+SE232) (SE207+SE208) (SE240+SE241)	Fusion PCR: SE115+SE242
1Kb amyG + GFP-AfpyrG + 1Kb amyG downstream (SE217+SE218)(AME27+AME28) (SE113+SE114)	Fusion PCR: SE219+SE116

Fig. S2-1 Deletion, promoter exchange and GFP-tagging schema and PCR constructs of each strain

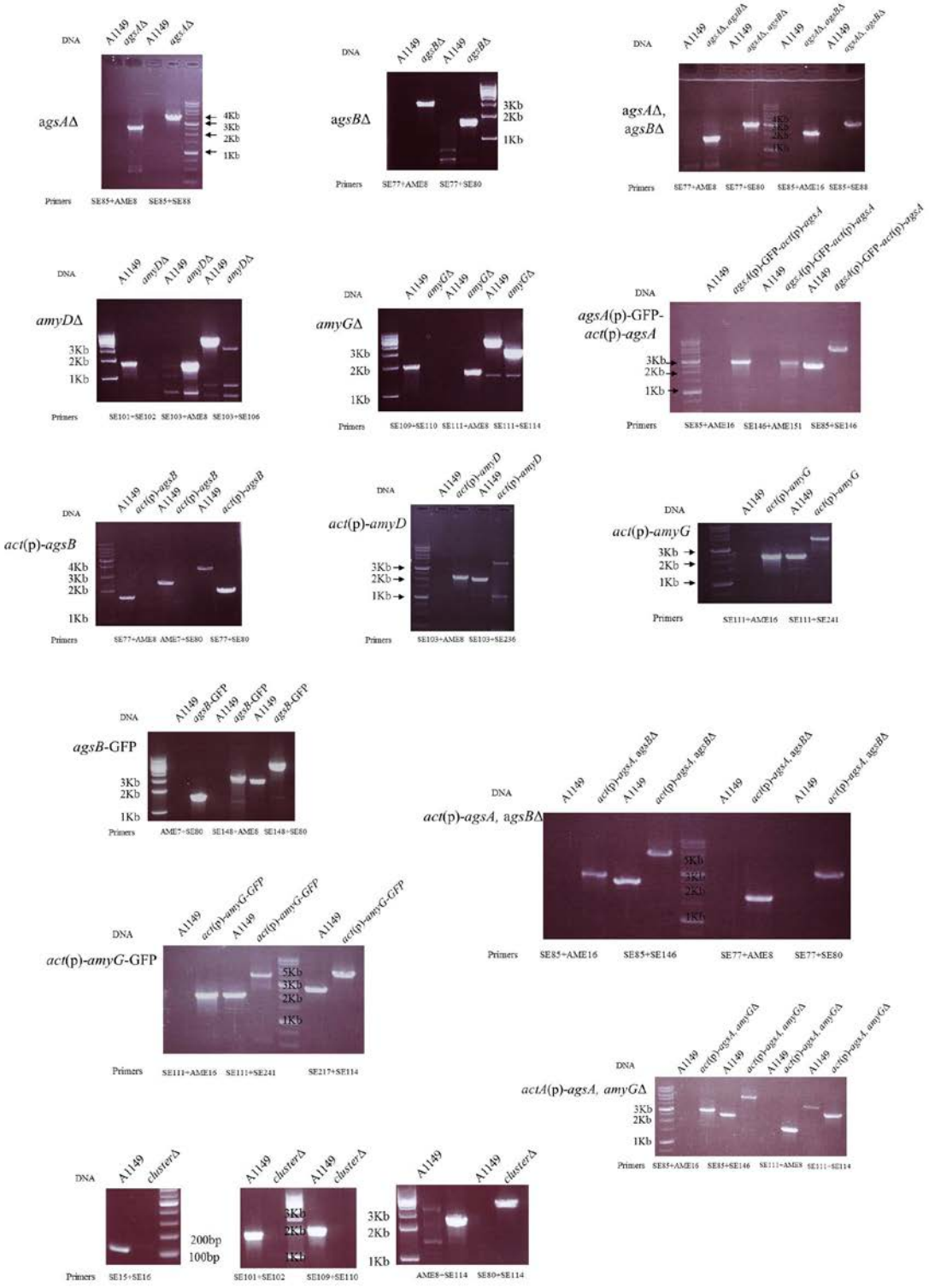

Fig. S2-2 PCR confirmation of all constructed strains. Strains labeled at right of each gel picture. Primers are indicated at the bottom and DNA templates are on the top.

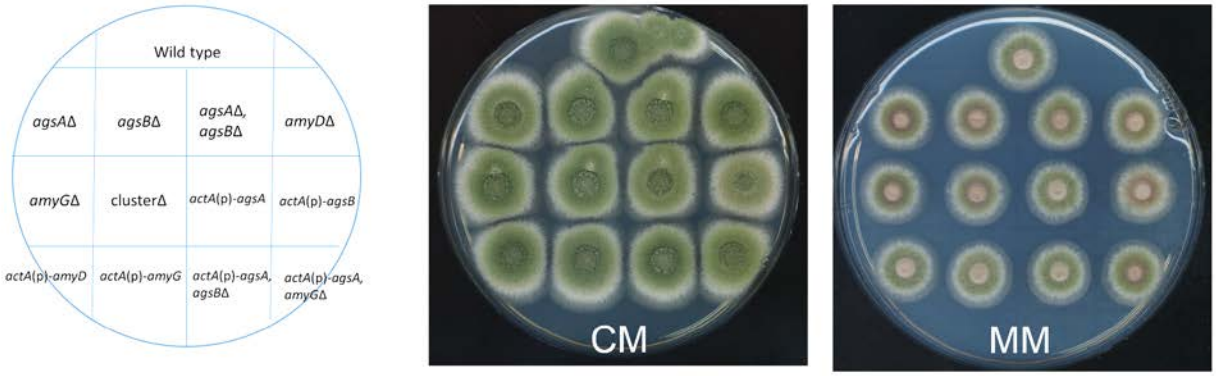

Fig. S2-3 Phenotype of all strains on CM and MM plates. 10^5 conidia of each strain were inoculated on CM and MM plates and incubated at 30 °C for 72 h. All strains showed a similar phenotype as wild type on both CM and MM. Only a moderate conidiation reduction was seen for *actA*(p)-*agsB* on both plates.

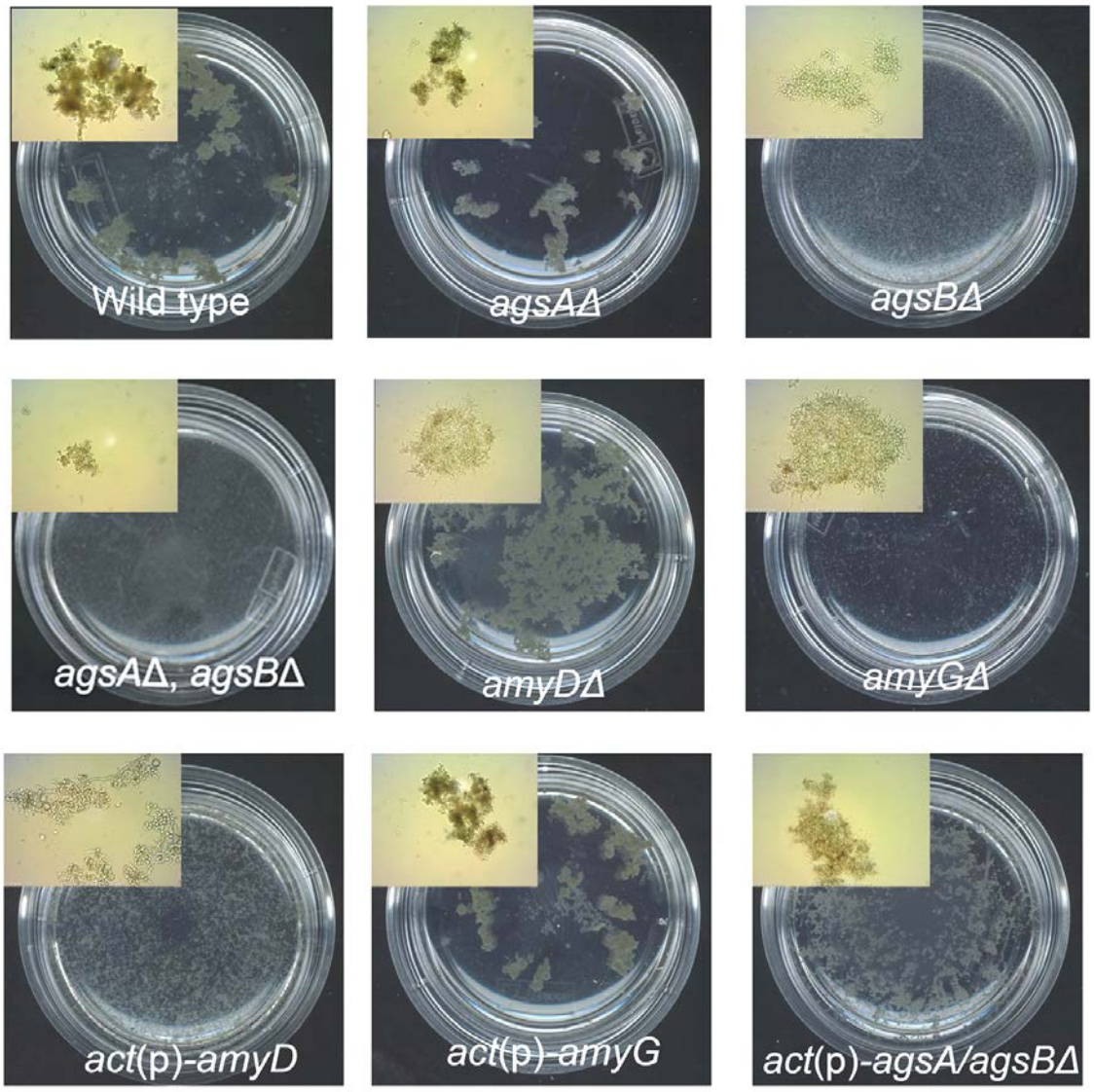

Fig. S2-4 Conidia cluster formation in A1149 and deletion strains. For each strain, $5x10^7$ freshly harvested conidia were inoculated in 20 mL complete medium, incubated at 37 °C, 150 r.p.m. for 6h. Then 3 mL medium were poured to petri dish for scanning to show the visible conidia cluster. 20 μL of medium with germlings were added to glass slide and examined under light microscope (10X objective lens). The pictures were captured by Dino-eye camera. The whole view pictures are shown are the left top of each petri dish.

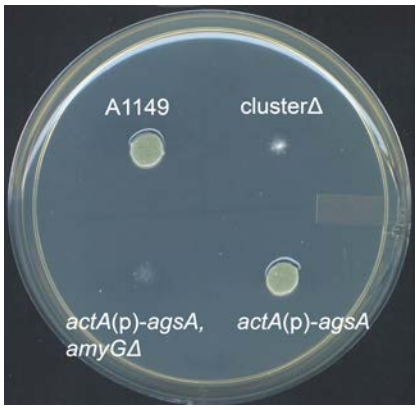

Fig. S2-5 Drug sensitivity of clusterΔ, *actA*(p)-*agsA* and [*actA*(p)-*agsA*, *amyG*Δ]. For each strain, 10^5 conidia were inoculated on plates and incubated for 48 h at 30 ºC. ClusterΔ and [*actA*(p)-*agsA*, *amyG*Δ] showed hypersensitivity to CFW (30 μg mL^{-1}), whereas *actA*(p)-*agsA* maintianed the same sensitivity as wild type strain.

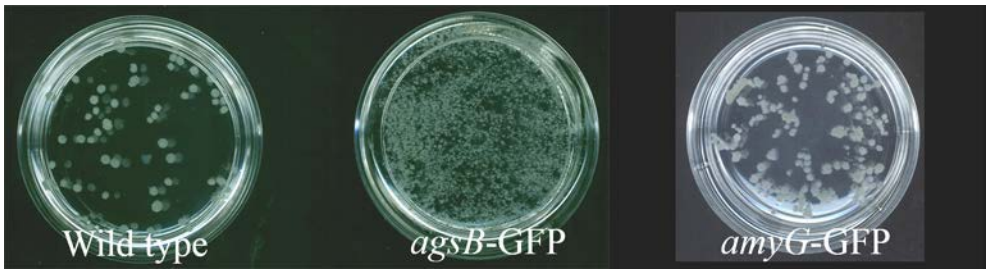

Fig. S2-6 *agsB*-GFP strain grown in shaken liquid medium

The *agsB*-GFP also showed fragmented colonies when grown in shaken liquid medium, indicating that function of AgsB was eliminated by C-terminal GFP tagging. But no such growth defect showed with AmyG-GFP strain, indicating a functional AmyG in this strain.

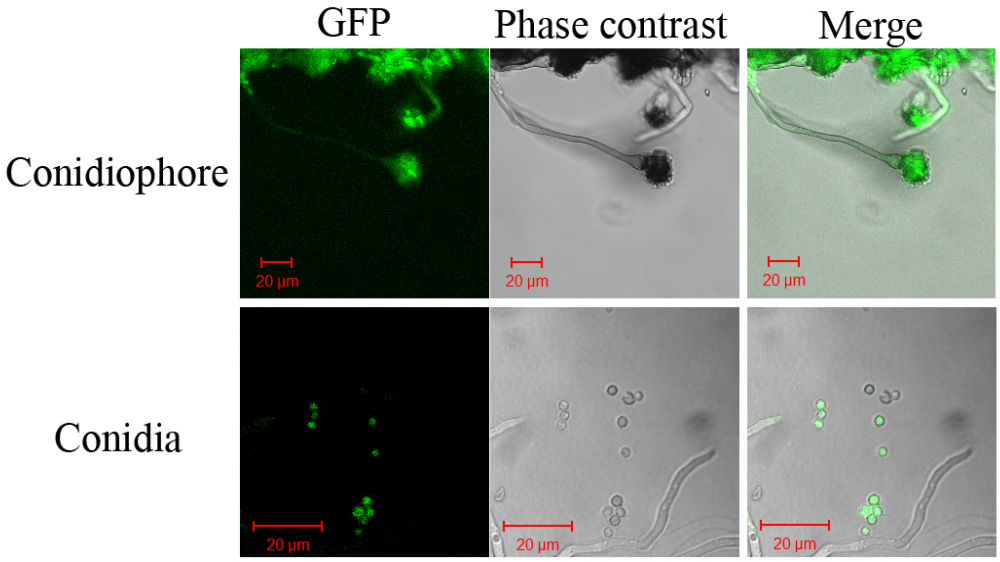

Fig. S2-7 Fluorescence examination of AgsB-GFP

GFP was seen both in conidiophore and conidia as well as hyphae (Fig. 5). All results together showed *agsB* constitutively expresses at all *A. nidulans* life stages.

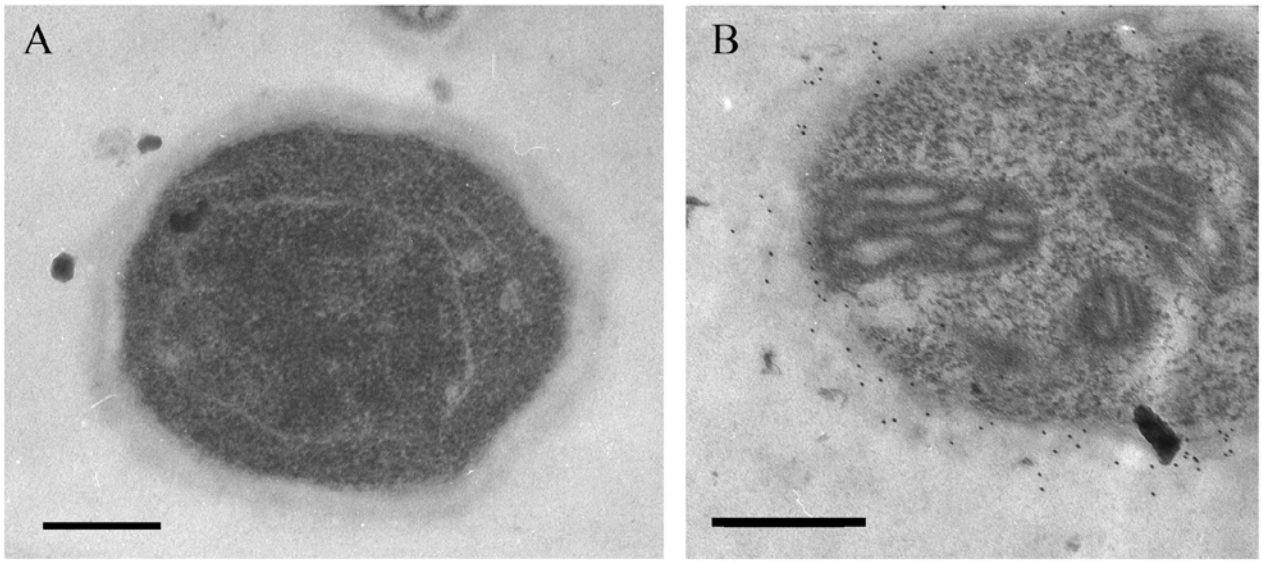

Fig. S2-8 Immunogold-TEM of A1149 with mouse IgM (A) and L10 (B). Scale bar = 500 nm

Cells were grown in shaken liquid medium, and embedded in LR White. Mouse IgM is the negative control for MOPC 104E. L10 targets galactofuranose in *A. nidulans*.

CHAPTER 3

OVEREXPRESSION OF AgsB IN *ASPERGILLUS NIDULANS* CAUSES CELL WALL DEFECTS AND REVEALS HIGHLY MUTABLE SITES IN AgsB

In chapter 2, I characterized the roles of α-1,3-glucan synthases in *A. nidulans*. I found AgsB is the major synthase due to its constant expression and its functional product. Deletion of α-1,3-glucan from the *A. nidulans* cell wall reduced conidial adhesion, but caused no other phenotypic change. In contrast, overexpression of AgsB using an actin promoter led to a moderate conidiation defect. To pursue the work on α-1,3-glucan, I choose to study it using overexpression analysis. Two different promoters were used to give a high expression for AgsA and AgsB. The phenotypic changes were detected using microscopy. This is the first study to show more α-1,3-glucan can cause severe phenotypic defects in an *Aspergillus* species. Results from this chapter further explain the roles of α-1,3-glucan in *A. nidulans* cell wall.

My role in this research: designed the study along with S Kaminskyj who funded it. I wrote thefirst draft; and contributed to the final revised draft.

This chapter has formed a manuscript as “Overexpression of AgsB in *Aspergillus nidulans* causes cell wall defects and reveals highly mutable sites in *agsB*” by Xiaoxiao He and Susan Kaminskyj. The manuscript is in revision at Fungal Genetics and Biology.

Overexpression of AgsB in *Aspergillus nidulans* causes cell wall defects and reveals highly mutable sites in *agsB*

Xiaoxiao He and Susan G.W. Kaminskyj*

Department of Biology, University of Saskatchewan, 112 Science Place, Saskatoon, SK S7N 5E2, Canada

*Author for correspondence

Tel: +1 306 966 4422; email: susan.kaminskyj@usask.ca

Keywords: alpha-1,3-glucan, alpha-1,3-glucan synthase, *Aspergillus nidulans*, replication slippage, conidial adhesion, cellular adhesion

3.1. Abstract:

Alpha-1,3-glucan (α-1,3-glucan) is a major cell wall component for *Aspergillus* species, and it has been shown to be important for the virulence of *A. fumigatus*. Studying wall α-1,3-glucan could help to clarify aspects of the pathogenesis process. Our previous work in *A. nidulans* showed that deletion of AgsB, the major α-1,3-glucan synthase, had no major impact for cell wall formation on agar medium, but substantially reduced conidial adhesion in liquid medium. In this work, we further studied the function of α-1,3-glucan using overexpression analysis. When *agsB* was overexpressed by a histone promoter [*H2A*(p)], a high α-1,3-glucan content was detected in the cell wall. This was coupled with phenotypic changes including conidiation defects and thicker hyphal walls. This is the first report of altered α-1,3-glucan affecting *A. nidulans* cell morphology. Notably, the *H2A*(p)-*agsB* strain did not show increased conidial adhesion, but had increased cellular adhesion to hydrophobic materials. Our results also suggested this high level of α-1,3-glucan content in the *H2A*(p)-*agsB* strain caused cell wall defects and remodeling. Intriguingly, spontaneous mutants with no α-1,3-glucan content were readily isolated from plates inoculated with the *H2A*(p)-*agsB* strain. DNA sequencing showed that these mutants had different short deletions within *agsB* that abolished its function, which appeared to have been generated by a common mechanism: replication slippage. These mutations revealed the highly mutable sites in *agsB* during DNA replication.

3.2. Introduction

Alpha-1,3-glucan is a major cell wall component in many fungi (Latgé, 2010). Characterization work on this wall component using synthase deletion analysis showed α-1,3-glucan is only essential for the morphology of *Schizosaccharomyces pombe* (Hochstenbach et al., 1998), but has no major impact on other investigated fungi, including *Aspergillus spp.* (Rappleye et al. 2004; Henry et al. 2012; Yoshimi et al. 2013; He et al. 2014). However, α-1,3-glucan is still required by these fungi, especially the pathogenic ones. Accumulated evidence has shown α-1,3-glucan is important for a successful pathogenesis (Rappleye et al. 2007; Fujikawa et al., 2012; Beauvais et al., 2013). Therefore, a better understanding of the roles of α-1,3-glucan may help to dissect the pathogenesis process.

In our previous work, we characterized α-1,3-glucan synthases in *A. nidulans* using gene deletion and overexpression approaches (He et al. 2014). We found deletion of the major α-1,3-glucan synthase (AgsB) had no impact on colony development on agar medium, whereas overexpression of AgsB by an actin promoter [*actA*(p)] caused a minor conidiation defect, suggesting further investigations on the roles of α-1,3-glucan could use overexpression analyses. Unfortunately, few data are available from α-1,3-glucan synthase overexpression in any fungal system.

To have a stronger expression level than our previously used promoter [*actA*(p)], we applied a histone promoter [*H2A*(p)] to regulate *agsB*. As expected, a much higher level of mRNA

expression was detected, however the α-1,3-glucan content in the walls was higher than wild type but surprisingly lower than the *actA*(p)-*agsB* strain (He et al., 2014). In addition, a series of phenotypic changes were noted in the *H2A*(p)-*agsB* strain, which had not been seen before in a α-1,3-glucan related strain in *A. nidulans*. Most intriguingly, phenotype-reversion mutants lacking α-1,3-glucan were readily isolated from plates inoculated with the *H2A*(p)-*agsB* strain, revealing several highly mutable sites within *agsB*. These data suggested α-1,3-glucan is already fully optimal at its normal expression level, and high α-1,3-glucan content is deleterious for cell morphology.

3.3. Materials and Methods

3.3.1. Strains and Media

All strains in this study are listed in Table S3-1. They were constructed from A1149, which was also the wild type control for all the experiments. The promoter exchange strategy was described in He et al. (2014), except in this study an *A. nidulans* histone promoter was used instead of an actin promoter. The PCR protocol, protoplast generation and transformation strategies followed Szewczyk et al. (2006) and El-Ganiny et al. (2008). Primers are shown in Table S3-2. Details for each strain construction and confirmation can be found in Fig. S3-1.

All strains were grown on complete medium (CM per litre: 1 % glucose, 0.2 % peptone, 0.1 % yeast extract, 0.1 % casamino acids, 50 mL 20 x nitrate salts, 1 mL trace elements, 1 mL vitamin solution, pH 6.5), or on minimal medium (MM per litre: 1 % glucose, 50 mL 20 x nitrate salts, 1 mL trace elements, 0.001 % thiamine, pH 6.5) supplemented with nutrition solution as required. Trace elements, vitamin solution, nitrate salt and all nutrition stocks are described in Kaminskyj (2001). For transformation medium, 1 M sucrose was added to MM as osmoticum. For phenotype rescue, 1 M sucrose was added to CM. Glucose concentration was tripled in 3 % CM. All strains were grown at 30 ºC, unless mentioned specifically.

3.3.2. Adhesion Tests

For conidial adhesion, 5 x 10^7 freshly harvested conidia were inoculated in 20 mL liquid CM and incubated at 30 ºC with shaking at 150 r.p.m. for 16 h. Then, 1 mL medium was taken from the flask and scanned for imaging.

For polystyrene bead adhesion, 10^5 freshly harvested conidia were mixed with 1 μL fluorescent-conjugated polystyrene beads (Sigma L5530: 0.5 μm mean particle size) and grown in 1 mL CM at 37 ºC for 7 h with shaking at 150 r.p.m. A 50 μL aliquot of this culture was scanned and imaged by confocal microscopy. Bead adhesion test samples were examined using a Zeiss META501 confocal epifluorescence microscope with a 63 × objective lens. Confocal imaging used 514 nm excitation with emission controlled by a BP 530–600 nm filter.

For the biofilm formation test, the method was adapted from Gravelat et al. (2010). Briefly, 300 μL of complete medium was added in each well of a 24-well plate. Then, 10^5 freshly harvested conidia were inoculated in each well, and the plate was incubated at 30 ºC for 48 h. Each well was washed three times by 1 mL of ultra-pure water to assess cell adhesion.

3.3.3. Microscopy Studies

For transmission electron microscopy (TEM), strains were grown on dialysis tubing overlying CM for 2 d at 30 ºC. The TEM protocol was described in Kaminskyj (2000) using fixation with glutaraldehyde and OsO_4. Samples were embedded in Epon 812 resin. Following polymerization, 70-90 nm sections were stained by uranyl acetate for 20 min, followed by lead

citrate for 2 min. Sections were rinsed with ultrapure water for 30 s after each staining solution. TEM images were taken by a Philips CM10 model TEM, collected on x-ray film, and digitized.

For scanning electron microscopy (SEM), strains were grown on dialysis tubing overlying CM for 3 d at 30 ºC. The SEM protocol was described in He et al. (2014). SEM images were taken by a Phenom™ G2 Pure model.

3.3.4. Alpha-1,3-glucan Quantification

This method was adapted from Momany et al. (2004) and Marion et al. (2006), previously described in He et al. (2014). Alpha-1,3-glucan was extracted from dry cell wall samples by 1 M NaOH, and then was digested to glucose by 3 M H_2SO_4. Glucose content was quantified by the anthrone assay (Ashwell, 1957). All experiments were repeated three times with duplicates each time.

3.3.5. Real Time PCR

For gene expression studies, 2 x 10^7 conidia were inoculated in liquid CM and incubated at 30 ºC with shaking at 150 r.p.m. for 16 h. Colonies were collected by filtration, immediately frozen in liquid nitrogen, then lyophilized. Total RNA was extracted using an RNeasy plant kit (Qiagen) following manufacturer's instructions. Genomic DNA elimination and reverse transcription used a QuaniTect reverse transcription kit (Qiagen). Quantitative real time PCR (qPCR) used a SYBR® select Master Mix kit (Applied Biosystems) following the protocol described in Alam et al. (2012). Histone was used as a reference gene (Fujioka et al., 2007).

Primers for qPCR are listed in Table S3-2. The relative expression was normalized to histone and calculated using the ΔΔCt method (Livak and Schmittgen, 2001). Three independent experiments with triplicates were performed for each reaction.

3.4. Results

3.4.1. Overexpression of AgsB Causes Severe Conidiation Reduction

In our previous study, we reported that overexpression of AgsB by *actA*(p) in *A. nidulans* caused a moderate conidiation defect, suggesting higher than wild type α-1,3-glucan content may somehow affect the conidiation process (He et al., 2014). In order to further study the roles of α-1,3-glucan on cell morphology, we used a histone promoter [*H2A*(p)] to overexpress AgsB for a higher expression level than with *actA*(p). As expected, the *H2A*(p)-*agsB* strain had a 14-fold overexpression level for *agsB* in qPCR assay (Table 3-1), which was much higher than the *actA*(p)-*agsB* strain (~2 fold; He et al., 2014). With a 14-fold overexpression of AgsB, the *H2A*(p)-*agsB* strain showed a severe reduction in conidiation, which was readily visualized by the pale color of the colony (Fig. 3-1A). We then used SEM to examine the conidiation phenotype. The individual conidiophores of the *H2A*(p)-*agsB* strain were comparable to wild type morphology (Fig. 3-1B), but their density and the number of conidia on each was much lower (Fig. 3-1B). Besides the conidiation deficiency, the *H2A*(p)-*agsB* strain also showed other phenotypic changes, including slower hyphal growth rate (Fig. 3-1A), a 3-fold thicker cell walls (Fig. 3-1C and Table S3-3), abnormal hyphal morphology (Fig. 3-1D), and greatly swollen germinated conidia (Fig. 3-1D and Table S3-4). Cleistothecia were already seen on a 3-day old *H2A*(p)-*agsB* colony (*data not shown*), which was taken as a sign for an early self-mating. However, unexpectedly, in α-1,3-glucan quantification test, while the α-1,3-glucan abundance in the *H2A*(p)-*agsB* strain was higher than the wild type strain (Table 3-1), it was lower than the

actA(p)-*agsB* strain (He et al., 2014).

3.4.2. Overexpression of AgsB did not Increase Conidial Adhesion but Increases Cellular Adhesion to Hydrophobic Materials

Previously, we found that deletion of AgsB substantially reduced conidial adhesion in shaken liquid culture, resulting in formation of many small colonies rather than fewer larger ones (He et al., 2014). Therefore we might expect that overexpression of AgsB would increase conidial adhesion, resulting in formation of fewer and larger colonies than the wild type strain. However, when the overexpression strains were grown in shaken liquid medium overnight, the *actA*(p)-*agsB* strain colonies resembled the wild type, whereas the *H2A*(p)-*agsB* strain formed many tiny colonies (Fig. 3-2A). Although superficially the *H2A*(p)-*agsB* strain colonies looked like those produced by the *agsB*Δ strain (Fig. 3-2A), compound microscope images showed they were actually different. The colonies of the *H2A*(p)-*agsB* strain were compact and small, whereas the colonies of the *agsB*Δ strain were loose and tiny (Fig. 3-2B), indicating the colony phenotypes of these two strains resulted from different reasons. Nevertheless, neither overexpression strain showed the signs of increased conidial adhesion.

In addition, we also noticed that the *H2A*(p)-*agsB* strain but not the *actA*(p)-*agsB* strain showed very strong adhesion to the glass surface treated with GelSlick® (Fig. 3-2A), in other words an increased cellular adhesion to a hydrophobic surface. To confirm that, we used fluorophore-conjugated polystyrene beads to assess the cellular adhesion of our strains. Polystyrene beads have been used to test cell surface adhesion ability for *Aspergillus* species

(Lamarre et al. 2009; Alam et al., 2014). When examined by fluorescence microscope, both overexpression strains had higher adhesion ability to polystyrene beads, especially the *H2A*(p)-*agsB* strain (Fig. 3-2C). However, the *agsB*Δ strain maintained a similar adhesion ability as the wild type strain (Fig. 3-2C).

With noticing the strong adhesion ability of the *H2A*(p)-*agsB* hyphae, we wondered whether this change could enable *A. nidulans* to form a biofilm. Strong adhesion to a hydrophobic surface is a characteristic of *A. fumigatus* biofilms (Kaur and Singh, 2014), which contributes to making *A. fumigatus* a successful pathogen (Kaur and Singh, 2014; Muszkieta et al., 2014). A simplified testing method for biofilm formation was developed by Gravelat et al. (2010) using adhesion to a plastic tissue culture well. Following their idea, we found that hyphal mats formed by wild type *A. nidulans*, *agsB*Δ and *actA*(p)-*agsB* strains could be washed away easily (Fig. 3-4D), indicating a weak adhesion and no biofilm formation. In contrast, the *H2A*(p)-*agsB* and wild type *A. fumigatus* strains formed a layer of hyphae that could not be removed by washing (Fig. 3-4D).

3.4.3. Overexpression of AgsB-α-1,3-glucan Causes Cell Wall Defects and Remodeling

Wide, slow-growing hyphae can be caused by a diversity of cellular defects (Harris et al., 1994; Shi et al., 2004; El-Ganiny et al., 2008). Given that in the *H2A*(p)-*agsB* strain a major cell wall carbohydrate was dramatically overexpressed, we wondered whether the reason for the slow-growing hyphae was resource depletion. Glucose is the main source for energy production and a major substrate for cell wall polysaccharides. If overexpression of AgsB consumed too much glucose, this might cause problems for cell growth. To test that, we tripled the glucose

concentration in the complete medium (from 1% w/v to 3% w/v). However, no improvement was seen for the phenotypes of the *H2A*(p)-*agsB* strain (Fig. 3-3A). We then tried 1M sucrose medium, which is commonly used as an osmoticum to remediate cell wall defective strains (Lin and Momany, 2004; El-Ganiny et al., 2008). The phenotypes of the *H2A*(p)-*agsB* stain were partially recovered on 1 M sucrose medium regarding hyphal growth rate and conidiation rate (Fig. 3-3A), suggesting overexpression of AgsB caused a cell wall defect.

As reported previously, the carbohydrate products of AgsA and AgsB are not equivalent with respect to their cellular functions (He et al. 2014): AgsB-α-1,3-glucan was more important for conidial adhesion in liquid medium and for CFW sensitivity. We were interested to see whether *H2A*(p)-overexpressed AgsA-α-1,3-glucan, on its own, could lead to similar phenotypic changes as the *H2A*(p)-*agsB* stain. To test this notion, we generated the [*H2A*(p)-*agsA, agsB*Δ] strain. The expression of *agsA* in this strain was greatly increased in qPCR assay (Table 3-1), and the α-1,3-glucan content was also dramatically elevated (Table 3-1). However, there was no phenotypic change observed in respect to hyphal growth rate or conidiation rate on solid medium (Fig. 3-3B). The conidial adhesion defect due to the loss of AgsB-α-1,3-glucan was also not recovered (Fig. 3-3B) by overexpression of AgsA-α-1,3-glucan. So overexpression of AgsA-α-1,3-glucan did not cause a cell wall defect, or recovery, under the conditions we tested.

Although the *H2A*(p)-*agsB* strain had a conidiation defect and a 3-fold thicker cell wall, the α-1,3-glucan abundance in this strain was not as high as the [*H2A*(p)-*agsA, agsB*Δ] strain (Table 3-1). We think this could because of cell wall remodeling. It is likely that overexpressing a

component of the cell wall by molecular genetic means will trigger a CWI-mediated restructuring. The dynamics of cell wall architecture have been recorded in *Aspergillus* species (Beauvais et al., 2013; Alam et al., 2014). In our lab, Alam et al. (2012) showed that loss or down-regulation of galactopyranose mutase (*ugmA*) expression in *A. nidulans* led to an expression increase for *agsB* and an expression decrease for β-glucan synthase (*fksA*). Therefore, we tested the expressions of *ugmA* and *fksA* in the *H2A*(p)-*agsB* strain to see how the cell responded to α-1,3-glucan overexpression. Results showed both *ugmA* and *fksA* had higher expression levels than the wild type strain (Fig. 3-3C). In contrast, when we tested the same genes in the [*H2A*(p)-*agsA*, *agsB*Δ] strain, both *ugmA* and *fksA* were maintained at comparable expression levels as the wild type strain (Fig. 3-3C).

3.4.4. Spontaneous Mutants from *H2A(p)-agsB* Reveal Highly Mutable Sites in *agsB* During DNA Replication

Intriguingly, the *H2A*(p)-*agsB* strain colonies streaked across a plate often became interspersed with wild type-appearing colonies, these typically arising after being grown for a few days (Fig. 3-4A indicated by the arrows). At first, we thought this could be contamination from a wild type strain. However, due to their delayed colony appearance and because their relatively high frequency, we wondered whether these wild type-like colonies were actually derived from the *H2A*(p)-*agsB* strain itself. Four potential mutant strains from four individual plates were collected to ensure these isolates had been generated independently. Mutants were named as *H2A*(p)-*agsB* mutant #1 to #4. Genomic DNA was extracted from each mutant and

tested for the source of the mutant. When we generated the *H2A*(p)-*agsB* strain, we had inserted a nutrition marker (*AfpyroA*) and a *H2A*(p) between *agsB* and its upstream (Fig. S3-1). Therefore, the sequence before *agsB* 5' end was changed in the *H2A*(p)-*agsB* strain, which could be tested by PCR (Fig. S3-2) and used to determine the source for these mutants. The results showed all the mutants had the same band as the *H2A*(p)-*agsB* strain rather than the wild type strain (Fig. 3-4B), suggesting they were derived from the *H2A*(p)-*agsB* strain. We then tested these mutants in shaken liquid medium to assess the α-1,3-glucan content. Surprisingly, they all formed the loose and small colonies like *agsB*Δ strain (Fig. 3-3C), indicating these mutants had no α-1,3-glucan in their cell walls. The lack of α-1,3-glucan in the mutants' cell wall was also confirmed by anti-α-1,3-glucan antibody staining (Fig. S3-2).

It was very interesting to see the α-1,3-glucan content in these mutants changed from a high level to none. Because we artificially overexpressed *agsB* in the *H2A*(p)-*agsB* strain, the most likely changes in these mutants were mutations within *agsB* or its promoter that eliminated AgsB function. We sequenced *agsB* as well as the inserted *H2A*(p) (about 8.5 kb in total) in these four mutants. Short sequence deletions within the *agsB* coding region were found in each of the mutant strains (Table 3-2). In mutant #1, four nucleotides were deleted in the middle of the gene (Table 3-2), which shifted the reading frame. In mutant #3, fourteen nucleotides were missing near the 3' end (Table 3-2), which also shifted the reading frame. Most intriguingly, in the other two mutants (mutant #2 and #4) exactly the same eighteen nucleotide deletions were found near the 3' end (Table 3-2), which did not change the reading frame but still abolished its function. So

all these mutants resulted from short sequence deletions and two of them even shared the same deletion. Obviously, these were not random mutations.

One of the most well defined mechanisms for short sequence deletion/insertion is replication slippage (Li et al., 2002; Lovett, 2004; Montgomery et al., 2013), which requires adjacent direct sequence repeats on genome. For each of our mutants the deleted sequences were repeated or partially repeated by the sequence right before them (Table 3-2). Therefore, these mutants were probably the results of replication slippage during DNA replication.

3.5. Discussion

Previous studies on α-1,3-glucan were mostly based on α-1,3-glucan synthase deletion (Hochstenbach et al., 1998; Rappeleye et al. 2004; Henry et al. 2012; Yoshimi et al. 2013). Data on α-1,3-glucan overexpression are rare (He et al 2014). In this study, we constructed α-1,3-glucan synthase overexpression strains to further study the roles of α-1,3-glucan in the *A. nidulans* cell wall.

3.5.1. Alpha-1,3-glucan Content is Optimally Expressed in *A. nidulans* Cell Wall under Regular Growth Conditions

When the major α-1,3-glucan synthase (AgsB) was overexpressed by *actA*(p) or *H2A*(p), more α-1,3-glucan was found in the hyphal cell wall (Table 3-1 and He et al., 2014) as well as the conidial cell wall of *actA*(p)-*agsB* strain (Table S3-5). However, neither of these overexpression strains showed higher conidial adhesion when grown in shaken liquid medium (Fig. 3-2A). Therefore, simply increasing cell wall α-1,3-glucan did not increase conidial adhesion, suggesting additional factors were involved. In addition, both overexpression strains showed phenotypic defects on solid medium. The *actA*(p)-*agsB* strain had a moderate conidiation defect related to conidia abundance (He et al., 2014), whereas the *H2A*(p)-*agsB* strain had more dramatic phenotypic changes, including a severe conidiation defect, slower growth rate and thicker hyphal cell wall (Fig. 3-1). These phenotypic changes were partially rescued by growth on 1 M sucrose medium, indicating more α-1,3-glucan appeared to cause a cell wall weakness

(Fig. 3-3A). Especially for the *H2A*(p)-*agsB* strain, the cell had remodeled its cell wall to cope with α-1,3-glucan overexpression, as shown by increased wall thickness (Fig. 3-1C). In fungi, cell wall remodeling is controlled by cell wall integrity pathways (Levin, 2005; Fujioka et al., 2007; Munro et al., 2007). Activation of such pathways can alter the expression of many wall components, as we found for *ugmA* and *fksA* (Fig. 3-3C). This explained why the α-1,3-glucan abundance in the *H2A*(p)-*agsB* strain was not as high as the [*H2A*(p)-*agsA*, *agsB*Δ] strain, because other cell wall components (at least β-glucan and galactofuranose) were also increased in *H2A*(p)-*agsB* cell walls. These increased wall components together made the abnormally thickened cell wall in the *H2A*(p)-*agsB* strain. All together, these data suggest α-1,3-glucan is already optimally expressed in the *A. nidulans* cell wall to support conidial adhesion under regular growth condition, whereas more α-1,3-glucan is deleterious for cell morphology.

3.5.2. Increased Cellular Adhesion in AgsB Overexpression Strains is not Due to α-1,3-glucan Itself

Although α-1,3-glucan is a major cell wall component in many filamentous fungi as well as some yeasts (Latgé, 2010), most existing data show it is dispensable for cell wall formation on solid medium (Henry et al., 2013; Yoshimi et al. 2013; He et al. 2014). This begs the question of why many fungi still produce α-1,3-glucan in a high abundance. Accumulated evidence has shown α-1,3-glucan contributes to the full virulence of some pathogenic fungi (Rappleye et al. 2007; Fujikawa et al., 2012; Beauvais et al., 2013). In our study, α-1,3-glucan content was related to the adhesion ability to hydrophobic materials (Fig. 3-2A, C and D). The *H2A*(p)-*agsB*

strain even restored the ability for biofilm formation in *A. nidulans* (Fig. 3-2D). Adhesion ability and biofilm formation are both important factors for the virulence of *Aspergillus* species (Yoshijima et al., 2010; Muszkieta et al., 2013). Therefore, our results supported the previous findings that α-1,3-glucan contributes to fungal virulence. However, based on our results, we cannot make a direct link between α-1,3-glucan and the cellular adhesion, especially when we found that α-1,3-glucan content in the *H2A*(p)-*agsB* strain was not the highest in our strain lists (Table 3-1), other cell wall components (β-glucan and galactofuranose) were also induced in this strain and more extracellular matrix was observed outside of many *H2A*(p)–*agsB* cells (Fig. S3-2), perhaps galactosaminogalactan (Gravelat et al., 2013). Therefore, our results suggested the change of adhesion property was triggered by the factors associated with the overexpression of α-1,3-glucan, but not because of α-1,3-glucan itself. For instance, increased hyphal surface adhesion could result from exposure of mannans in *A. fumigatus* (Lamarre et al 2009). Further studies on cell wall analysis are needed to figure out the reasons for this high cellular adhesion, and this could also help to dissect the biofilm formation itself. Nevertheless, the current data showed *A. nidulans* also has the potential to form a biofilm under extreme α-1,3-glucan overexpression.

3.5.3. *H2A*(p)–*agsB* Provides a Tool to Study Important Sites in *agsB*

Spontaneous phenotype-reversion mutants were frequently isolated from the *H2A*(p)-*agsB* strain. Since we found these mutants had no α-1,3-glucan, it was clear that the function of AgsB had been eliminated, presumably by mutation(s). When we sequenced *agsB* in these mutants, we

expected to find single base-pair mutations disabling AgsB. If so, these mutations might have provided useful information related to the essential amino acids within AgsB, and these mutations could help for the further protein study of α-1,3-glucan synthase. However, so far, we were only able to find short sequence deletions but not single base-pair mutations (Table 3-2).

According to the sequencing result, we found these mutants were not generated by totally random events. The most likely mechanism was replication slippage, which is a common type of DNA replication error that requires adjacent direct sequence repeats (mechanism reviewed by Lovett, 2004). Replication slippage mainly happens at tandem repeat sequences (Li et al., 2002), but is not restricted to those regions (Li et al., 2004). In the human genome, it is estimated that up to 75 % short sequence deletions/insertions could be due to replication slippage (Montgomery et al., 2013). In fungi, replication slippage has been reported in yeast (Mar Albà et al., 1999), and our result suggests it also happens in *A. nidulans*. The *agsB* sequence was ideal for detecting this type of mutation, because the overexpression strain had a phenotype on solid medium whereas the deletion strain did not. The sequencing results also confirmed our previous finding that the transmembrane domain is essential for AgsB function (He et al., 2014). Even loss of 6 amino acids in this critical domain was not affordable for the protein (see results for mutants #2 and #4).

In summary, our overexpression study showed that more α-1,3-glucan did not increase conidial adhesion in shaken liquid medium, but triggered a higher cellular adhesion to hydrophobic materials. Abnormally high α-1,3-glucan content in the *A. nidulans* cell wall was

shown to be harmful, causing cell wall defects and remodeling. Intriguingly, phenotype reversion mutants from the *H2A*(p)–*agsB* strain could be readily isolated on the agar cultures. To date, our results suggest the mutations were generated by replication slippage, and these mutations were at non-random mutable sites in *agsB*. More independent mutants have been isolated and archived. Preliminary sequencing showed they do not share any previous identified mutations. Further work on more mutants may provide new insights for α-1,3-glucan synthase protein.

3.6. Acknowledgements

S.G.W.K is pleased to acknowledge support from the Natural Science and Engineering Council of Canada Discovery Grant program. X.H. is supported by Graduate Teaching Fellowship from University of Saskatchewan. We thank Dr. Peta Bonham-Smith (Department of Biology, University of Saskatchewan) for the access to qPCR. Finally, we thank the Department of Biology and other units and individuals at the University of Saskatchewan for funding the Phenom G2 Pure scanning electron microscope.

3.7. Tables

Table 3-1 Expression changes and α-1,3-glucan quantification for *H2A*(p) overexpression strains

Strains	Expression changes for target gene (in folds) [a]	Relative α-1,3-glucan abundance in hyphal cell wall (%) [b]
Wild type	1	15 ± 1
H2A(p)-*agsB*	13.5 ± 3.0	28 ± 4
H2A(p)-*agsA*, *agsB*Δ	1523 ± 478	34 ± 2

[a] **:** Expression changes were measured by qPCR as mentioned in Materials and Methods. Target gene expression in the wild type strain was defined as 1. Results represent the mean ± SD from three independent experiments with triplicates each time.

[b:] Alpha-1,3-glucan was quantified by an anthrone assay as mentioned in Materials and Methods. Relative α-1,3-glucan abundance represents the percentage of total α-1,3-glucan weight in 1 mg dry cell wall. Mean ± SD was shown for each strain. Each experiment was repeated three times with duplicates each time.

Table 3-2 Deleted sequences in *H2A*(p)-*agsB* mutants

Strains	Sequences position [a]	Deleted sequence [b] (5'to 3') with repeat sequence at 5'
Mutant #1	3784-3787	CTTG~~CTTG~~
Mutant #2	6582-6599	TCGGCCT~~CCTGCTGATCTTCGGCCT~~
Mutant #3	6316-6329	GCGGCTTC~~TATGCTGCGGCTTC~~
Mutant #4	6582-6599	TCGGCCT~~CCTGCTGATCTTCGGCCT~~

[a]: Sequence position represents position in cDNA

[b]: Deleted sequence shown by ~~strikethrough.~~

3.8. Figures

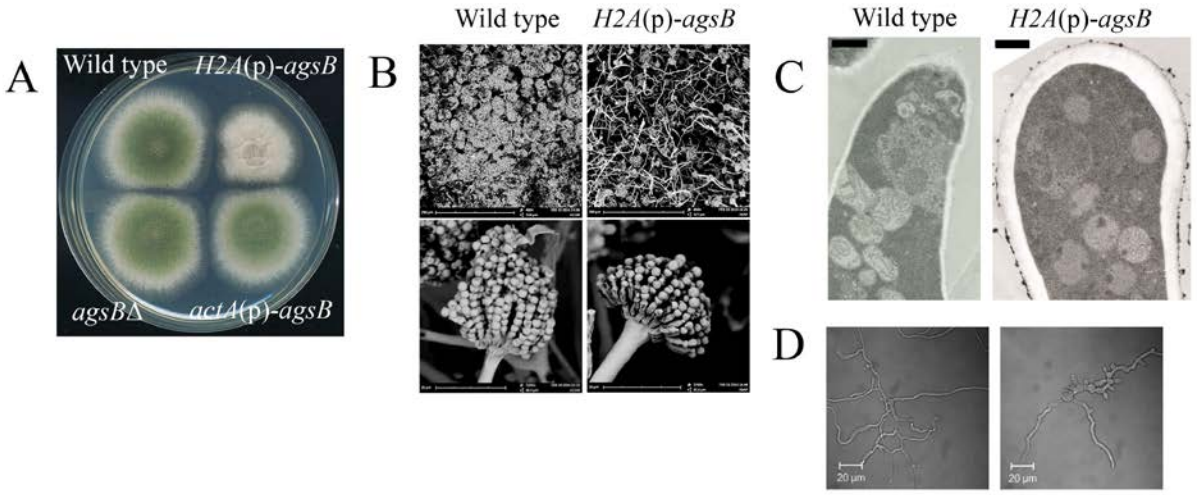

Fig. 3-1 The *H2A*(p)-*agsB* strain exhibits phenotypic changes compared to wild type.

A. 10^5 freshly harvested conidia of each strain were inoculated on complete medium and incubated at 30 ºC for 72 h. Only the *H2A*(p)-*agsB* strain showed obvious growth and conidiation defects.

B. SEM showed the *H2A*(p)-*agsB* strain has fewer conidiophores and fewer conidia per conidiophore.

C. TEM showed cell wall thickness is obviously increased in the *H2A*(p)-*agsB* strain. Bar = 500 nm

D. 63× phase contrast images showed the *H2A*(p)-*agsB* strain has bigger germinated conidia and abnormal hyphal morphology.

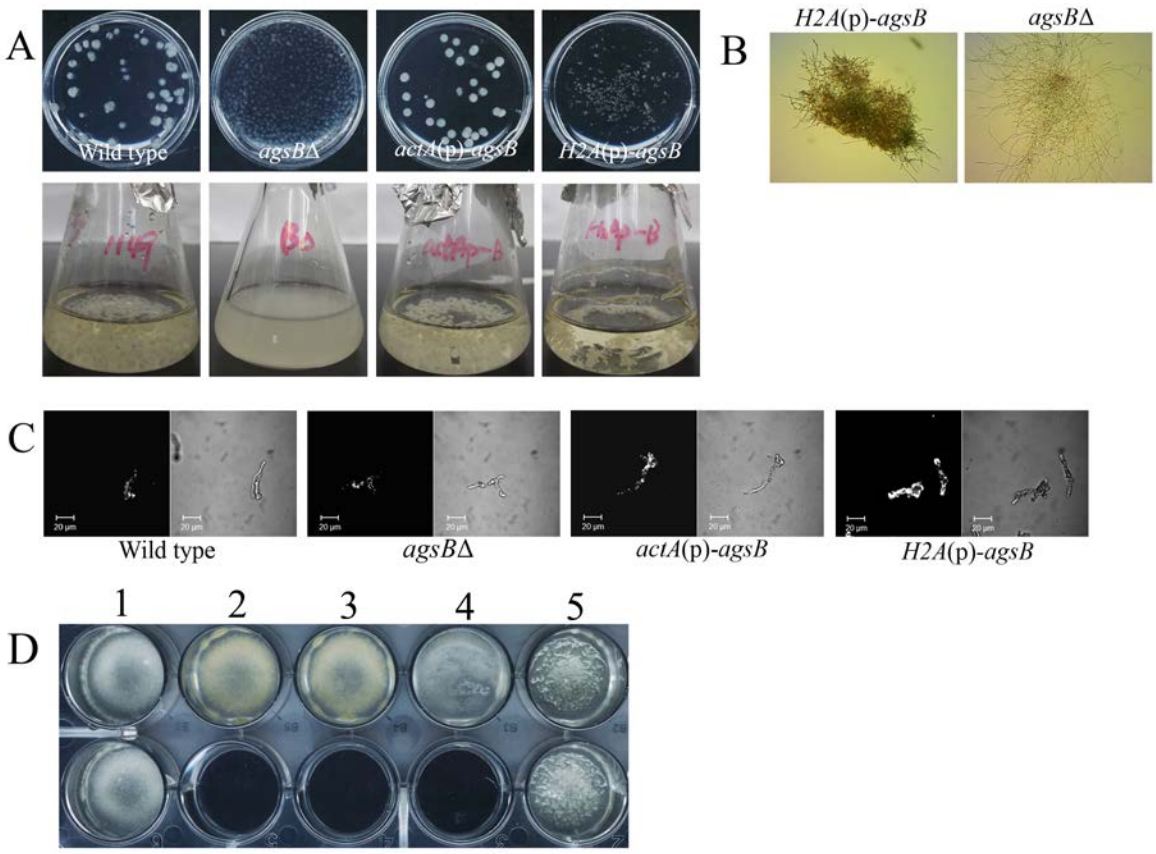

Fig. 3-2 Adhesion test for wild type and AgsB deletion and overexpression strains

A. 2 x 10^7 freshly harvested conidia of each strain were inoculated in 20mL complete medium. Flask was incubated at 30 ºC for 16 h with 150 r.p.m. The *actA*(p)-*agsB* strain behaved the same as the wild type strain, whereas the *agsB*Δ and *H2A*(p)-*agsB* strains formed many tiny colonies. In addition, only the *H2A*(p)-*agsB* strain showed strong adhesion to Gel Slick pre-treated flask walls (Lower panel).

B. Compound microscope magnified individual colony of the *H2A*(p)-*agsB* and *agsB*Δ strains showed these two small colonies are actually different.

C. 10^5 freshly harvested conidia of each strain and 1 µL polystyrene beads were grown in 1 mL complete medium at 37 ºC for 7 h with 150 r.p.m. Images were captured by a Zeiss META501 confocal epifluorescence microscope at 63× objective lens. Confocal imaging used 514 nm excitation with emission controlled by a BP 530–600 nm filter. The *actA*(p)-*agsB* strain had more adhered beads than wild type, whereas the *H2A*(p)-*agsB* strain was fully covered by beads.

D. 10^5 freshly harvested conidia of each strain were grown in 300 µL complete medium at 30 ºC for 48 h (upper panel), then washed by ultra-pure water (lower panel). Strains are 1) wild type *A.fumigatus*, 2) wild type *A. nidulans*, 3) *agsB*Δ, 4) *actA*(p)-*agsB* and 5) *H2A*(p)-*agsB*. Only the colonies formed by wild type *A. fumigatus* and *H2A*(p)-*agsB* cannot be removed by washing, indicating the formation of biofilm.

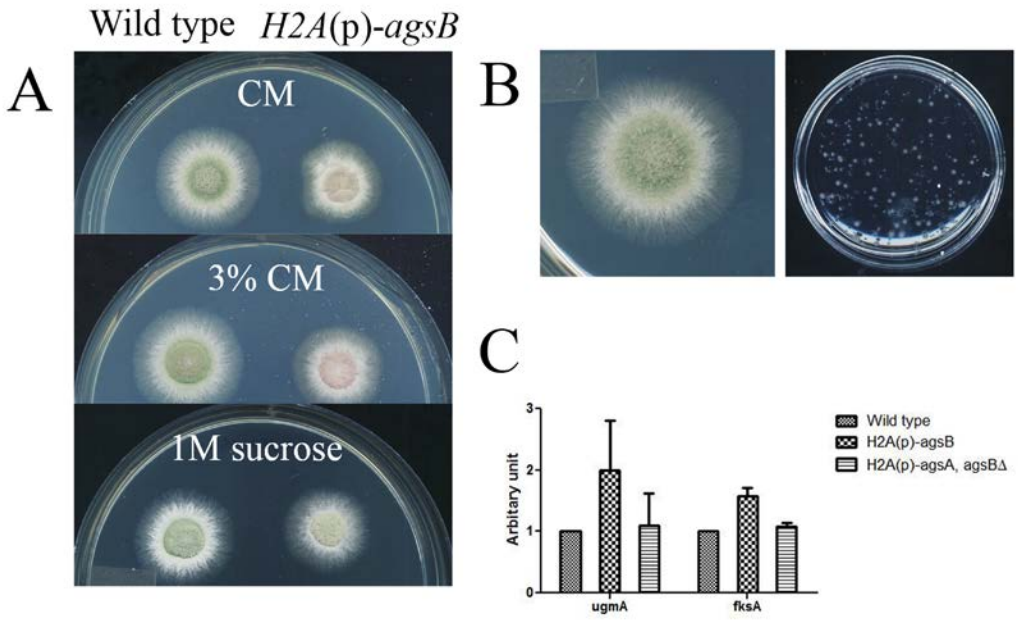

Fig. 3-3 Overexpression of AgsB-α-1,3-glucan causes cell wall defects and remodeling

A. 10^5 freshly harvested conidia of each strain were inoculated on indicated medium. Plates incubated at 30 ºC for 48 h. Compare to wild type control on each medium, the *H2A*(p)-*agsB* strain showed faster growth rate and higher conidiation rate on 1 M sucrose medium than CM or 3 % CM.

B. The phenotype of the [*H2A*(p)-*agsA*, *agsB*Δ] strain is indistinguishable from wild type when grown on solid complete medium (left). But the conidial adhesion defect due to the loss of AgsB was not recovered in shaken liquid complete medium (right).

C. The expressions of *ugmA* and *fksA* were up-regulated in the *H2A*(p)-*agsB* strain but not in the [*H2A*(p)-*agsA*, *agsB*Δ] strain.

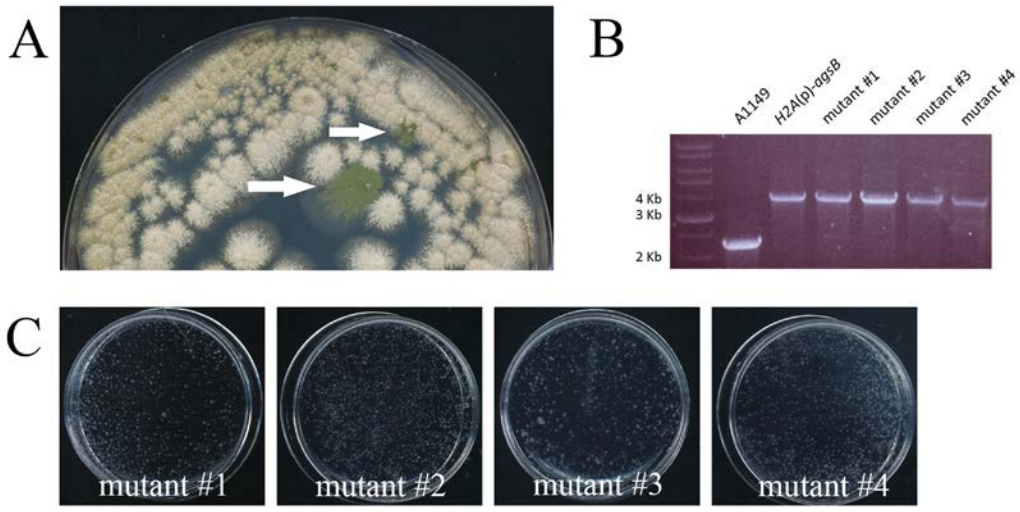

Fig. 3-4 Spontaneous mutants from the *H2A*(p)-*agsB* strain have no α-1,3-glucan

A. Wild type-like colonies (indicated by arrows) spontaneously grew on the *H2A*(p)-*agsB* plate.

B. These isolated strains had the same PCR band as the *H2A*(p)-*agsB* strain. Therefore they are the mutants from the *H2A*(p)-*agsB* strain].

C. The spontaneous mutants formed tiny colonies comparable to the *agsB*Δ strain, indicating they had no α-1,3-glucan in their cell walls.

3.9. Supplemental Materials

Table S3-1 *Aspergillus nidulans* and *Aspergillus fumigatus* strains in this study

Strains	Name	Genotype	Origin
Aspergillus nidulans	A1149	*pyrG89*; *pyroA4*; *nkuA*::*argB*	FGSC
*agsB*Δ	AXH1	*AN3307*::*AfpyrG*; *pyrG89*; *pyroA4*; *nkuA*::*argB*	He et al. 2014
actA(p)-*agsB*	AXH17	*agsB*p::*AfpyrG*:*actA*p:*agsB*; *pyrG89*; *pyroA4*; *nkuA*::*argB*	He et al. 2014
H2A(p)-*agsB*	AXH20	*agsB*p::*AfpyrG*:*H2A*p:*agsB*; *pyrG89*; *pyroA4*; *nkuA*::*argB*	this study
H2A (p)-*agsA*, *agsB*Δ	AXH59	*agsA*p:: *agsA*p: *AfpyroA*:*H2A*p:*agsA*; *AN3307*::*AfpyrG*; *pyrG89*; *pyroA4*; *nkuA*::*argB*	this study
H2A(p)-*agsB* mutant #1	AXH65	*agsB*p::*AfpyrG*:*H2A*p:*agsB*; *pyrG89*; *pyroA4*; *nkuA*::*argB*	this study
H2A(p)-*agsB* mutant #2	AXH67	*agsB*p::*AfpyrG*:*H2A*p:*agsB*; *pyrG89*; *pyroA4*; *nkuA*::*argB*	this study
H2A(p)-*agsB* mutant #3	AXH68	*agsB*p::*AfpyrG*:*H2A*p:*agsB*; *pyrG89*; *pyroA4*; *nkuA*::*argB*	this study
H2A(p)-*agsB* mutant #4	AXH70	*agsB*p::*AfpyrG*:*H2A*p:*agsB*; *pyrG89*; *pyroA4*; *nkuA*::*argB*	this study
A. fumigatus	A1151	*pyrG^AF*::*Delta KU80; pyrG-*	FGSC

Table S3-2 Primers in this study

Primers	Sequence 5' to 3'	Description
Selective marker and strain confirmation		
AME1	ATGTCGTCCAAGTCGCAATT	Af*pyrG**
AME2	TCATGACTATGCCGCATACTAC	Af*pyrG**
SE231	GGACATCAGATGCTGGATTACTAAAG	Af*pyroA* with native promoter
SE232	TTACCATCCTCTCTTGGCCA	Af*pyroA* with native promoter
AME7	CAATACCGTCCAGAAGCAATAC	Af*pyrG* confirmation*
AME8	CACATCCGACTAGCACTATCC	Af*pyrG* confirmation*
AME15	ATTCCTGTCATGGCCAAAG	Af*pyroA* confirmation*
AME16	TCAACAACATCTCCGGTACC	Af*pyroA* confirmation*
Gene deletion		
SE77	CATACAAAAATCCATGGACCG	*agsB* upstream F

SE78	AATTGCGACTATGGACGACATACTAGATGAAGCGAGAACGAG	*agsB* upstream R (*pyrG* tail)
SE79	GAGTATGCGGCAAGTCATGAGGCTTAGCAACCGTAGTTTGG	*agsB* downstream F (*pyrG* tail)
SE80	CTGGATTAAACATGAGAGGGAGA	*agsB* downstream R
SE81	AGCAAACGATTTTCAGGGTC	*agsB* Fusion F
SE82	AGCAACCCAAACGCTACG	*agsB* Fusion R
Promoter exchange		
SE211	GAGTATGCGGCAAGTCATGATCGAAAGTTGAATTCGGTAATG	*H2A* promoter F (*pyrG* tail)
SE212	TTTGATTGATTTGGAGAATCAGG	*H2A* promoter R
SE311	TGGCCAAGAGAGGATGGTAATCGAAAGTTGAATTCGGTAATG	*H2A* promoter F (*pyroA* tail)
SE213	CCTGATTCTCCAAATCAATCAAAATGGGGAGGCTCCAGCTC	*agsB* F (*H2A*(p) tail)
SE143	GATAGACCCAAAAGTATTGCCTCC	*agsB*_1210 R
SE144	AGGCAATGATCATGCATGTG	*H2A*(p)-*agsB* Fusion R
SE85	TAGACGAGGAACATTTACCGG	*agsA* upstream F
SE242	CTTAGTAATCCAGCATCTGATGTCCGGTCGATTTTTCCGGATGT	*agsA* upstream R (pyroA tail)
SE312	CCTGATTCTCCAAATCAATCAAAATGAGGTGGAGGCCTTTAAAC	*agsA* F (*H2A*(p) tail)
SE146	ATTGGTTGGGCTGTCTTCC	*agsA*_1200 R
SE89	GGCTTGTAGACTAGGAATGGTATCT	*H2A*(p)-*agsA* Fusion F
SE147	CACACTACACGATAAGCACTACG	*H2A*(p)-*agsA* Fusion R
qPCR		
SE244	CACCCGGACACTAGGTATCTC	Histone qPCR F#
SE245	GAATACTATCGTAACGGCCTTGG	Histone qPCR R#
SE246	ATCGGACACTAACCTTCCCTG	*agsB* qPCR F#
SE247	GACTATGGCTGACGATCAACG	*agsB* qPCR R#
SE248	GCTTTCCAAATCCCACAGTTGG	*agsA* qPCR F#
SE249	GTGAAGCAGATATGCATCCGTG	*agsA* qPCR R#
SE11	GTGTGGTCCGTTTCGCTATT	*fksA* qPCR F*
SE12	GCTCAAGAAGGATGCCACTC	*fksA* qPCR R*
AME84	CGTTCCCAGCTTTCAGGATA	*ugmA* qPCR F*
AME85	CTTTGCAGCACCCAATCC	*ugmA* qPCR R*

#, Fujioka et al. (2007)

*, Alam et al. (2012)

Table S3-3 Quantification of cell wall thickness (nm)

Strains	Cell wall thickness (nm)
Wild type	53 ± 10
H2A(p)-*agsB*	157 ± 38

TEM images were used for the measurement of cell wall thickness. 30 individual cells from each group were measured. Results represent mean ± SD.

Table S3-4 Quantification of conidia diameter (μm)

Strains	Ungerminated	Germinated
Wild type	3.4 ± 0.4	6.0 ± 0.4
H2A(p)-*agsB*	3.5 ± 0.4	8.1 ± 1.1

Conidia were spread on dialysis tubing overlying CM without incubation (ungerminated) or incubated overnight (germinated). Then slides were made from dialysis tubing and imaged by a Zeiss META501 confocal epifluorescence microscope at 63×. All images were processed by Zeiss LSM Image Browser. At least 30 conidia were measured for each strain under each condition. Results represent mean ± SD.

Table S3-5 Abundance of α-1,3-glucan in conidial cell wall (%)

Strains	Ungerminated	Germinated
Wild type	5.3 ± 0.4	7.1 ± 0.7
actA(p)-*agsB*	8.5 ± 0.8	9.8 ± 0.6

The ungerminated conidia were freshly collected from the medium and the germinated conidia were grown in liquid CM for 8 h at 30 °C with 150 r.p.m. The α-1,3-glucan quantification process followed the method previously described. Due to the poor conidiation rate of *H2A*(p)-*agsB* strain, this strain was not used in this experiment.

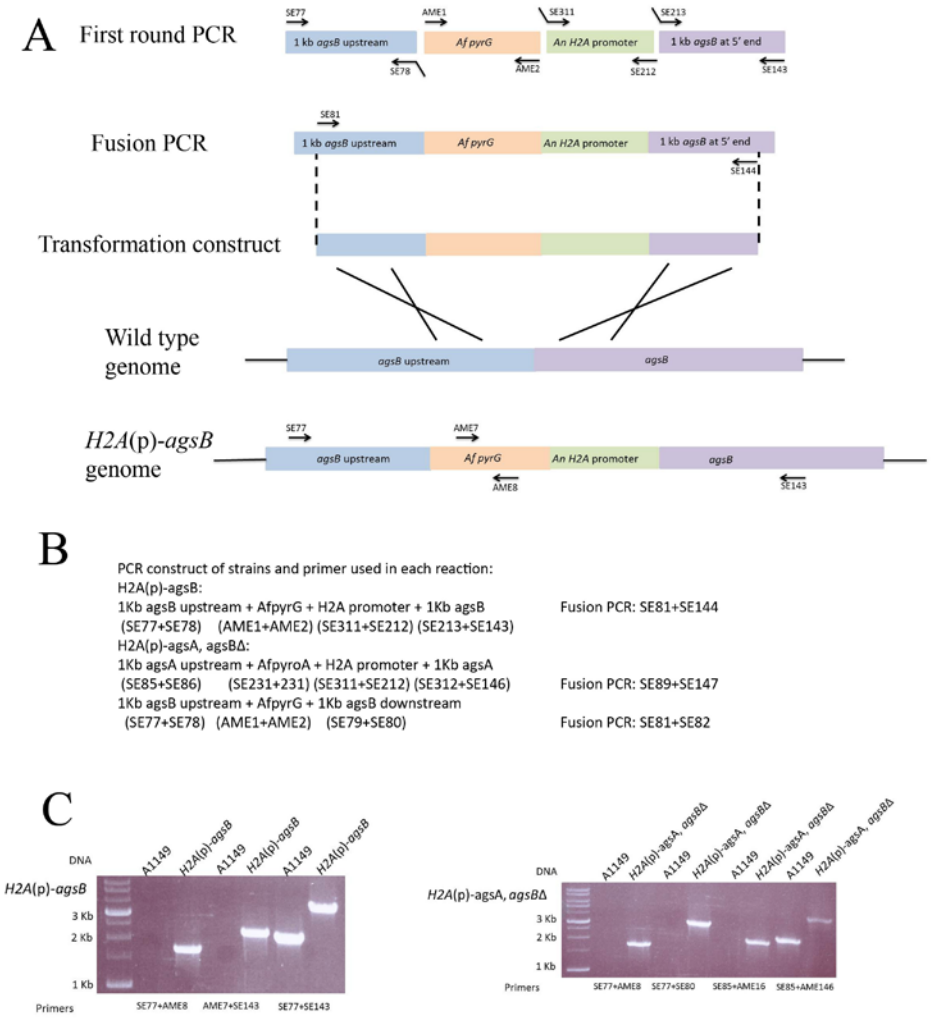

Fig. S3-1 Promoter exchange strategy, PCR construct for each strain, and strain confirmation.

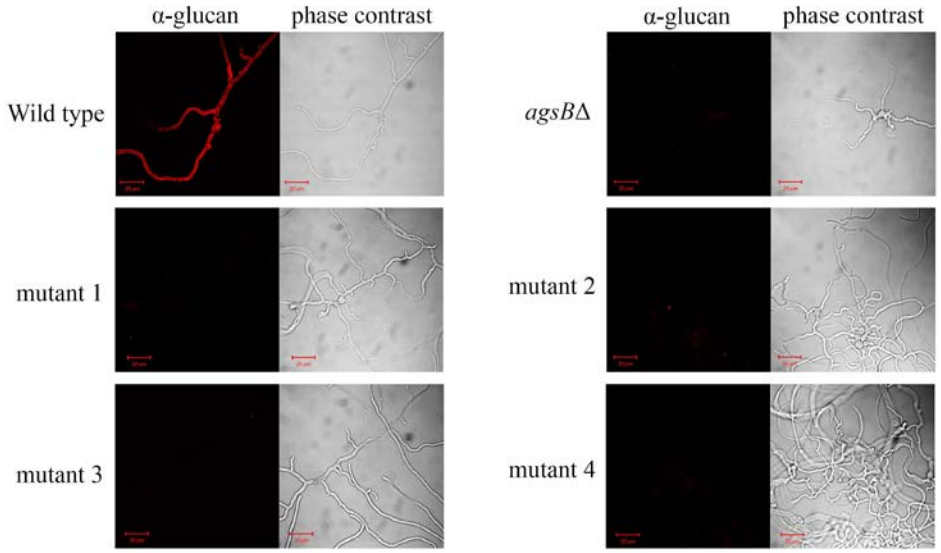

Fig. S3-2 MOPC 104E straining for wild type, *agsB*Δ and *H2A*(p)-*agsB* strains.

Primary antibody MOPC 104E and secondary antibody TRITC-conjugated goat-anti-mouse (Sigma) were used at 1:20 and 1:50 respectively. Samples were examined using a Zeiss META501 confocal epifluorescence microscope at 63 x objective lens. Confocal imaging used 543 nm excitation, with emission controlled by BP 560-615 nm filter.

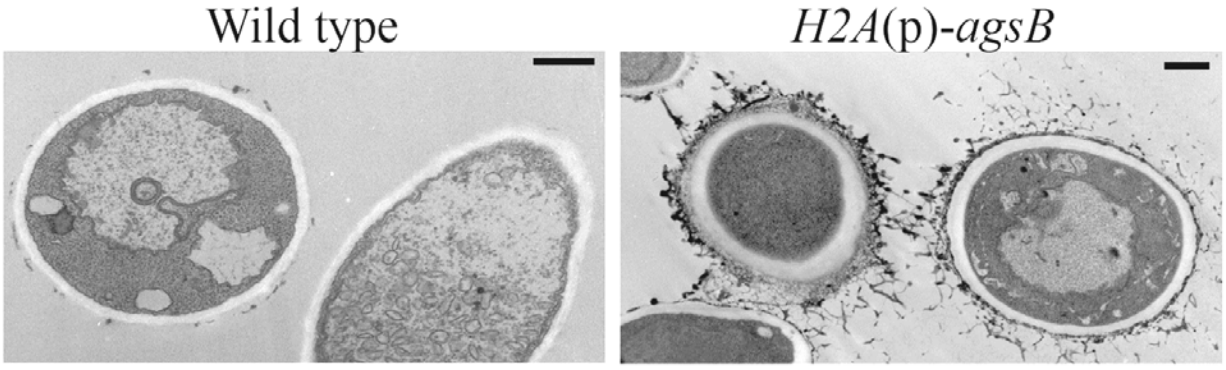

Fig. S3-3 Typical TEM images of wild type and *H2A*(p)-*agsB* strains. Many cells of *H2A*(p)-*agsB* strain are surrounded by excessive extracellular matrix (black materials). Scale bar = 500 nm

CHAPTER 4

AN AMYLASE-LIKE PROTEIN, AmyD, IS THE MAJOR NEGATIVE REGULATOR FOR ALPHA-1,3-GLUCAN SYNTHESIS IN THE *ASPERGILLUS NIDULANS* ASEXUAL LIFE CYCLE

In chapter 2, I found AmyD can repress α-1,3-glucan synthesis in *A. nidulans*. Previously, the only proteins reported to have repressive effects on α-1,3-glucan synthesis were α-1,3-glucanases. Both AmyD and the three annotated α-1,3-glucanases in *A. nidulans* were predicted to have an N-terminal signal peptide and a C-terminal GPI-anchor site. Considering the similar localizations of AmyD and α-1,3-glucanases, I hypothesized that AmyD works together with α-1,3-glucanases to degrade α-1,3-glucan in *A. nidulans*. In this chapter, I examined the function of AmyD in the α-1,3-glucan degradation process along with three putative α-1,3-glucanases to verify that hypothesis. Results from this chapter further explain the α-1,3-glucan metabolism process in *A. nidulans*.

My role in this research: designed the study along with S Kaminskyj who funded it. I wrote thefirst draft; and contributed to the final revised draft.

Results from this chapter have formed a manuscript as “An amylase-like protein, AmyD, is the major negative regulator for α-1,3-glucan synthesis in *Aspergillus nidulans* during the asexual life cycle” by Xiaoxiao He and Susan Kaminskyj.

An amylase-like protein, AmyD, is the major negative regulator for α-1,3-glucan synthesis in *Aspergillus nidulans* during the asexual life cycle

Xiaoxiao He, Susan G. W. Kaminskyj*

Department of Biology, University of Saskatchewan, 112 Science Place, Saskatoon, SK S7N 5E2, Canada

*Author for correspondence

Tel: +1 306 966 4422; email: susan.kaminskyj@usask.ca

Key words: alpha-1,3-glucan, cell wall, alpha-amylase, alpha-1,3-glucanase, *Aspergillus nidulans*

4.1. Abstract

Alpha-1,3-glucan affects fungal cell-cell interactions and is important for the virulence of pathogenic fungi. Interfering with production of α-1,3-glucan could help to prevent fungal infection. In our previous study, we reported that an amylase-like protein, AmyD, could repress α-1,3-glucan accumulation in *Aspergillus nidulans*. To further explore the mechanism of AmyD, we studied its function in the α-1,3-glucan degradation process along with two other predicted amylase-like proteins and three annotated α-1,3-glucanases. AmyC and AmyE share substantial sequence identity with AmyD, however neither affects α-1,3-glucan synthesis. In contrast, AgnB and MutA (but not AgnE) are functional α-1,3-glucanases that also repress α-1,3-glucan accumulation. Nevertheless, the functions of AmyD and these glucanases were independent from each other. The dynamics of α-1,3-glucan accumulation showed different patterns between the AmyD overexpression strain and the α-1,3-glucanase overexpression strains, suggesting AmyD may not be involved in the α-1,3-glucan degradation process. In addition, we confirmed that the final localization of AmyD is on cell membrane. These results suggest the function of AmyD is to directly suppress α-1,3-glucan synthesis, but not to facilitate its degradation.

4.2. Introduction

Alpha-1,3-glucan and β-glucan are major cell wall components for many filamentous fungi as well as for many yeasts (Latgé, 2010). However, they have very different impacts on fungal cells. Beta-glucan is essential for fungal cell survival, at least for species of *Aspergillus* and *Candida* (Douglas et al., 1997; Firon et al., 2002). Hence, β-glucan synthase inhibitors (echinocandins) are used clinically to treat systemic aspergillosis and candidiasis (Denning, 2003). In contrast, α-1,3-glucan has only found to be important for the morphology of *Schizosaccharomyces pombe* (Hochstenbach et al., 1998), particularly for cell integrity at cytokinesis (Cortés et al., 2012). For other fungal species, α-1,3-glucan synthase deleted strains cause minor or no phenotypic change (Rappeleye et al. 2004; Henry et al. 2012; Yoshimi et al. 2013; He et al. 2014). Nevertheless, accumulated evidence has suggested α-1,3-glucan has a role in host-pathogen interaction (Rappleye et al. 2007; Fujikawa et al., 2012; Beauvais et al., 2013), which is important for a successful pathogenesis. Thus, treatments that could eliminate fungal α-1,3-glucan might be able to prevent fungal infection. Unfortunately, to our knowledge no drug is developed yet targeting α-1,3-glucan synthase. As an alternative strategy to blocking the synthesis of α-1,3-glucan, we could potentially degrade α-1,3-glucan from fungal cell walls to achieve the same purpose.

Alpha-1,3-glucanase (hereafter, α-1,3-glucanase) expressed by fungal cells can recycle α-1,3-glucan from their cell walls. In *S. pombe*, α-1,3-glucanase (*Sp*Agn1p) was shown to have

an endo-catalytic hydrolysis ability on α-1,3-glucan (hydrolyzing α-1,3-glucan into pentasaccharides), and thereby was important for successful cell division (Dekker et al, 2004). *Paracoccidioides brasiliensis* α-1,3-glucanase (*Pb*Agn1p) has comparable activity (Villalobos-Duno et al., 2013). In *Trichoderma* species, two α-1,3-glucanases have been characterized, and these were suggested to have anti-fungal effects because their expression was highly induced under antagonistic conditions (Ait-Lahsen et al., 2001, Sanz et al., 2005). Together this is strong evidence that α-1,3-glucanase has the potential to digest α-1,3-glucan from fungal cell walls. Consistent with this, a strain of transgenic rice plants that expressed a bacterial α-1,3-glucanase was more resistant to *Magnaporthe oryzae* (Fujikawa et al., 2012). Therefore, degrading α-1,3-glucan from fungal cell walls is a possible way to prevent fungal infection, and characterization of glucanase-like protein is expected to provide additional useful information about this major but enigmatic wall carbohydrate.

In our previous study, we reported that an amylase-like protein (AmyD) had a repressive effect on α-1,3-glucan synthesis in *A. nidulans* (He et al., 2014). Amylase-like proteins with similar effects were also seen in *S. pombe* (Morita et al., 2006) and *A. niger* (van der Kaaij et al., 2007). These data suggest some amylase-like proteins may have the same potential as α-1,3-glucanase to eliminate α-1,3-glucan from fungal cell walls. To further explore this possibility, we studied the function of AmyD along with two other amylase-like proteins and three α-1,3-glucanases in the α-1,3-glucan degradation process. We found that AmyD was the only amylase-like protein in *A. nidulans* that could repress α-1,3-glucan accumulation, and that

AmyD function was independent from α-1,3-glucanase. The functional α-1,3-glucanases maintained low expression levels in the *A. nidulans* asexual life cycle. Therefore, AmyD is the major negative regulator for α-1,3-glucan accumulation in *A. nidulans* during asexual life cycle. The function of AmyD is more likely to repress α-1,3-glucan synthesis, but not to facilitate its degradation.

4.3. Materials and Methods

4.3.1. Strains, Plasmids and Media

All strains in this study were constructed in *A. nidulans* A1149. The A1149 strain was also the wild type control for all assays in this paper. Strains used in this study are listed in Table S4-2. Primers and plasmids are listed in Table S4-3. Strategies for gene deletion and confirmation methods were described by Szewczyk et al. (2006) and El-Ganiny et al. (2008). Briefly, a targeted replacement construct was constructed by fusion PCR including 1 kb upstream, a selectable marker, and 1 kb downstream (details see Fig. S4-1A). This construct was transformed to A1149 protoplasts. *A. fumigatus pyrG* and *pyroA* were used as selectable markers (details for each strain see Fig. S4-1B). The strategy for promoter exchange was previously described in He et al. (2014). For promoter exchange, the transformation construct was 1 kb upstream of the target, the selectable marker, *actA*(p) and 1 kb of the target gene from 5' end (Fig. S4-1A). The *actA* promoter was amplified from A1149 genomic DNA and the sequence was given in Fig. S4-3. Again, details for each construction are given in Fig. S4-1B. PCR confirmation of each constructed strain is shown in Fig.S4-2. The sequence of each overexpression strain was confirmed by DNA sequencing, and only clones with no mutation were used for further study.

All strains were grown on complete medium (CM per litre: 10 g glucose, 2 g peptone, 1 g yeast extract, 1 g casamino acids, 50 mL 20 x nitrate salts, 1 mL trace elements, 1 mL vitamin solution, pH 6.5) or minimal medium (MM: 10 g glucose, 50 mL 20 x nitrate salts, 1 mL trace

elements, 0.001 % thiamine, pH 6.5) supplemented with nutrition solution as required. Trace elements, vitamin solution, nitrate salt and all nutrition stocks are described in Kaminskyj (2001). For transformation medium, 1 M sucrose was added to MM as osmoticum. All strains were grown at 30 ºC, unless mentioned specifically.

4.3.2. Quantification of Conidiation

1.5 mL CM agar were added to each well of a 24-well plate and seeded with 10^5 conidia after solidification. Plates were incubated for 4 d, then 1 mL ultra-pure water from Barnstead™ Nanopure™ system was used to collect conidia from each well. Conidia were quantified by hemocytometer.

4.3.3. Alpha-1,3-glucan Quantification

The method was adopted from Momany et al. (2004) and Marion et al. (2006). Briefly, 2 x 10^7 conidia were grown at 30 ºC in 100 mL liquid CM, shaken at 150 r.p.m. for 24 h (or the indicated time). Colonies were collected by filtration and washed with 0.5 M NaCl. Cells were frozen at -80 ºC for 2-4 h, then broken in disruption buffer (DB: 20 mM Tris, 50 mM EDTA, pH 8.0) using a Virsonic Ultrasonic Cell Disrupter, until hyphal ghosts formed. Cell walls were separated by centrifugation at 3500 x *g* for 10 min. The pellet containing the cell wall fraction was washed in DB with stirring for 4 h at 4 ºC followed by a wash with sterile ultrapure water under the same conditions, pelleted again, and lyophilized. Dry cell wall samples were weighed, then suspended in 1 M NaOH at 0.5 mg mL^{-1}. Alkaline extraction was performed overnight at

37 ºC. Then 2 mL alkaline-soluble fraction (containing 1 mg cell wall) was used for the following process. The alkali was neutralized by acetic acid until pH 5.5. Alpha-1,3-glucan was collected by centrifugation 12000 x *g* for 10min, and then washed twice in ultrapure water. Finally, α-1,3-glucan was hydrolyzed by 2 mL 3 M H_2SO_4, at 100 ºC for 1 h. Glucose content (mainly from α-1,3-glucan in the alkali-soluble fraction) was quantified by anthrone assay (Ashwell, 1957). All experiments were repeated three times with duplicates each time.

4.3.4. RT-PCR and qPCR

For the time-course expression study, 2 x 10^7 conidia were inoculated in liquid CM and incubated at 30 ºC with or without shaking at 150 r.p.m., then colonies were collected at 14 h and 24 h for both groups. In static condition, only the colonies grown on the liquid surface were collected. Collected colonies were immediately frozen in liquid nitrogen, then lyophilized.

For the overexpression study, 2 x 10^7 conidia were inoculated in liquid CM and incubated at 30 ºC with shaking at 150 r.p.m. for 14 h. Colonies were collected by filtration, immediately frozen in liquid nitrogen, then lyophilized.

Total RNA was extracted using an RNeasy plant kit (Qiagen) following manufacturer's instructions. RNA concentration was measured using a Nanodrop®, then diluted to 500 ng μL^{-1}. Genomic DNA elimination and reverse transcription used a QuaniTect reverse transcription kit (Qiagen) following the manufacturer instructions.

Quantitative real time PCR (qPCR) was performed in 96-well optical plates in an iQ5

real-time PCR detection system (Bio-Rad). Gene expression was assayed in a total volume of 20 µL per reaction containing cDNA at an appropriate dilution and SYBR green fluorescein (Qiagen). A no-template control was used for each pair of primers. Histone was used as a reference gene (Fujioka et al., 2007). Primers for qPCR are listed in Table S4-3.

The qPCR amplification used the following conditions: 95 ºC /15 min for one cycle, 95 ºC /15 s, 55 ºC /40 s and 72 ºC /30 s for 40 cycles and final extension cycle of 72 ºC /2 min. Melting curve analysis was done using the following cycle: 15 s at 65 ºC with an increase of 0.5 ºC each cycle to 95 ºC. The relative expression was normalized to histone and calculated using the ΔΔCt method (Livak and Schmittgen, 2001). Three independent experiments with triplicates were performed for each reaction.

4.3.5. Drug Sensitivity Test

Calcofluor White (American Cyanamid Company) was prepared as a stock at 10 mg mL^{-1} in 25 mM KOH (Hill et al., 2006). The stock solution was sterilized by filtration. For testing, CFW stock solution was added to CM agar cooled to 55~60 ºC. Then, 10^5 conidia of each strain were inoculated on plate on the same day. Plates were incubated for 48 h at 30 ºC.

4.4. Results

4.4.1. AmyC and AmyE do not Affect α-1,3-glucan Accumulation

In the *A. nidulans* genome, there are two putative/annotated amylase-like proteins, AmyC (encoded by ANID4507) and AmyE (encoded by ANID6324) that share high sequence similarity with AmyD. Like AmyD, both are predicted to have an N-terminal signal peptide and a C-terminal GPI-anchor site (de Groot et al. 2009). Their overall amino acid sequence identities to AmyD are 59 % (AmyC) and 47 % (AmyE) respectively, suggesting they could have conserved functions with AmyD.

To study their functions, we first examined their expression levels to see when we could expect to detect their activities. Samples were grown in shaken liquid medium and in static liquid medium for 14 h and 24 h respectively. In shaken liquid medium, *A. nidulans* grows vegetatively (hyphal elongation only) but does not undergo colony development. In static liquid medium, *A. nidulans* could undergo a complete asexual life cycle. Conidiophores with some conidia were seen when we collected the static samples at 24 h. Unlike *amyD* (He et al., 2014), we found *amyC* and *amyE* maintained low expression levels throughout the *A. nidulans* asexual life cycle (represented by high Ct value in qPCR) (Table 4-1). Therefore, their activities are not expected in all asexual life stages.

We chose to overexpress these putative amylase genes instead of deleting them to examine their effects on α-1,3-glucan. In our previous study, we showed that the actin promoter [*actA*(p)] gave a ~2-fold expression for *amyD* in *A. nidulans* (He et al., 2014), so we also used it in this

study for gene overexpression. The *actA*(p)-*amyC* and *actA*(p)-*amyE* strains had no obvious phenotypic change when tested on solid medium, or when grown in shaken liquid medium in respect to the colony size (Fig. 4-1A and B). In contrast, the *actA*(p)-*amyD* strain formed many tiny colonies in shaken liquid (Fig. 4-1B). This suggests that AmyC and AmyE may not have the same function as AmyD. Our qPCR results showed *amyC* and *amyE* were each overexpressed by several hundred-fold when regulated by *actA*(p), consistent with their low expression under native promoters (Table 4-1). However, the α-1,3-glucan content in *actA*(p)-*amyC* and *actA*(p)-*amyE* was comparable to wild type cells (Fig. 4-1C), unlike *actA*(p)-*amyD* (Fig. 4-1C). We interpret this to mean AmyC and AmyE did not reduce α-1,3-glucan accumulation in *A. nidulans*. So far, AmyD is the only reported amylase-like protein that has a repressive effect on α-1,3-glucan accumulation in *A. nidulans*.

4.4.2. MutA as well as AgnB but not AgnE can Repress α-1,3-glucan Accumulation

In order to verify whether AmyD could facilitate α-1,3-glucan degradation, we needed to find a functional α-1,3-glucanase. MutA (encoded by ANID7349) is the only characterized α-1,3-glucanase in *A. nidulans.* However its expression has only been studied for the sexual life cycle (Wei et al., 2001). Two more α-1,3-glucanase encoding genes, *agnB* (ANID3790) and *agnE* (ANID1604) have also been annotated in the *A. nidulans* genome (de Groot et al., 2009). Therefore, AgnB and AgnE were chosen as our study candidates and MutA was included as a positive control.

A time-course expression study showed that both *agnB* and *mutA* had very low expression

throughout the *A. nidulans* asexual life cycle (Table 4-1), whereas expression of *agnE* was highly induced during conidiation (Table 4-1). When the α-1,3-glucanases were individually deleted, this change had no impact on colony phenotypes or α-1,3-glucan content (Fig. 4-2A-C), as we expected due to their low expression levels in vegetative growth. When the α-1,3-glucanases were individually overexpressed by *actA*(p), each had a many hundred-fold increase in expression level (Table 4-1), but only the overexpression of AgnB and MutA led to a lower α-1,3-glucan content (Fig. 4-2F). Therefore, AgnB and MutA are the functional α-1,3-glucanases in our test. Intriguingly, both *actA*(p)-*agnB* and *actA*(p)-*mutA* behaved the same as wild type in shaken liquid medium (Fig. 4-2E), unlike *actA*(p)-*amyD* that formed tiny colonies (Fig. 4-1B).

The *actA*(p)-*agnB* strain had a pale conidia color for colonies grown on solid medium (Fig. 4-2D), although quantification of conidiation did not show obvious difference (Table S4-1). This suggests that the conidia color difference could be due to a defect in pigment formation somehow related to the overexpression of *agnB*.

We then also deleted AgnB and MutA together, just in case they might compensate for each other when individually deleted. However, the double deletion strain still had no impact on α-1,3-glucan content (Fig. 4-2C).

4.4.3. Functions of AgnB and MutA are Independent from AmyD

Our results showed that AgnB, MutA and AmyD all had similar repressive effects on α-1,3-glucan content when overexpressed (Fig. 4-1D and 4-2F). Considering they each have a

signal peptide and a GPI-anchor site (de Groot et al., 2009), we hypothesized that AmyD may work together with either or both α-1,3-glucanases to degrade α-1,3-glucan (He et al., 2014). If our hypothesis was correct, the repressive effects on α-1,3-glucan content from AgnB and MutA should be abolished or reduced when AmyD was deleted. To verify this, we generated [*actA*(p)-*agnB, amyD*Δ] and [*actA*(p)-*mutA, amyD*Δ] strains. We found these two strains had wild type phenotypes on solid medium and in shaken liquid medium (Fig. 4-3A and B). The pigment defect in *actA*(p)-*agnB* was recovered with the deletion of *amyD* (Fig. 4-2D and 4-3A). However, both strains still showed low α-1,3-glucan content similar as in *actA*(p)-*agnB* and *actA*(p)-*mutA* (Fig. 4-3C and 4-2F), indicating the effects of AgnB and MutA were still present. Therefore, the functions of AgnB and MutA appear to be independent from AmyD.

4.4.4. Dynamics of α-1,3-glucan Accumulation Affects Colony Formation in Liquid as well as Calcofluor White Drug Sensitivity

It was interesting to see that *actA*(p)-*agnB*, *actA*(p)-*mutA*, and *actA*(p)-*amyD* strains had similar α-1,3-glucan content (Fig. 4-1D and 4-2F), but behaved differently in shaken liquid medium (compare Fig. 4-1B with 4-2E). We think this may be because of how α-1,3-glucan accumulates in these strains. In all our previous quantification experiments, we collected the fungal cell samples at 24 h post inoculation. In contrast, visualization of colonies in shaken liquid medium had typically been done earlier, usually around 16 h post inoculation. So, we also collected additional samples at 16 h and 20 h post inoculation to examine the dynamics of α-1,3-glucan accumulation in cell walls. Results showed very different patterns of α-1,3-glucan

accumulation in these strains (Fig. 4-4A). In wild type, α-1,3-glucan content did not stay at a constant level but showed a continuous growing trend from 16 h to 24 h. In *actA*(p)-*amyD*, the growing trend was maintained, but at each time point the concentration of α-1,3-glucan was only about 50 % of wild type. However, in *actA*(p)-*agnB* and *actA*(p)-*mutA*, α-1,3-glucan content showed a decreasing trend from 16 h to 24 h. We also noticed that at 16 h the α-1,3-glucan content in wild type, *actA*(p)-*agnB* and *actA*(p)-*mutA* was very similar, whereas the α-1,3-glucan content in *actA*(p)-*amyD* was much lower.

In our previous work, we found that α-1,3-glucan content was correlated with sensitivity to Calcofluor White (CFW) (He et al., 2014). We wondered if this change was also correlated with α-1,3-glucan content in early life stage. We tested all stains on 50 μg mL^{-1} CFW. Only *actA*(p)-*amyD* showed delayed germination and/or slower growth, whereas all other strains maintained the same growth ability (Fig. 4-4B).

4.4.5. The localization of AmyD associates with cell membrane

In order to understand the mechanism of AmyD, it is important to figure out the localization of this protein. However, due to the hinder from the AmyD protein structure and the GPI-anchor site, we did not get viable signal when the GFP was tagged after the signal peptide (between 26th and 27th amino acid) or tagged after the GPI-anchor site. To sovle these problems, we replaced the amylase domain of AmyD (from the 63^{th} to the 507^{th} amino acid) by a GFP (details of strain's construction see Fig. S4-4). The N-terminal signal peptide and C-terminal GPI anchor site of AmyD were maintained, which are the elements determined the localization of AmyD.

The GFP signal of the constructed strain (AmyD-GFP) showed strong association with septa (Fig. 4-5A) and cell membrane (Fig. 4-5B), although some signal also presented in the cytoplasm. We interpret these as showing the final localization of AmyD is on cell membrane, which is the same as a GPI-anchor protein.

4.5. **Discussion**

In our previous study, we reported that AmyD repressed α-1,3-glucan accumulation in *A. nidulans*, and we hypothesized that AmyD might work together with one or more α-1,3-glucanases to degrade α-1,3-glucan (He et al., 2014). In our current study, we extended our work to α-1,3-glucan degradation-related genes to further understand the function of AmyD.

4.5.1. AmyD is the Major Negative Regulator of α-1,3-glucan Accumulation in the *A. nidulans* Asexual Life Cycle

AmyC and AmyE share high sequence similarity with AmyD, however our results showed they do not affect α-1,3-glucan accumulation. They also had no impact on starch digestion when tested on starch-only medium (*unpublished data*), so their functions are still unclear. So far, AmyD is the only reported amylase-like protein that can repress α-1,3-glucan accumulation in *A. nidulans*. From our results, two α-1,3-glucanases (AgnB and MutA) showed similar repressive effects as AmyD when overexpressed (Fig. 4-2F). However, each maintained a very low expression level in the *A. nidulans* asexual life cycle (Table 4-1). Altogether, we conclude AmyD is the major negative regulator of α-1,3-glucan accumulation during the *A. nidulans* asexual life cycle.

4.5.2. Functions of α-1,3-glucanases and AmyD are Independent from Each Other

Our results confirmed MutA as a functional α-1,3-glucanase and also revealed AgnB but not

AgnE had the same effect as AmyD to repress α-1,3-glucan accumulation. However, the low expression level of *mutA* and *agnB* in the *A. nidulans* asexual life cycle (Table 4-1) suggested α-1,3-glucan degradation is not active during these stages. This is consistent with why even the *mutA* and *agnB* double deletion strain maintained the same α-1,3-glucan content as wild type. This also could explain why the most prominent anti-α-1,3-glucan antibody-staining signal was from the older hyphae (He et al., 2014), because α-1,3-glucan was not recycled during the asexual life cycle. With this in mind, we think the function of AmyD is not based on α-1,3-glucanase.

On the other hand, *amyD* had a relatively high expression level during *A. nidulans* asexual development (He et al., 2014). It is still possible the function of α-1,3-glucanase depends on AmyD. However, when *amyD* was deleted from *actA*(p)-*agnB* and *actA*(p)-*mutA*, the repressive effects on α-1,3-glucan from AgnB and MutA were maintained (Fig. 4-3C). Therefore, the functions of these glucanases are independent from AmyD. Evidence from other α-1,3-glucanase characterization work also showed α-1,3-glucanase is functional by itself (Ait-Lahsen et al., 2001; Dekker et al, 2004; Villalobos-Duno et al., 2013). In our study, we did find the deletion of *amyD* in an *actA*(p)-*agnB* strain reversed the pigment formation defect (compare Fig. 4-2D with 4-3A), which was a specific phenotypic change in *actA*(p)-*agnB*. Otherwise, we have never found low α-1,3-glucan content leads to a pigment defect. Therefore, we think this phenotypic change does not relate to α-1,3-glucan content.

4.5.3. Alpha-1,3-glucan Content in Early Life Stage is Critical for Colony Formation in Shaken Liquid as well as Drug Sensitivity

Our dynamics study showed the α-1,3-glucan accumulation processes in *actA*(p)-*agnB* and *actA*(p)-*mutA* are very different from *actA*(p)-*amyD* (Fig. 4-4A). Although these colonies had similar α-1,3-glucan content after 24 h growth, the α-1,3-glucan content at earlier times (16 h and 20 h) was very different. Especially at 16 h, the α-1,3-glucan content in *actA*(p)-*agnB* and *actA*(p)-*mutA* was almost the same as wild type, whereas in *actA*(p)-*amyD* it was only half that of wild type. This could explain why *actA*(p)-*agnB* and *actA*(p)-*mutA* formed the regular size colonies as wild type (Fig. 4-3E), because colony formation in shaken liquid was already complete at 16 h. Even though the α-1,3-glucan content decreased in these two strains at later time, the formed colonies were unable to disassemble. The same principle also explained why *actA*(p)-*agnB* and *actA*(p)-*mutA* maintained the same drug sensitivity as wild type (Fig. 4-4B). When *A. nidulans* was stressed by CFW, spore germination was delayed. However, the higher α-1,3-glucan content in early life stage enabled the *actA*(p)-*agnB* and *actA*(p)-*mutA* strains to form colonies faster than *actA*(p)-*amyD*.

Why the effects of AgnB and MutA started later than AmyD still needs further investigation, however it is clear the mechanism of AmyD is different from α-1,3-glucanase. According to the different α-1,3-glucan accumulation patterns (Fig. 4-4A), it is more likely that AmyD directly represses α-1,3-glucan synthesis rather than facilitates α-1,3-glucan degradation. One of the possible reasons is AmyD may affect the major α-1,3-glucan synthase (AgsB) expression.

However, when we replaced the native promoter of *agsB* with *alcA*(p) and grew the strain under constant expression condition (100 mM threonine) (as per Alam et al., 2012), we found the repressive effect from AmyD overexpression was still present (*unpublished data*), suggesting that AmyD did not affect *agsB* expression.

AgtA, the homologue of AmyD in *A. niger*, has been enzymatically characterized (van der Kaaij et al., 2007). Their results showed AgtA has very low starch hydrolysis ability but serves as a glucanotransferase on α-1,4-glucosidic linkages. The amino acid sequence identity between AmyD and AgtA is 70 %, so it is highly likely AmyD will have a similar function as AgtA, but this will need enzymatic study to confirm and is beyond the scope of our current work. Further study on the mechanism of AmyD will also require establishing an *in vitro* α-1,3-glucan synthesis system to find out how AmyD prevents the synthesis. Nevertheless, considering the different mechanisms between AmyD and α-1,3-glucanase, AmyD likely cannot be used the same way as α-1,3-glucanase to prevent fungal infection.

In summary, AmyD localizes on cell membrane and is the only reported amylase-like protein that can repress α-1,3-glucan accumulation in *A. nidulans*. Expression analysis showed AmyD is the major negative regulator during the *A. nidulans* asexual life cycle. The function of AmyD is independent from the α-1,3-glucanases MutA and AgnB. The dynamics study showed the effect of AmyD started earlier than α-1,3-glucanase, and the mechanism of AmyD is different from the α-1,3-glucanase. These data suggested AmyD may not serve for α-1,3-glucan degradation, but directly represses α-1,3-glucan synthesis at the protein level.

4.6. Acknowledgements

We are pleased to acknowledge support from the Natural Science and Engineering Council of Canada Discovery Grant program (SGWK), and the Graduate Teaching Fellowship from University of Saskatchewan (XH). We thank Dr. Peta Bonham-Smith lab (Department of Biology, University of Saskatchewan) for access to qPCR.

4.7. Tables

Table 4-1: Time-course expression study

	Shaken growth		Static growth		Overexpression by *actA*(p)
genes	14 h	24 h	14 h	24 h	14h
amyC	1	1.44 ± 0.44	1.28 ± 0.28	18.84 ± 6.36	794.13 ± 190.28
amyE	1	1.72 ± 0.71	1.93 ± 0.49	27.82 ± 9.79	484.82 ± 140.61
agnB	1	2.16 ± 0.63	2.39 ± 0.83	11.71 ± 3.93	871.00 ± 191.59
agnE	1	1.92 ± 0.57	1.59 ± 0.53	274.90 ± 85.55	1268.84 ± 292.38
mutA	1	2.97 ± 0.89	2.31 ± 0.96	6.96 ± 1.99	1753.59 ± 654.97

2×10^7 conidia were inoculated in liquid CM and incubated at 30 ºC under indicated conditions. The overexpression strains were grown in shaken condition for 14 h. Expression of each gene in 14 h shaken growth group was defined as 1. Results present the mean of three independent qPCR tests with triplicates each time ± standard deviation.

4.8. Figures

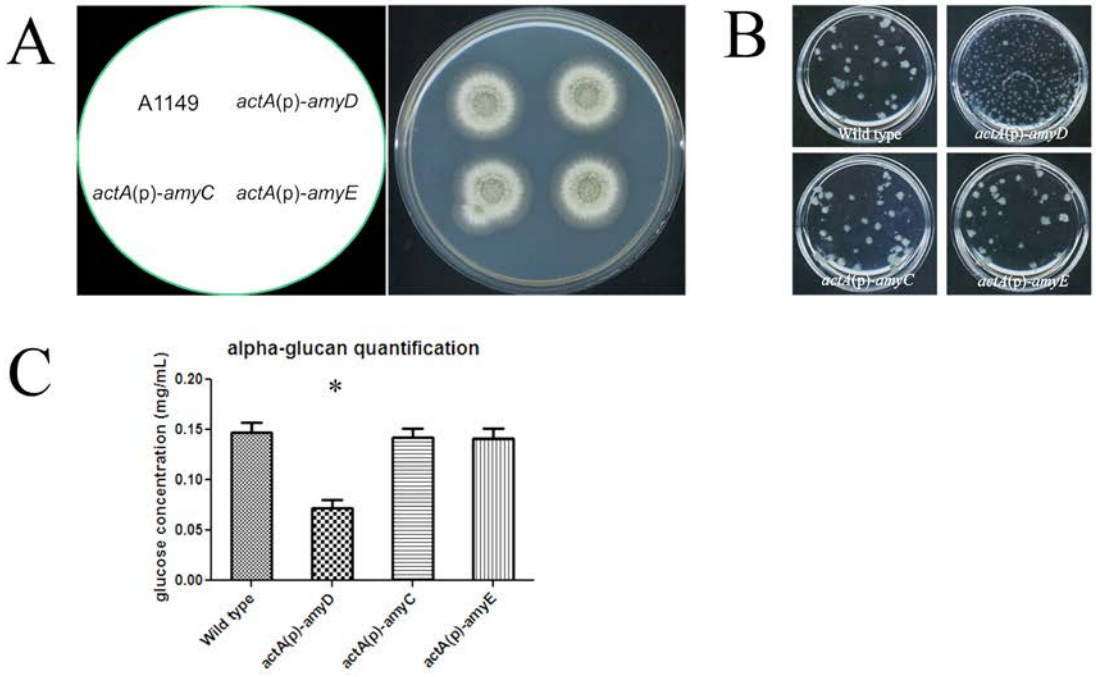

Fig. 4-1 AmyC and AmyE do not affect α-1,3-glucan accumulation

A. 10^5 freshly harvested conidia of each strain were inoculated on complete medium and the plates were incubated at 30 °C for 48 h. All constructed strains showed the wild type colony phenotype on solid medium.

B. 5 x 10^7 freshly harvested conidia were inoculated in flasks with 20 mL complete medium, then was incubated at 30 °C, 150 r.p.m. overnight. Only *actA*(p)-*amyD* formed tiny colonies.

C. 2 x 10^7 spores of each strain were inoculated in flasks with 100 mL complete medium. Samples were grown at 30 °C with 150 r.p.m. for 24h. Alpha-1,3-glucan was extracted from 1 mg dry cell wall, and then digested to glucose and quantified by anthrone assay. Results represent the mean of three independent quantification tests with duplicates each time ± standard deviation. The data of each mutant were compared with the data of wild type (column 1) individually by Mann Whitney U Test. The significant difference ($P<0.05$) was indicated by asterisks.

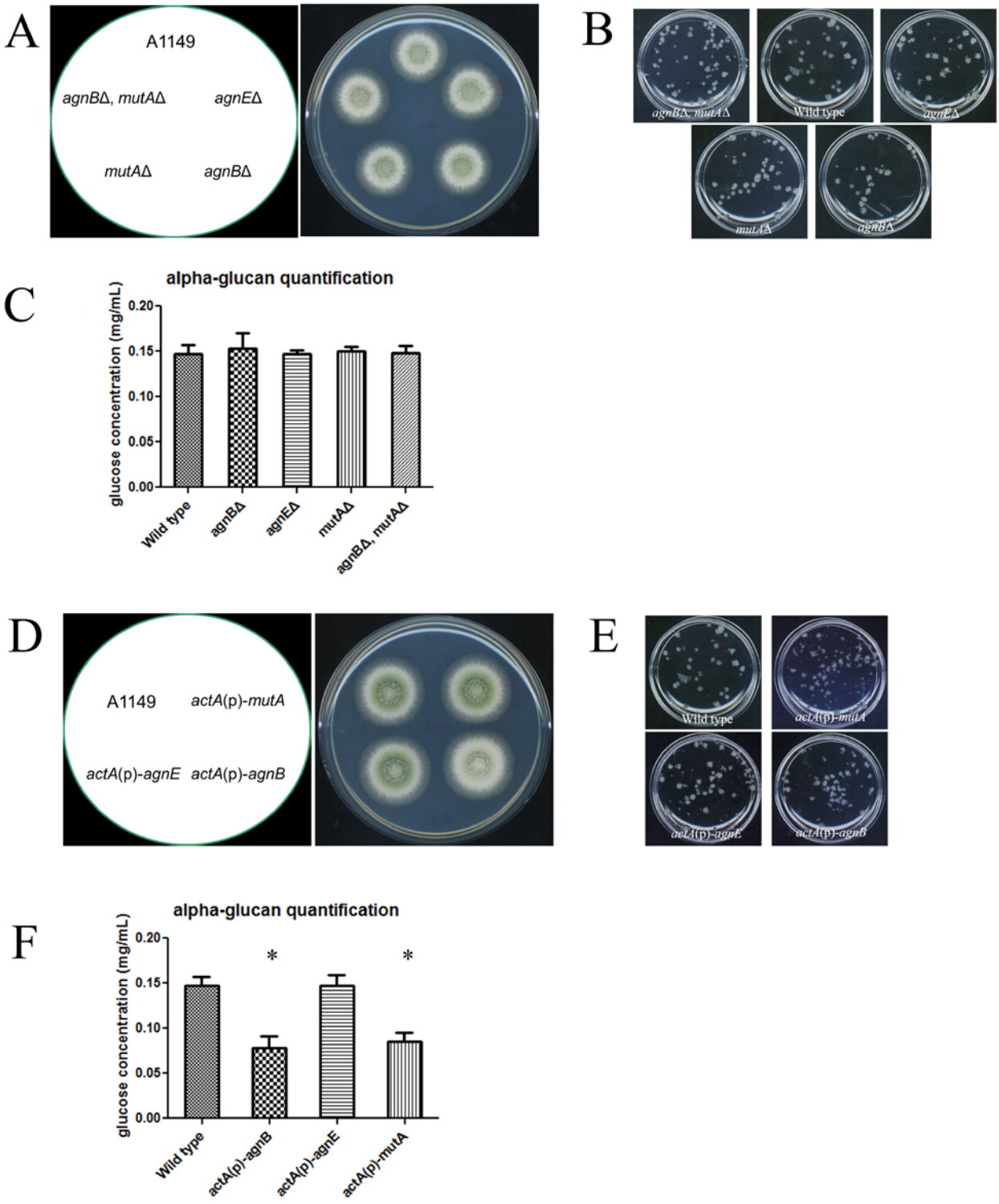

Fig. 4-2 AgnB and MutA are functional α-1,3-glucanases

A. 10^5 freshly harvested conidia of each strain were inoculated on complete medium and the

plates were incubated at 30 °C for 48 h. All constructed strains showed the wild type colony phenotype on solid medium.

B. 5 x 10^7 freshly harvested conidia were inoculated in flasks with 20 mL complete medium, then were incubated at 30 °C, 150 r.p.m. overnight. All strains behaved the same as wild type.

C. 2 x 10^7 spores of each strain were inoculated in flasks with 100 mL liquid complete medium. Samples were grown at 30 °C with 150 r.p.m. for 24h. Alpha-1,3-glucan was extracted from 1 mg dry cell wall, and then digested to glucose and quantified by anthrone assay. Results represent the mean of three independent quantification tests with duplicates each time ± standard deviation. The data of each mutant were compared with the data of wild type (column 1) individually by Mann Whitney U Test. No significant difference was found.

D. 10^5 freshly harvested conidia of each strain were inoculated on complete medium and the plates were incubated at 30 °C for 48 h. Only *actA*(p)-*agnB* showed pigment deficiency.

E. 5 x 10^7 freshly harvested conidia were inoculated in flasks with 20 mL liquid complete medium, then incubated at 30 °C, 150 r.p.m. overnight. All strains behaved the same as wild type.

F. 2 x 10^7 spores of each strain were inoculated in flasks with 100 mL liquid complete medium. Samples were grown at 30 °C with 150 r.p.m. for 24h. Alpha-1,3-glucan was extracted from 1 mg dry cell wall, and then digested to glucose and quantified by anthrone assay. Results represent the mean of three independent quantification tests with duplicates each time ± standard deviation. The data of each mutant were compared with the data of wild type (column 1) individually by Mann Whitney U Test. The significant difference ($P<0.05$) was indicated by asterisks.

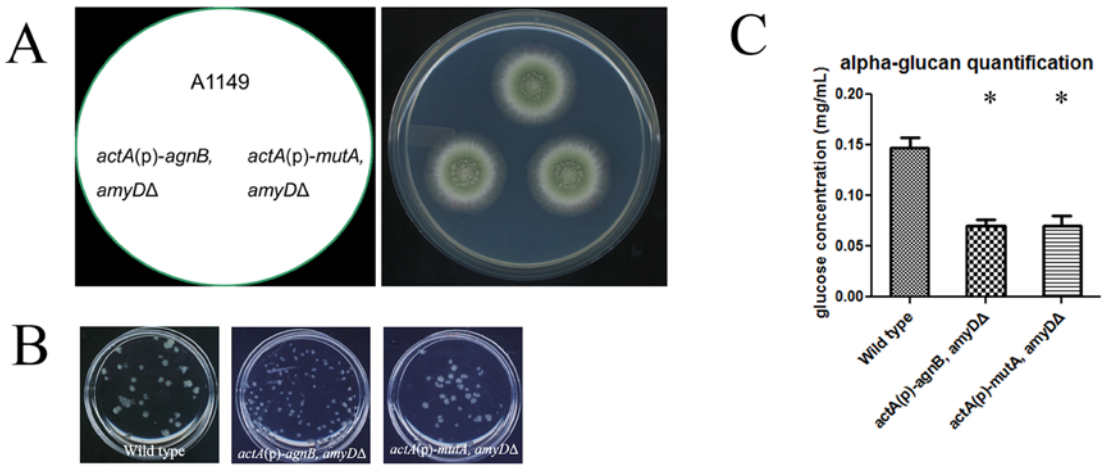

Fig. 4-3 AmyD is not required for the functions of AgnB and MutA

A. 10^5 freshly harvested conidia of each strain were inoculated on complete medium and the plates were incubated at 30 °C for 48 h. All constructed strains showed the wild type colony phenotype on solid medium.

B. 5 x 10^7 freshly harvested conidia were inoculated in flasks with 20 mL liquid complete medium, then the flask was incubated at 30 °C, 150 r.p.m. overnight. All strain behaved the same as wild type.

C. 2 x 10^7 spores of each strain were inoculated in flasks with 100 mL liquid complete medium. Samples were grown at 30 °C with 150 r.p.m. for 24h. Alpha-1,3-glucan was extracted from 1 mg dry cell wall, and then digested to glucose and quantified by anthrone assay. Results represent the mean of three independent quantification tests with duplicates each time ± standard deviation. The data of each mutant were compared with the data of wild type (column 1) individually by Mann Whitney U Test. The significant difference ($P<0.05$) was indicated by asterisks.

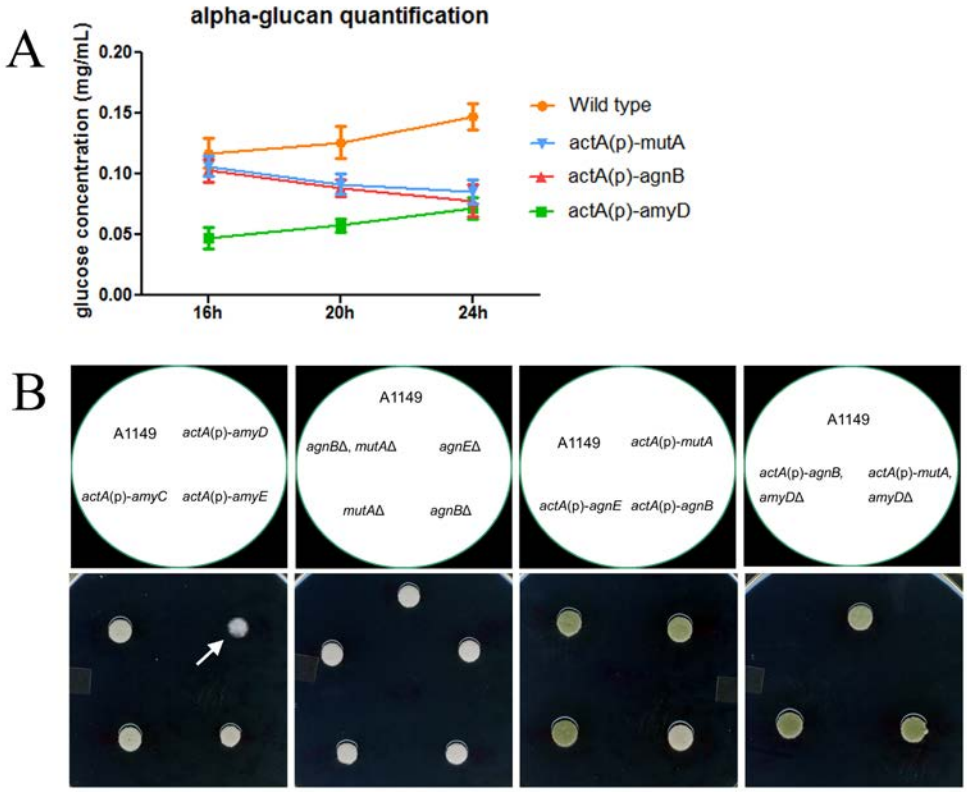

Fig. 4-4 Alpha-1,3-glucan content in early germination and growth is critical for colony formation in shaken liquid medium and drug sensitivity against CFW

A. Dynamics of α-1,3-glucan accumulation in each strain. 2 x 10^7 spores of each strain were inoculated in flasks with 100 mL liquid complete medium. Samples were grown at 30 °C with 150 r.p.m. for 16h, 20h and 24h respectively. Alpha-1,3-glucan was extracted from 1 mg dry cell wall, and then digested to glucose and quantified by anthrone assay. Wild type and *actA*(p)-*amyD* showed the same increasing trend from 16 h to 24 h, except the glucose concentration in *actA*(p)-*amyD* was much lower than wild type at each time point. The *actA*(p)-*agnB* and *actA*(p)-*mutA* had the same decreasing trend from 16 h to 24 h.

B. 10^5 freshly harvested conidia of each strain were inoculated on 50 μg mL^{-1} CFW plate and the plates were incubated at 30 °C for 48 h. Only *actA*(p)-*amyD* (arrow) showed delayed germination and growth.

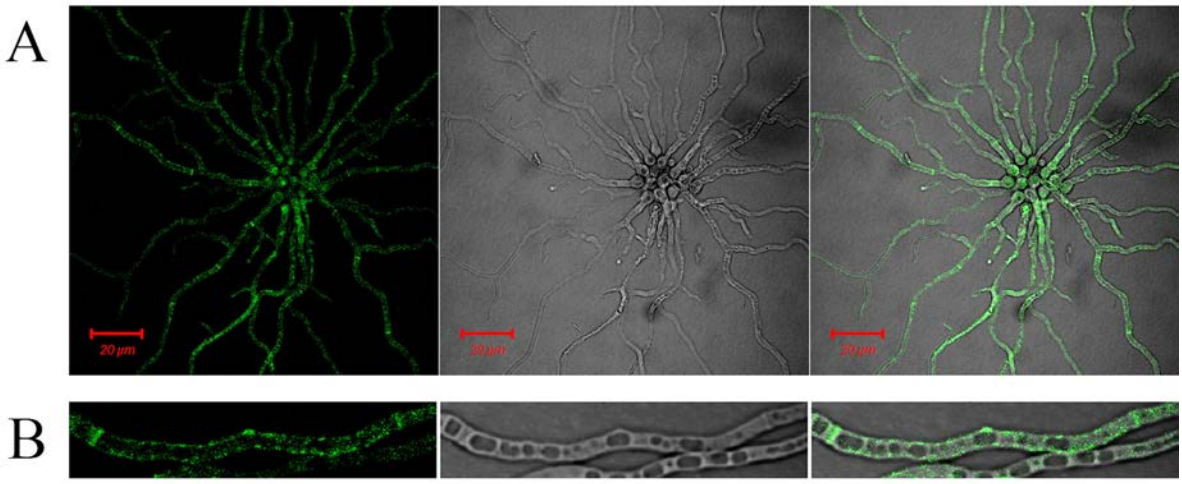

Fig. 4-5 Localization of AmyD associates with cell membrane

Then samples were examined using a Zeiss META501 confocal epifluorescence microscope at 63 x or 25 x objective lens. Confocal imaging used 488 nm excitation with emission controlled by BP 505-530 nm filter. The GFP singal mostly associated with septa and cell membrane.

4.9. Supplemental Materials

Table S4-1 Quantification of conidiation

Medium	**CM**	
Strains	Wild type	*actA*(p)-*agnB*
Conidiation	100% ± 9.7%	94.7% ± 5.9%

10^5 conidia were grown on 1.5mL medium in 24-well plates at 30 °C for 4 d. 1 mL ultra-pure water was used to collect conidia from each well. Conidia were quantified by hemocytometer. Results represent the average of three independent quantification tests with triplicates each time ± standard deviation.

Table S4-2 *Aspergillus nidulans* strains in this study

Strains	alias	Genotype	Origin
A1149	A1149	*pyrG89*; *pyroA4*; *nkuA*::*argB*	FGSC*
actA(p)-*amyD*	AXH38	*amyD*p:: *AfpyroA*:*actA*p:*amyD*; *pyrG89*; *pyroA4*; *nkuA*::*argB*	He et al. 2014
actA(p)-*amyC*	AXH52	*amyC*p:: *AfpyroA*:*actA*p:*amyC*; *pyrG89*; *pyroA4*; *nkuA*::*argB*	this study
actA(p)-*amyE*	AXH53	*amyE*:: *AfpyroA*:*actA*p:*amyE*; *pyrG89*; *pyroA4*; *nkuA*::*argB*	this study
*agnB*Δ	AXH78	*AN3790*:: *AfpyroA*; *pyrG89*; *pyroA4*; *nkuA*::*argB*	this study
*agnE*Δ	AXH42	*AN1604*:: *AfpyroA*; *pyrG89*; *pyroA4*; *nkuA*::*argB*	this study
*mutA*Δ	AXH79	*AN7349*::*AfpyrG*; *pyrG89*; *pyroA4*; *nkuA*::*argB*	this study
*agnB*Δ, *mutA*Δ	AXH80	*AN3790*:: *AfpyroA*; *AN7349*::*AfpyrG*; *pyrG89; pyroA4*; *nkuA*::*argB*	this study
actA(p)-*agnB*	AXH50	*agnB*p:: *AfpyroA*:*actA*p:*agnB*; *pyrG89*; *pyroA4*; *nkuA*::*argB*	this study
actA(p)-*agnE*	AXH47	*agnE*p:: *AfpyroA*:*actA*p:*agnE*; *pyrG89*; *pyroA4*; *nkuA*::*argB*	this study
actA(p)-*mutA*	AXH51	*mutA*p:: *AfpyroA*:*actA*p:*mutA*; *pyrG89*; *pyroA4*; *nkuA*::*argB*	this study
actA(p)-*agnB, amyD*Δ	AXH55	*agnB*p:: *AfpyroA*:*actA*p:*agnB*; *AN3308*::*AfpyrG*; *pyrG89*; *pyroA4*; *nkuA*::*argB*	this study
actA(p)-*mutA, amyD*Δ	AXH56	*mutA*p:: *AfpyroA*:*actA*p:*mutA*; *AN3308*::*AfpyrG*; *pyrG89*; *pyroA4*; *nkuA*::*argB*	this study
AmyD-GFP	AXH86	*amyD*:: *AfpyroA*:*actA*p:*gfp*; *pyrG89*; *pyroA4*; *nkuA*::*argB*	this study

* Fungal Genetics Stock Center

Table S4-3 Primers and plasmids in this study

Primers	Sequence 5' to 3'	Description
Selective marker and strain confirmation		
AME1	ATGTCGTCCAAGTCGCAATT	Af*pyrG**
AME2	TCATGACTATGCCGCATACTAC	Af*pyrG**
SE231	GGACATCAGATGCTGGATTACTAAAG	Af*pyroA* with native promoter
SE232	TTACCATCCTCTCTTGGCCA	Af*pyroA* with native promoter
AME7	CAATACCGTCCAGAAGCAATAC	Af*pyrG* confirmation*
AME8	CACATCCGACTAGCACTATCC	Af*pyrG* confirmation*
AME15	ATTCCTGTCATGGCCAAAG	Af*pyroA* confirmation*
AME16	TCAACAACATCTCCGGTACC	Af*pyroA* confirmation*
SE101	ATGAAAATCCTCCCATCCTTG	*amyD* clone F
SE102	TCACGCCAAAAGCAGTACG	*amyD* clone R
Gene deletion		
SE103	CGGCCATTGACCATGAAC	*amyD* upstream F
SE104	AATTGCGACTATGGACGACATTGTGACGATGTCTGGACCG	*amyD* upstream R (pyrG tail)
SE105	GAGTATGCGGCAAGTCATGATTTGATCTGTTTTCATCTTTTTGC	*amyD* downstream F (pyrG tail)
SE106	GTCATAGATGTCATACCCGTTTCC	*amyD* downstream R
SE107	GTCTTCATCCGGTCCACTATC	*amyD* Fusion F
SE108	GAAGATGAGGGTGTTGTCG	*amyD* Fusion R
SE343	GGGGAGTCGAGTTTACACCA	*agnB* upstream F
SE344	CTTAGTAATCCAGCATCTGATGTCCGATCTGGACCGTCAGTTTCG	*agnB* upstream R (pyroA tail)
SE408	TGGCCAAGAGAGGATGGTAATTAGCGCATTGTTTCTGCAG	*agnB* downstream F (pyroA tail)
SE409	GTAGAGACCGCGCTCTGTCT	*agnB* downstream R
SE347	TTCTCAGTAACCCCCAAGACG	*agnB*Δ Fusion F
SE410	CGAAGACTGACTTTGGTACCG	*agnB*Δ Fusion R
SE320	ATGCCATTGAGCTGGACATT	*agnE* F
SE321	TCATATCAGGCAAGAGAGCAGG	*agnE* R
SE322	CTGGCGAGAGATTCTGGAAC	*agnE* upstream F
SE323	TCCATTACCCATTTCGAAGC	*agnE* upstream R (pyroA tail)
SE324	TGGCCAAGAGAGGATGGTAACACCTAATACCAGGCCAGTTTT	*agnE* downstream F (pyroA tail)
SE325	CCTCATATAGAGACCGCGCA	*agnE* downstream R
SE326	CTAGCCTAGCATCTTTACCGACTG	*agnE*Δ Fusion F
SE327	GTAGAGTTGGGACTTAAGCTAGTCG	*agnE*Δ Fusion R
SE349	AGTAATTTCGCGCGATACCC	*mutA* upstream F
SE411	GGGCGAGCCTTTAACGTACAGTTGCTTGCTTGAGGCT	*mutA* upstream R (pyrG tail)
SE190	AATTGCGACTTGGACGACATGGTGTTTAGGGGTG	*actA*p R (pyrG tail)
SE191	TACGTTAAAGGCTCGCCC	*actA*p F
SE412	GAGTATGCGGCAAGTCATGATGCTAGAAGGATCGAGCCA	*mutA* downstream F (pyrG tail)
SE413	GTTTTCCTCTGACCCAGTCG	*mutA* downstream R
SE353	GTTCGAGTTGGTTGCGAGTC	*mutA*Δ Fusion F
SE414	CCAAGTTGAGTCTTACGCCG	*mutA*Δ Fusion R

Promoter exchange and GFP tagging		
SE234	TGGCCAAGAGAGGATGGTAATACGTTAAAGGCTCGCCC	*actA*(p) F (pyroA tail)
SE208	GGTGTTTAGGGGTGGATTAGAA	*actA*(p) R
SE355	AGAGCTCATCGTGAAGGATGA	*amyC* upstream F
SE356	CTTAGTAATCCAGCATCTGATGTCCGGTTTGATAGACGGATCTTGTCTT	*amyC* upstream R (pyroA tail)
SE357	TTCTAATCCACCCCTAAACACCATGACTGACAGATTCGCCC	*amyC* F (*actA*(p) tail)
SE358	CGTGTTGTAAAGTGGGGAGG	*amyC*_1100 R
SE359	CCTGGAAGTACCTAGGAAACTGG	*actA*(p)-*amyC* Fusion F
SE360	AAATTATTGAGTCTAATGGGCGAC	*actA*(p)-*amyC* Fusion R
SE361	GGCGCTCCAGTTATACCG	*amyE* upstream F
SE362	CTTAGTAATCCAGCATCTGATGTCCCCTTAGAAAGGTAGGTTGCTGTG	*amyE* upstream R (pyroA tail)
SE363	TTCTAATCCACCCCTAAACACCATGCGGCGCCTCACATGT	*amyE* F (*actA*(p) tail)
SE364	GTCAGTAGAAGTATGCAGCAGGTTCT	*amyE*_1100 R
SE365	AAATACCGTTCACCTTGGACG	*actA*(p)-*amyE* Fusion F
SE366	CATGGGGTAATTCAGGAGACC	*actA*(p)-*amyE* Fusion R
SE343	GGGGAGTCGAGTTTACACCA	*agnB* upstream F
SE344	CTTAGTAATCCAGCATCTGATGTCCGATCTGGACCGTCAGTTTCG	*agnB* upstream R (pyroA tail)
SE345	TTCTAATCCACCCCTAAACACCATGTATCTGAAAACGCTCTTTTTG	*agnB* F (*actA*(p) tail)
SE346	TTCTCGTCTTGAATGTACTGGTC	*agnB*_1140 R
SE347	TTCTCAGTAACCCCCAAGACG	*actA*(p)-*agnB* Fusion F
SE348	GAATGCTGCTCACATGTCCA	*actA*(p)-*agnB* Fusion R
SE322	CCGACTGACCATTTGCATC	*agnE* upstream F
SE323	CTTAGTAATCCAGCATCTGATGTCCTTTGCTTCAGGTTCGCTTC	*agnE* upstream R (pyroA tail)
SE340	TTCTAATCCACCCCTAAACACCATGCCATTGAGCTGGACATT	*agnE* F (*actA*(p) tail)
SE341	ACAGCTTGATGAGAGCTCTTGC	*agnE*_1100 R
SE326	CTAGCCTAGCATCTTTACCGACTG	*actA*(p)-*agnE* Fusion F
SE342	TCACAGGGCCGATATAATGG	*actA*(p)-*agnE* Fusion R
SE349	AGTAATTTCGCGCGATACCC	*mutA* upstream F
SE350	CTTAGTAATCCAGCATCTGATGTCCCAGTTGCTTGCTTGAGGCT	*mutA* upstream R (pyroA tail)
SE351	TTCTAATCCACCCCTAAACACCATGAAGATCTTCCACCGCTG	*mutA* F (*actA*(p) tail)
SE352	CTAGGCGCTAAAAGAGCCAA	*mutA*_1100 R
SE353	GTTCGAGTTGGTTGCGAGTC	*actA*(p)-*mutA* Fusion F
SE354	TACGTCAACCGAAAACTCCAG	*actA*(p)-*mutA* Fusion R
SE429	CCAGTGAAAAGTTCTTCTCCTTTACTGCAGTATAGACCAGCGGTCG	*amyD*_186R gfp tail
SE427	CATGGCATGGATGAACTATACAAAGCTGGGGGGAACGTTAGT	*amyD*_1633F gfp tail
SE328	AGTAAAGGAGAAGAACTTTTCACTGG	gfp F no start codon
SE315	TTTGTATAGTTCATCCATGCCATG	gfp R no stop codon
qPC		
SE244	CACCCGGACACTAGGTATCTC	Histone qPCR F#
SE245	GAATACTATCGTAACGGCCTTGG	Histone qPCR R#
SE153	GGATGGAGATGACCCTGCTA	*amyD* qPCR F
SE154	TGCGCATCATGGTAGTCATT	*amyD* qPCR R
SE334	GGATTCCAGCCAAGTGTTGT	*amyC* qPCR F

SE335	AAAGCCCACTCCCTCTCATT	*amyC* qPCR R
SE336	TCTGGGTAAAGGGACTGGTG	*amyE* qPCR F
SE337	GTAGACTTCCCCCATCGTGA	*amyE* qPCR R
SE332	CTGGCGAGAGATTCTGGAAC	*agnB* qPCR F
SE333	TCCATTACCCATTTCGAAGC	*agnB* qPCR R
SE330	CATGATGGGTGGAGGAGTCT	*agnE* qPCR F
SE331	CAGGAGAGAGCCGATACCAG	*agnE* qPCR R
SE338	CCAAATGGAATCAACCTGCT	*mutA* qPCR F
SE339	ATGGGGAAGCTGTTTGTCAC	*mutA* qPCR R

#, Fujioka et al. (2007)

*, Alam et al. (2012)

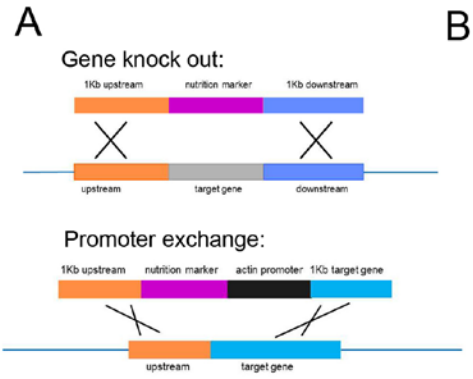

B

actA(p)-amyC:	
1Kb amyC upstream + AfpyroA + actAp+ 1Kb amyC	
(SE355+SE356) (SE231+SE232) (SE234+SE208) (SE357+SE358)	Fusion PCR: SE359+SE360
actA(p)-amyE:	
1Kb amyE upstream + AfpyroA + actAp+ 1Kb amyE	
(SE361+SE362) (SE231+SE232) (SE234+SE208) (SE363+SE364)	Fusion PCR: SE365+SE366
agnBΔ:	
1 Kb agnB upstream + AfpyroA + 1Kb agnB downstream	
(SE343+SE344) (SE231+SE232) (SE408+SE409)	Fusion PCR: SE347+SE410
agnEΔ:	
1 Kb agnE upstream + AfpyroA + 1Kb agnE downstream	
(SE322+SE323) (SE231+SE232) (SE324+SE325)	Fusion PCR: SE326+SE327
mutAΔ:	
1Kb mutA upstream + actAp+ AfpyrG + 1Kb mutA downstream	
(SE349+SE411) (SE190+SE191) (AME1+AME2) (SE412+SE413)	Fusion PCR: SE353+SE414
agnBΔ, mutAΔ:	
1 Kb agnE upstream + AfpyroA + 1Kb agnE downstream	
(SE322+SE323) (SE231+SE232) (SE324+SE325)	Fusion PCR: SE326+SE327
1Kb mutA upstream + actAp+ AfpyrG + 1Kb mutA downstream	
(SE349+SE411) (SE190+SE191) (AME1+AME2) (SE412+SE413)	Fusion PCR: SE353+SE414
actA(p)-agnB:	
1Kb agnB upstream + AfpyroA + actAp+ 1Kb agnB	
(SE343+SE344) (SE231+SE232) (SE234+SE208) (SE345+SE346)	Fusion PCR: SE347+SE348
actA(p)-agnE:	
1Kb agnE upstream + AfpyroA + actAp+ 1Kb agnE	
(SE322+SE323) (SE231+SE232) (SE234+SE208) (SE340+SE341)	Fusion PCR: SE326+SE342
actA(p)-mutA:	
1Kb mutA upstream + AfpyroA + actAp+ 1Kb mutA	
(SE349+SE350) (SE231+SE232) (SE234+SE208) (SE351+SE352)	Fusion PCR: SE353+SE354
actA(p)-agnB, amyDΔ:	
1Kb agnB upstream + AfpyroA + actAp+ 1Kb agnB	
(SE343+SE344) (SE231+SE232) (SE234+SE208) (SE345+SE346)	Fusion PCR: SE347+SE348
1 Kb amyD upstream + AfpyrG + 1Kb amyD downstream	
(SE103+SE104) (AME1+AME2) (SE105+SE106)	Fusion PCR: SE107+SE108
actA(p)-mutA, amyDΔ:	
1Kb mutA upstream + AfpyroA + actAp+ 1Kb mutA	
(SE349+SE350) (SE231+SE232) (SE234+SE208) (SE351+SE352)	Fusion PCR: SE353+SE354
1 Kb amyD upstream + AfpyrG + 1Kb amyD downstream	
(SE103+SE104) (AME1+AME2) (SE105+SE106)	Fusion PCR: SE107+SE108

Fig. S4-1 Deletion and promoter exchange schema and PCR constructs of each strain

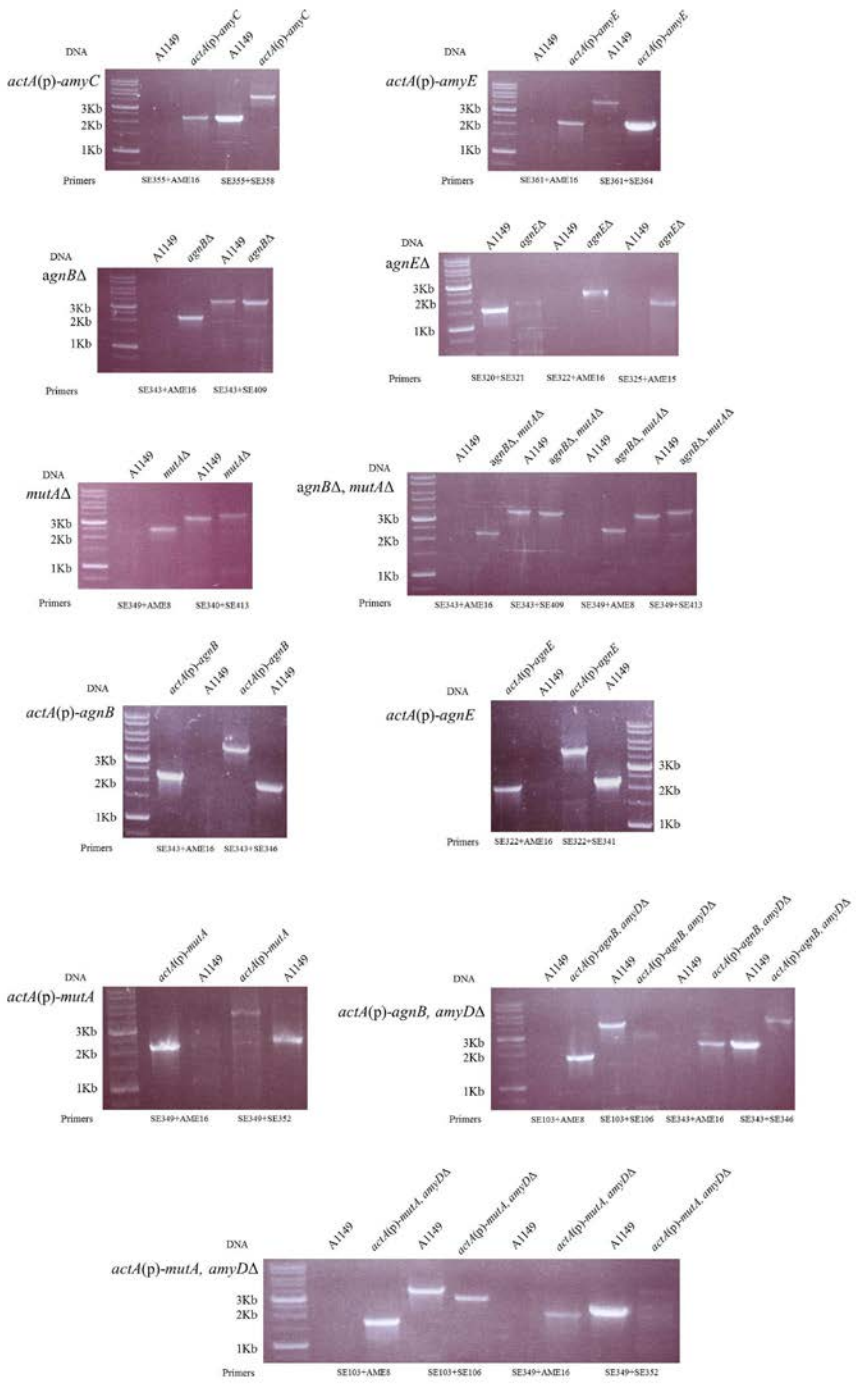

Fig. S4-2 PCR confirmation of all constructed strains.
Strains labeled at right of each gel picture. Primers are indicated at the bottom and DNA templates are on the top.

>AN6542 upstream COORDS:ChrI_A_nidulans_FGSC_A4
TACGTTAAAGGCTCGCCCCAACCTCGAAAAGGCGGTAAAATACTAAAAACGGTCCTTAGA
AGGCCTTTTCGACAACGATTTAGAAGGGCTGAGTACAAAAGGAGATCAACCACAGATAGT
ATCGAGCGTGGTTATAGAGAACTAGTTCAGCACATGCCTTATTCCTTTTTTTTCTTCCCATTT
TTTTTTTCTTTCTTAAAGGACAGATATAAAAATCTGGAAGCCTGGAGTAGGATCCCCTTAG
GCATTGTTGAACTTCAGGAAAAAGTGAGTCGTCATCGTGCTTACAAGCAGAGAGCGATAA
TAATAGAACGAATGAGAGGACAGACCCTGTTCTTTGAAAACTGGACACGCTGGGCTGAA
CCATCATTACGGCCTTGGTCGTCGGTCTCTGCCCCACGAGGATTCATCATCTCGCGAGGCC
ACCTCAGCGCGCAATCATTCTGCCTGAGAGGCAACACTTGGTCGCCAGTATAAAAGAACC
AATTGAACAAGAGACACCTATCTCGTAGCAGTCTTTGTGTAGTCTGTACTTTATTCGTTTTA
CCCTCTGAGGAAACGCGGTGGCGGTGACCATTCGACTAGACGAGACTAAGCCCCTTTGG
CGCCTGAACCTCCAGCCCCTTTCCAGTCCTTCTGTTCAGTTCGAGCGGCTGTCGAGCTGCT
GCTGACTACTCCGCCTACCGCTACAACCTCCACCACCACCGACCACCAACAAACCCTCGAC
TCTCTCCCCTTCTCTCCTCCACTTCTCAACATCCAACTCCCCATTCTCGCTCTGTTCATCATCT
CTCCTCCTCCCTTCCTTACCTGTCAACCTCTCATTTCTTTTTCTCTTTGTTCTTCGTAGTTCGA
TTCTAATCCACCCCTAAACACC

Fig. S4-3 Sequence of *actA* upstream

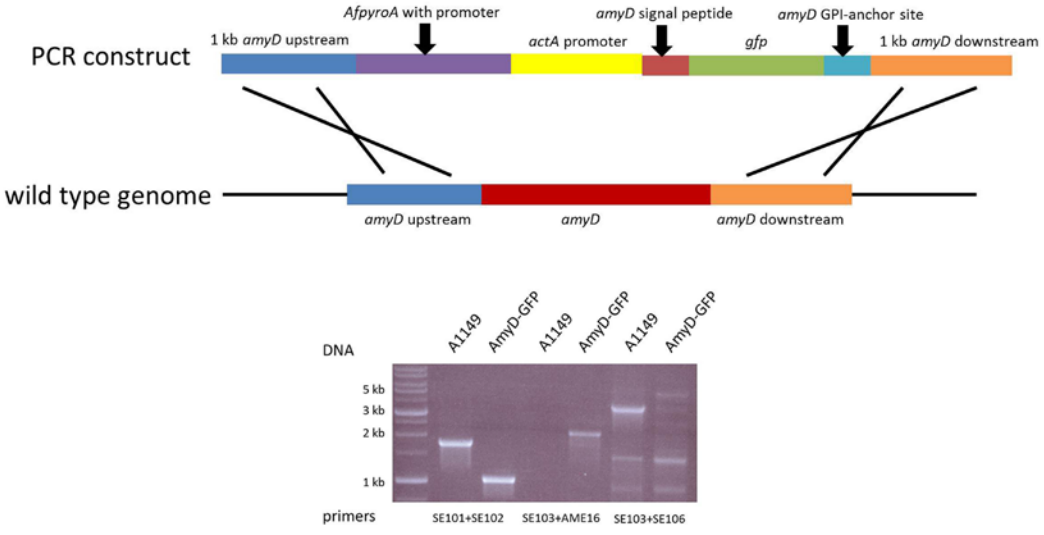

Fig. S4-4 AmyD-GFP construction and PCR confirmation

CHAPTER 5

USING *ASPERGILLLUS NIDULANS* TO IDENTIFY ANTI-FUNGAL DRUG RESISTANCE MUTATIONS

While scientists are trying to develop new effective and safe anti-fungal drug, the existing ones are being challenged by emerging drug resistance. Given the fact that new broad-spectrum drug targets candidates are few and drug development is expensive, studies exploring resistance mechanisms against the current anti-fungal agents are important. In this chapter, I develope a strategy to identify drug resistance mutations using *A. nidulans* and next generation sequencing. As a proof-of-principle study, I use this strategy to investigate the drug resistance mutations against calcofluor white. Results showed this is a promising strategy to reveal the drug resistance causing mutations in a time-saving manner.

My role in this research: designed the study along with S Kaminskyj who funded it. I wrote thefirst draft; and contributed to the final revised draft. S Li provided technical assistance during the project.

The manuscript of this chapter has been published as “Using *Aspergillus nidulans* to identify anti-fungal drug resistance mutations” by Xiaoxiao He, Shengnan Li and Susan Kaminskyj in Eukaryotic Cell 2014:13(2):288-94.

Using *Aspergillus nidulans* to identify anti-fungal drug resistance mutations.

Xiaoxiao He, Shengnan Li, Susan GW Kaminskyj*

Department of Biology, University of Saskatchewan, Canada

Running Head: Strategy for identifying drug resistance genes

*Address correspondence to susan.kaminskyj@usask.ca

Key words: drug resistance, *Aspergillus nidulans*, next generation sequencing, calcofluor white, anti-fungal drug

5.1. Abstract

Systemic fungal infections contribute to at least 10 % of deaths in hospital settings. Most anti-fungal drugs target ergosterol (polyenes) or its biosynthetic pathway (azoles and allylamines), or beta-glucan synthesis (echinocandins). Anti-fungal drugs that target proteins are prone to the emergence of resistant strains. Identification of genes whose mutations lead to targeted resistance can provide new information on those pathways. We used *Aspergillus nidulans* as a model system to exploit its tractable sexual cycle, and Calcofluor White as a model anti-fungal agent to cross-reference our results with other studies. Within two weeks from inoculation on sub-lethal doses of Calcofluor White, we isolated 24 *A. nidulans* adaptive strains from sectoring colonies. Meiotic analysis showed that these strains had single-gene mutations. In each case the resistance was specific to Calcofluor White, since there was no cross-resistance to Caspofungin (echinocandin). Mutation sites were identified in two mutants by next generation sequencing. These were confirmed by re-engineering the mutation in a wild type strain using a gene replacement strategy. One of these mutated genes was related to cell wall synthesis and one to drug metabolism. Our strategy has wide application for many fungal species, for anti-fungal compounds used in agriculture as well as health, and potentially during protracted drug therapy once drug resistance arises. We suggest our strategy will be useful for keeping ahead in the drug-resistance arms race.

5.2. Introduction

Fungal infection is growing problem in the developed world, particularly over the last several decades. Fungi readily infect immune-compromised patients, and systemic infections typically cause high morbidity (Pfaller et al., 2010; Brown et al., 2012; Lilic, 2012; Netae and Brown, 2012). In addition, reports of fungal infections in healthy populations are rising (Brown et al., 2012; Netae and Brown, 2012), for example due to increasing virulence of pathogens such as *Aspergillus fumigatus* (Brown et al., 2012). Fungi are now as serious a threat to human health as bacteria, viruses and parasites (Netae and Brown, 2012).

Fungi and animals have conserved metabolic pathways, which limits the options for drug targets. There are four major classes of anti-fungal drugs. Azoles and polyenes interfere with biosynthesis or distribution of ergosterol, the sterol in fungal membranes (Chen and Sorrell, 2007). Although these drugs have a wide spectrum of effect against fungal growth, the structural similarity between ergosterol in fungi and cholesterol in mammals leads to toxicity and limits human drug usage (Carrillo-Munoz et al., 2006; Cowen, 2008). Azoles also have substantial application as agricultural fungicides and there are cases of cross-resistance (Verweij et al., 2009). The newest anti-fungal drug class to be released clinically, echinocandins, targets cell wall beta-1,3-glucan synthase (Denning, 2003). Human toxicity of echinocandins is low, but their narrow spectrum of activity and already emerging resistance was a severe disappointment to the community (Walker et al., 2010). Collectively, we are still searching for new anti-fungal

drug targets, but progress is slow.

With new broad-spectrum drug targets being few, and drug development being expensive, studies exploring resistance mechanisms against our current anti-fungal agents are important. Cowen (2008) notes that the effectiveness of *all* existing anti-fungal drugs is reduced by resistant strains. Especially for echinocandins, clinically resistant strains were isolated shortly after their launch (Alexander et al., 2013; Fekkar et al., 2013). The strong adaptation ability of fungi is well documented (Schoustra et al., 2006; Schoustra et al., 2007; Schoustra et al., 2009; Gifford et al., 2011) so it was not surprising to see anti-fungal drug resistance emerging quickly. Mutation hot spots in *FKS1*, which encodes beta-glucan synthase, were detected in some of the resistant strains, but not in all (Walker et al., 2010; Alexander et al., 2013; Fekkar et al., 2013). Our strategy can efficiently identify mutations in this latter group.

Aspergillus nidulans is used as a model for adaptation studies (Schoustra et al., 2006; Schoustra et al., 2009). Vegetative nuclei in a colony are mitotically derived from a single spore nucleus, so the only source of genetic variation in an *A. nidulans* colony is somatic mutation, which then is clonally propagated as a mycelial sector (Schoustra et al., 2006). In *A. nidulans*, the asexual nuclear duplication cycle is roughly comparable to a somatic generation in yeast. In growing *A. nidulans* hyphae the nuclear duplication cycle is ~100 min (Trinci, 1970), and a typical hyphal growth rate is ~1 μm/min (Hubbard and Kaminskyj, 2007).

We used Calcofluor White (CFW) as an anti-fungal agent to cross-reference with earlier studies. We found that robust, heritable adaptation against CFW could rapidly be acquired in

multiple ways, each requiring only one mutation based on analysis of meiotic progeny. Two adaptive strains were selected for Next Generation Sequencing (NGS), to determine if this would be sufficient to identify adaptive mutations. Potential mutation sites were confirmed by gene replacement in parental strain. In this study, one adaptive strain was related to cell wall synthesis and the other to drug metabolism. We suggest our strategy can help us stay ahead in the fungal drug-resistance arm race.

5.3. Materials and Methods

5.3.1. Strains, Plasmids and Media

All of the strains in this study were derived from *A. nidulans* A1149, which was the wild type control for all assays in this paper. All strains, primers and plasmids are listed in Table S5-1. All strains were grown on complete medium (CM: 1 % glucose, 0.2 % peptone, 0.1 % yeast extract, 0.1 % casamino acids, 50 mL 20 x nitrate salts, 1 mL trace elements, 1 mL vitamin solution, pH 6.5) or minimal medium (MM: 1 % glucose, 50 mL 20 x nitrate salts, 1 mL trace elements, 0.001 % thiamine, pH 6.5) supplemented with nutrients for auxotrophies as required. Trace elements, vitamin solution, nitrate salt and all nutrition stocks are described in (Kaminskyj, 2001). For transformation medium, 1 M sucrose was added as osmoticum to MM. All strains were grown at 30 ºC, unless mentioned specifically. For adaptive strain induction, CFW stock solution (10 mg/mL in 25 mM KOH) was added as required into CM when it cooled to 60 ºC.

Strategies for gene deletion and gene replacement methods used a fusion PCR method (Szewczyk et al., 2006; El-Ganiny et al., 2008). Briefly, deletion constructs were constructed by fusion PCR including 1 kb upstream, a selectable marker, and 1 kb downstream. Gene replacement constructs were made by fusion PCR including 1 kb upstream, the mutated gene sequence, a selectable marker, and 1 kb downstream (details see Fig. S5-1A). Constructs were transformed to A1149 protoplasts. *Aspergillus fumigatus pyrG* and *pyroA* were used as selectable markers (details see Fig. S5-1A and Fig. S5-1B). Mutations in replacement strains were confirmed by Sanger sequencing.

5.3.2. Drug Sensitivity Test

The disc-diffusion assay was adapted from (Alam et al., 2012). Briefly, freshly harvested spores (10^6/mL) were added to CM at 55 ºC, and poured immediately into 9 cm diameter Petri plates. After the agar solidified, a sterilized paper disc was put at the designated places, followed by 20 µL of drug stock solution CFW (10 mg/mL in 25mM KOH), Congo Red (CR, 10 mg/mL in H_2O), or Caspofungin (20 mg/mL in H_2O). Plates were incubated at 30 ºC for 1 d.

For the growth sensitivity assay, drug stock solution was added to CM at 60 ºC at the designated concentration and poured immediately into 9 cm diameter Petri plates. Then 10^5 freshly harvested spores were spread over medium after it solidified. Plates were incubated at 30 ºC for 2 d.

5.3.3. Mating of *Aspergillus nidulans*

Mating experiments were performed as described in the work of Kaminskyj (2001). AXM5 and AXM20 are white spore-color, morphologically wild type and CFW-sensitive strains. They were obtained from previous mating experiments in our lab. The genotypes of AXM5 and AXM20 are given in Table S5-1. For assessing the drug sensitivity of progeny, at least 100 ascospores from each outcrossed cleistothecium were selected and tested for growth sensitivity on 30 µg/mL CFW.

5.3.4. Next Generation Sequencing

NGS was performed at the Beijing Genomic Institute as a commercial service using platform

Illumina HiSeq 2000. Two strains were sequenced in separate lanes. 1 GB draw data was generated from each run and an average 31x depth of each nucleotide (genome size 30Mb) was gained. Sequence assembly and single nucleotide polymorphism (SNP) analysis were also done at the Beijing Genomic Institute. The details of Illumina DNA sequencing technique can be found in Metzker 2010.

5.4. Results

5.4.1. *Aspergillus nidulans* Has Strong Adaptive Ability against Sub-Lethal Levels of Calcofluor White.

Schoustra and colleagues (Schoustra et al., 2009; Gifford et al., 2011) showed that *A. nidulans* readily gained fitness against the anti-fungal agent fluodioxinil under partially suppressed growth conditions. One to three mutations were sufficient to recover full fitness, with the first having the greatest phenotypic effect (Schoustra et al., 2009; Gifford et al., 2011). Following this idea, we grew 10^5 freshly harvested *A. nidulans* spores on CFW-containing medium (15 or 30 μg/mL). As expected, CFW suppressed *A. nidulans* growth *in vitro*: colony growth was restricted to ~50 % and ~30 %, respectively of that on drug-free medium (Fig. 5-1A). Colonies that were grown on 30 μg/mL CFW plates developed rapid-growing sectors (Fig.5-1B), which we called adaptive strains, in about a week after inoculation. We named two of the adaptive strains AXE5 and AXE8: these arose at 5 d and 8 d after inoculation, respectively. No adaptive sectors developed on the 15 μg/mL CFW plates during this experiment.

To test whether adaptive sectors would eventually emerge on 15 μg/mL CFW, and to increase the number of adaptive strains in our collection, we performed the inducing experiment with 20 replicas at each CFW concentration and extended the incubation time to 10 d (15 μg/mL) and 15 d (30 μg/mL) by which time the Petri plates were completely covered. No adaptive sectors developed on 15 μg/mL CFW. However, as before, adaptive sectors emerged on 30 μg/mL CFW beginning at 5 d. Eventually, 22 adaptive strains were isolated from twenty

30 μg/mL CFW plates (Table 5-1, AXE20 to AXE69). Finally, a total of 24 adaptive strains collection were generated in our experiment (Table 5-1). All of the adaptive strains were stably resistant to 30 μg/mL CFW after re-streaking and also after storing at -80 °C in glycerol (Fig. 5-2).

5.4.2. Adaptation to CFW can be Acquired by Single Mutations

We hypothesized that the adaptive sectors were each due to the first mutation that increased hyphal growth rate on CFW. To test this, each adaptive strain was crossed with AXM5 and with AXM20, both of which are wild type for CFW sensitivity, and have white spores. Mating with mutant strains is less consistent than with wild type ones (El-Ganiny et al., 2008). We performed each mating experiment in duplicate and unsuccessful mating experiments were repeated once more. Compared to wild-type strains, many matings with adaptive strains showed delayed cleistothecium formation and/or reduced ascospore production. Nevertheless, we had mating results from 19 adaptive strains. For each of these strains, the ratio of CFW-resistant to CFW-sensitive progeny was ~1:1 (Table 5-1 and Fig. 5-3), consistent with single-gene defects and χ^2 goodness-of-fit analysis. Five strains from our collection failed to mate with either AXM5 or AXM20, producing at best only tiny cleistothecia. We dissected some of these, but they produced only white-spored colonies. Therefore we were not able to assess the number of mutations in these adaptive strains. However, our mating results have revealed that adaptation in first-arising sectors was most likely due to one mutation, and that this adaptation was sexually heritable.

5.4.3. Adaptation to CFW is Specific

To test whether any of our adaptive strains had cross-resistance to other wall-targeting agents, we assessed their response to Congo Red (CR, which binds to cellulose fibres) and to Caspofungin. For AXE5 and AXE8, which were isolated from our preliminary test, we used a disc diffusion method (Alam et al., 2012). Weak cross-resistance to CR was found for both strains, but there was no cross-resistance to Caspofungin (Fig. 5-2A). For the remainder of the adaptive mutant strains, we used a more efficient method to compare drug sensitivity by testing their survival ability on drug-containing medium. A few strains (AXE 37, 51, 62, 64 and 69) showed a weak resistance to 500 μg/mL CR (Fig. 5-2B), whereas all strains maintained the same sensitivity to 10 μg/mL Caspofungin as the A1149 (Fig. 5-2B). We interpret this as showing that the adaptation in these mutants was specific to CFW compared to Caspofungin.

5.4.4. Adaptation to CFW Appears to be Acquired by Many Different Mutations

Calcofluor inhibits chitin crystallization during cell wall formation (Elorza et al., 1983), which is likely to require many protein products. To estimate the number of different CFW-adaptive mutants in our collection, we assessed their phenotypes under a suite of growth conditions. Precise analysis would have required 552 pairwise matings.

Based on this information, the 24 strains were grouped into five classes. Five strains (AXE 8, 52, 62, 66 and 69) showed obvious growth defects on drug-free medium (Fig. S5-2). Three strains (AXE 5, 33 and 37) were temperature sensitive, since they could not conidiate at 37 °C.

Five strains (AXE 29, 30, 35, 41 and 58) showed resistance only to 30 μg/mL CFW but not to 50 μg/mL CFW (Fig. S5-2). Six strains (AXE 35, 52, 58, 62, 64 and 69) showed growth defects on 1M NaCl (Fig. S5-2). Ten strains (AXE 20, 22, 43, 44, 46, 49, 51, 54, 63 and 65) had no obvious growth defect under any condition tested (Fig. S5-2). Within these groups, there were minor differences between strains. This suggested they may share the same overall resistance mechanism (perhaps mutations in the same gene or genes in the same pathway) but not necessary the same mutation (*e.g.* a non-conservative mutation vs a premature stop). For example, AXE5, AXE33 and AXE37 were all temperature sensitive, but their phenotypes at 37 °C differed (Fig. S5-2 and S5-3), suggesting they are related but different mutations. Eventually we found only strains AXE 20 and 22; AXE29 and 30; AXE35 and 58; AXE 44 and 51; AXE 52, 62 and 69 could *not* be distinguished based on these criteria. We interpret this to mean that there were at least 18 different mutations in our adaptive strain collection.

Since many mutations appeared to be unique in our collection, our current screen for CFW-resistance mutation is not exhaustive. However, the goal of this study was to assess whether we could efficiently identify fast-emerging resistance mutations to an anti-fungal agent, not to discover new genes involved in CFW resistance, so we concentrated on two strains and archived the rest.

5.4.5. Next Generation Sequencing (NGS) Revealed Potential Mutations in Adaptive Strains.

Plasmid complementation is a well-established method for gene identification in *A. nidulans* mutants,(e.g. Lin and Momany, 2004) but is not optimal for drug resistance mutants, due to their

relatively subtle phenotypes, and need for a reverse-selection strategy. Instead, we used NGS to identify candidate genes, a strategy that has been used in other organisms to identify single mutations (Srivatsan et al., 2008; Laitinen et al., 2010; Schmitt et al., 2012). We selected AXE5 and AXE8 for whole genome sequencing. Sequence assembly was based on the *A. nidulans* A4 genome (Arnaud et al., 2012). Compared to the A4 reference strain, about 400 single nucleotide polymorphisms (SNPs) were detected in each of the adaptive strains (Table 5-2). These were roughly evenly distributed across the 17 scaffolds that represent whole genome (Fig. S5-4). Since the two adaptive strains were both induced from the A1149 parent, the SNP distributions were very similar. After removing common SNPs, and SNPs that were not in a coding region, there were only 15 (AXE5) and 13 (AXE8) unique SNPs (Table 5-2 and Table S5-2). In this way, we successfully narrowed our targets from genome scale to a limited number of genes. Based on two well-established *Aspergillus* genome databases (AspGD and Broad Institute), we comprehensively analyzed each candidate gene (Table S5-2). Two SNPs that caused 3' truncations and had 99 % confidence scores drew our attention and were selected for closer examination.

5.4.6. CFW Resistance Mutations were Confirmed by Mutation-Reintroduction

For the AXE5 gene sequence, a C1198T mutation was detected in ANID_10647, which created a premature stop codon in the predicted protein product. Lin and Momany (2004) had previously characterized this gene and annotated it as a predicted cytochrome P450 protein. Their study had been based on a different genetic mutation (G1225T), which also introduced a

premature stop codon near the 3' end. All of the AXE5 phenotypes were consistent with those described in Lin and Momany (2004), including temperature sensitivity, resistance to CFW, and being osmotically remediable for temperature sensitivity (Fig. 5-2 and Fig. S5-3).

For AXE8 gene sequence, a G1081T mutation created a premature stop codon in ANID_03445. This is an uncharacterized gene in *A. nidulans*. However, *CHS4* in *S. cerevisiae*, the orthologue of ANID_03445, has been characterized (Choi et al., 1994; Ono et al., 2000). *CHS4* encodes the activator of the major chitin synthase (*CHS3*) in *S. cerevisiae*, which positively regulates chitin formation (Choi et al., 1994; Ono et al., 2000). Chs4p has been shown to physically interact with Chs3p (DeMarini et al. 1997), and this binding relies on the C-terminal 86 amino acids of Chs4p. Sequence analysis by ClustalW2 showed a 54 % sequence identity between ANID_03445 and *CHS4*. The G1081T mutation in ANID_03445 created a premature stop codon in the middle of the predicted protein product, thereby truncating 371 amino acids from the C-terminal. It is possible the ANID_03445 G1018T mutation affects the binding between this activator and chitin synthase in *A. nidulans*. In turn, the lack of this chitin synthase activation could lead to reduced chitin in the *A. nidulans* cell wall, and resistance to CFW.

To test whether these two specific mutations caused the CFW resistance, we first confirmed the sequence of the target genes in AXE5/ANID_10647 and AXE8/ANID_03445 by Sanger sequencing, revealing the same mutation as with NGS. Using PCR-based methods we re-constructed the mutations and separately replaced each gene in A1149 (Fig. S5-1). The PCR

constructs contained 1 kb of target gene upstream + the whole mutated gene + a nutrition marker with its native promoter (*A. fumigatus pyroA* in our case) + 1kb of target gene downstream.

All of the constructed ANID_10647 C1198T strains showed CFW resistance, however this was only so for some ANID_03445 G1081T strains. We sequenced the constructed strains and found only the CFW-resistant colonies from ANID_03445 G1081T transformation plates had the desired mutation, whereas the other colonies did not. This is likely because the mutation site in ANID_03445 G1081T is far (1174 bp) from the nutrition marker in PCR construct. Therefore, homologous recombination can happen after the mutated site. In that case, the selective marker would be introduced to the A1149 genome without mutation site, and those transformants would not have CFW resistance. In contrast, the mutation in ANID_10647 C1198T is close (242bp) to the 3' end of the gene, so there was a low possibility that homologous recombination can happen after this site.

The proper re-constructed strains showed the same drug resistance as AXE5 and AXE8 respectively (Fig. 5-4). All other associated phenotypic changes in AXE5 (*e.g.* temperature sensitivity) (Fig. S5-3) and AXE8 (*e.g.* growth defect on drug free medium; Fig. 5-4) were also present in our re-constructed strains. Therefore, the drug resistance mutations were confirmed. In addition, we deleted ANID_03445, and found that deletion strain was phenotypically indistinguishable from AXE8 (Fig. 5-4). As expected, the premature stop mutation in AXE8 may prevent the interaction between this activator and its correspondent chitin synthase. Lack of this interaction may lead to less chitin deposition in the *A. nidulans* cell wall and in turn lead to CFW

resistance as it did in *S. cerevisiae* (Choi et al., 1994; Ono et al., 2000). Furthermore, AXE8 showed phenotype defects in the absence of CFW, which is consistent with changes in its wall composition. Lin and Momany 2004 had already deleted ANID_10647 (Lin and Momany, 2004), so this was not repeated in our study.

5.5. **Discussion**

Excitingly, our strategy enabled us to generate and isolate adaptive strains in *A. nidulans* that had single-gene mutations, and to rapidly identify the mutated genes. Working with single gene mutations was important to simplify NGS analysis. We expect that our strategy should be generally applicable to fungi regardless of whether they have a tractable sexual life cycle to test the number of mutations.

Is our single-gene mutation collection a special case for CFW? We think not. First: Schoustra and colleagues found that single-gene mutations were sufficient to create a high level of resistance to fluodioxinil (Schoustra et al., 2009; Gifford et al., 2011). They did not identify the mutated genes, probably due to factors mentioned earlier. Second: echinocandin resistance mutations are typically at single sites in *FKS1* (Walker et al., 2010; Alexander et al., 2013; Fekkar et al., 2013). Third: single mutations in Erg11 lead to resistance against azoles (Kanafani and Perfect, 2008). Fourth: we were able to generate a single adaptive strain with resistance to 500 mg/mL CR. Mating results for that strain were consistent with a single-gene mutation (*data not shown*). Fifth: if multiple mutations were necessary for drug resistance, anti-fungal adaptation that required a particular combination of mutations would be expected to be extremely rare. Taken together, several lines of evidence besides our study show drug resistance based on protein function can emerge quickly given the appropriate selection pressure (Kanafani and Perfect, 2008; Schoustra et al., 2009; Fekkar et al., 2013), consistent with single-gene mutations. In contrast, resistance to polyenes that target ergosterol distribution, rather than its

synthesis, has been relatively durable, although even it has been overcome recently (Kanafani and Perfect, 2008).

Based on phenotype analysis, we have evidence to suggest there are at least 18 different single-gene mutations that cause resistance to ≥30 μg/mL CFW, suggesting the screen is not exhaustive. Multiple resistance mutations against CFW have been reported for fungi (Roncero et al., 1988; Garcia-Rodriguez et al., 2000), however at least one mutated gene [ANID_03445] that we identified had not been characterized in *A. nidulans*. The objective of our study was not to determine how many mutations lead to CFW resistance, and in addition, the protein basis for the mode of action of CFW is not fully understood. The ways that fungi can gain resistance will depend on the mechanism of a certain drug. And this will also decide the adaptation rate. However, as long as single mutations can lead to resistance, then we should expect to isolate such mutants.

We were able to identify many adaptive sectors on the 30 μg/mL CFW treatment but none on the 15 μg/mL plates, suggesting that the degree of inhibition may be important for induction of adaptive mutations. An interesting additional phenotype for the colonies on 30 μg/mL CFW was the marked increase in Hülle cells (see Fig. 5-1A). Schoustra et al (2007) proposed that mitotic recombination has the potential accelerate adaptation rates in *A. nidulans*. We suggest that the presence of large numbers of Hülle cells could be a sign that the colony has become potentiated for cell fusion. Hülle cells are seen with increasing frequency in older *A. nidulans* colonies, which may be associated with cleistothecia. Hyphal fusion and subsequent nuclear

migration could lead to enhanced spread of nuclei bearing a beneficial mutation, and a more efficient formation of a fast-growing sector (Trinci, 1970). We suggest that Hülle cell formation could be a harbinger of potential spread of adaptive mutations, and is consistent with the differences in adaptation rate between the two CFW concentrations we used.

Identifying a single critical mutation site in a whole genome is not trivial. Since the development of NGS in 2008 (Mardis, 2008), its application in resolving questions of adaptation has been applied in many organisms (reviewed in Stapley et al., 2010). NGS still suffers from short reads and high cost, which reduce its commercial availability, nevertheless, the small (30 Mb) haploid genome of *A. nidulans* made NGS more practical. We had ~ 31x coverage of each nucleotide and had high accuracy for most sites. Most SNPs were shared between the two strains, as expected since they were derived from the same parent, A1149. Despite this, we were able to use the A4 genome, which is thoroughly annotated, as a reference strain. In the end, only a few useful SNPs were identified in each adaptive strain. In our experiment, two samples were sequenced in separated lanes in order to assemble accurate genome sequence. However, if the purpose is to figure out the mutation sites, this is still not the optimal way for cost efficiency. Recently, a new type of "phenotype sequencing" would enable us to identify all potential causal-genes when all collected mutants were pooled and sequenced together (Lee and Harper, 2013). This would provide a more cost-saving manner for such studies; however stringent criteria must be met for this strategy.

The downstream work is straightforward for *A. nidulans*, since two well-established

databases (AspGD and Broad Institue) were available and all molecular techniques for gene manipulation were developed (Szewczyk et al., 2006). As a result, the target mutations were readily verified. For some fungal species, genome databases may be less well established. Until these resources are expanded, the metabolic conservation between fungi should enable us to apply most results to other species. Beginning with a model system such as *A. nidulans* should facilitate development.

In this proof-of-principle study, we developed a strategy to use *A. nidulans* and NGS to rapidly identify potential drug resistance mutations to CFW, which otherwise are difficult to locate. Our strategy has wide applicability to all anti-fungal drugs. Especially, we suggest this strategy could be using during drug development in order to predict where these new treatments will fail in the future. The value of this will be in having a combination therapy in anticipation of future need. In summary, we suggest that our strategy will be broadly useful in the drug-resistance arms race between humans and pathogenic microorganisms.

5.6. Acknowledgement

We are pleased to acknowledge support from the Natural Science and Engineering Council of Canada Discovery Grant program (SGWK), a Graduate Teaching Fellowship from University of Saskatchewan (XH), and a Canada Institutes for Health Research Training in Health Research using Synchrotron Techniques (CIHR-THRUST) Fellowship (SL). We thank Merck for the Caspofungin.

5.7. Tables

Table 5-1 Isolation day and meiotic progeny for each adaptive strain

Strain	Isolation day	Ratio of CFW resistant : sensitive progeny	Strain	Isolation day	Ratio of CFW resistant : sensitive progeny
AXE5	5	81:85	AXE46	10	41:59
AXE8	8	40:60	AXE49	10	58:42
AXE20	5	54:46	AXE51	5	N/A
AXE22	7	40:60	AXE52	5	45:55
AXE29	8	58:41	AXE54	5	53:46
AXE30	8	N/A	AXE58	6	N/A
AXE33	5	49:51	AXE62	8	44:56
AXE35	5	41:59	AXE63	9	52:48
AXE37	5	N/A	AXE64	9	51:49
AXE41	7	N/A	AXE65	9	53:47
AXE43	8	48:52	AXE66	13	35:65
AXE44	8	46:54	AXE69	13	37:62

Isolation date represents by days post-inoculation. Strains without successful mating results show as N/A.

Table 5-2 Summary of single nucleotide polymorphisms in AXE5 and AXE8

Strain	Total SNPs	Unique SNPs	Synonymous mutation	Non-synonymous mutation	Premature stop mutation
AXE5	393	15	5	8	2
AXE8	384	13	5	7	1

5.8. Figures

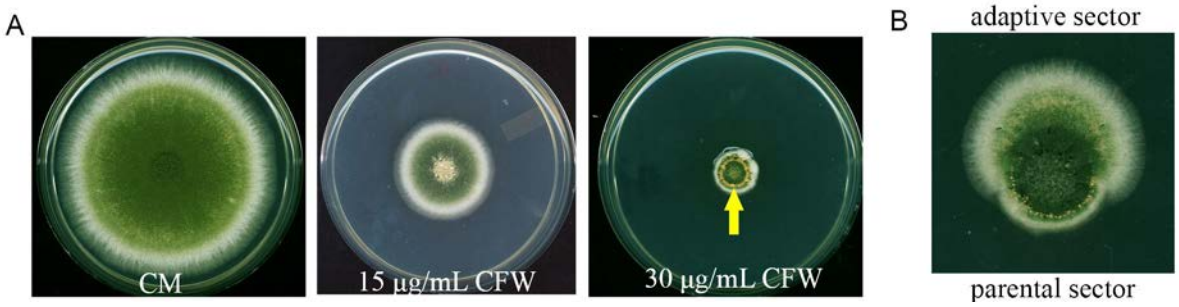

Fig. 5-1 Induction of adaptive strains

A. 10^5 freshly harvested spores were inoculated on CM, CM+15 μg/mL CFW, and CM+30 μg/mL CFW and plates were incubated at 30 °C for 5 d. *A. nidulans* colony growth was restricted on CFW containing medium.

B. Example of accelerated growth sector (top). AXE5 was shown, which was isolated on the fifth day post inoculation.

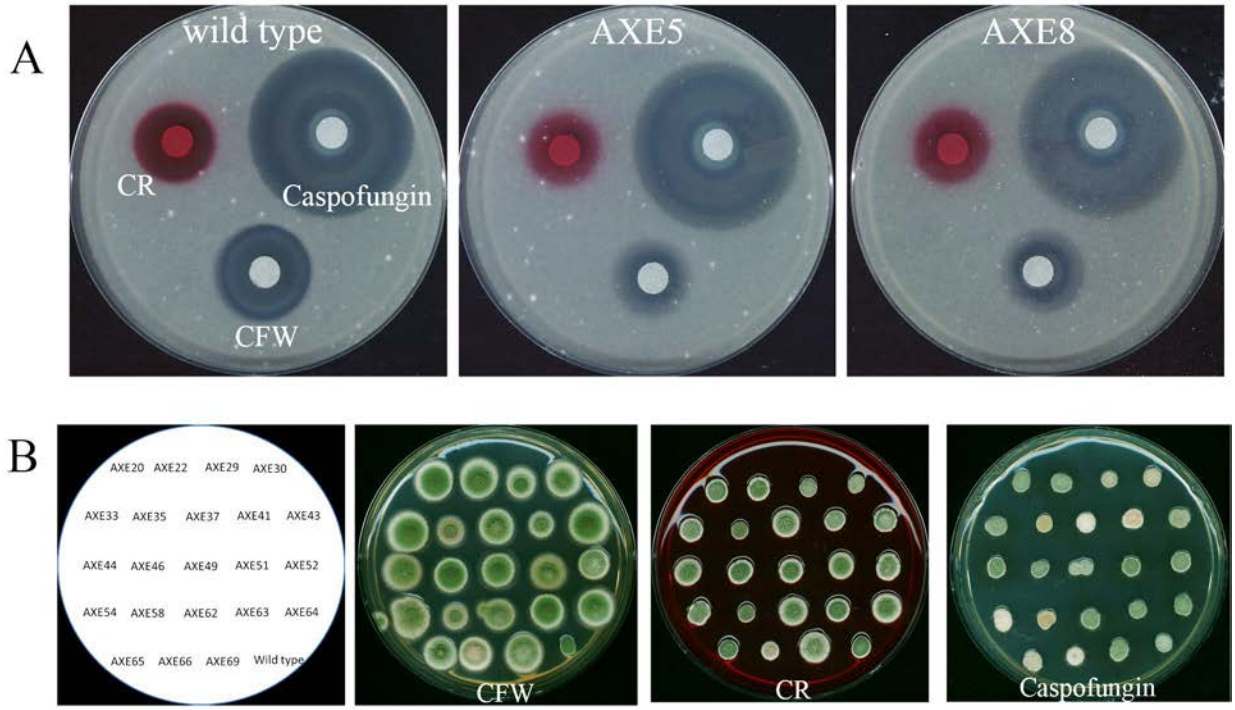

Fig. 5-2 Drug sensitivity of adaptive strains against CFW, CR and Caspofungin

A. Disc diffusion method was used to test drug sensitivity for AXE5 and AXE8. Freshly harvested spores were added to CM at a final concentration of 10^6 /mL. After solidification, 10 µL of each drug solution (CFW: 10mg/mL; CR: 10mg/mL; Caspofungin: 20mg/mL) was added on medium. Plates were incubated at 30 °C for 2 d. Both strains showed strong resistance to CFW and a weak cross-resistance to CR, but not to Caspofungin.

B. Survival ability test was used to show the drug sensitivity of other adaptive strains. 10^5 freshly harvested spores from each strain was added on CM, which was supplemented with 30µg/mL CFW, 500µg/mL CR and 10µg/mL Caspofungin respectively as indicated. Plates were incubated at 30 °C for 2 d. Again, all strains have stable resistance to CFW, some of them showed weak resistance to CR, but all maintained the same sensitivity to Caspofungin.

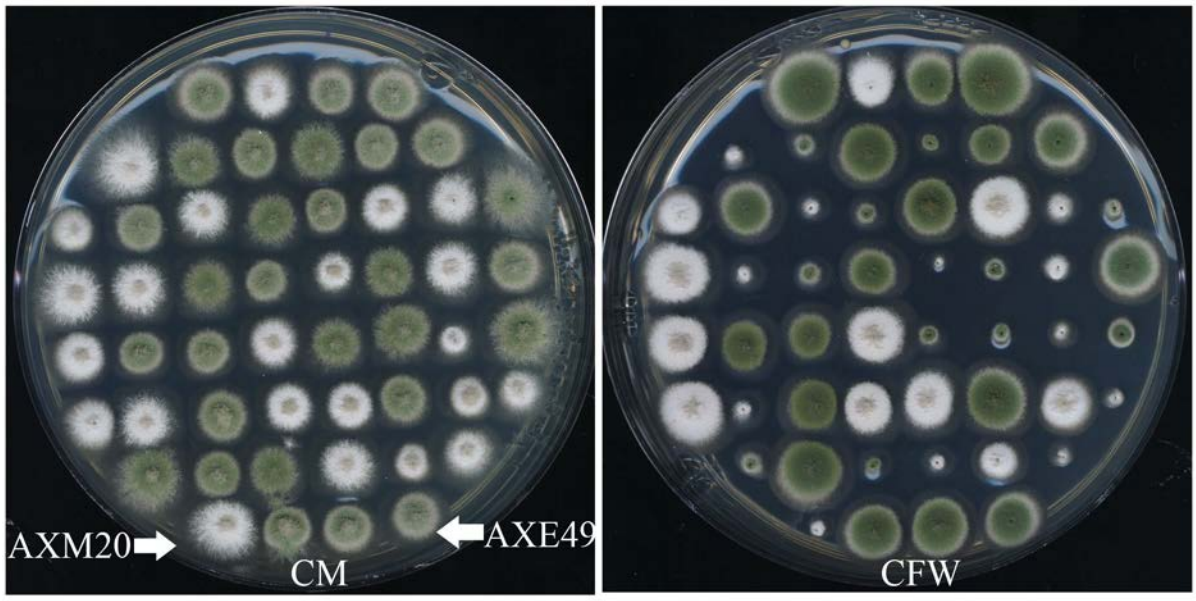

Fig. 5-3 Example of mating result between an adaptive strain and a wild type strain

Ascospores from AXM20::AXE49 were randomly inoculated on CM and CM+50 μg/mL CFW plates by toothpick. Parental strains were used as control (indicated by arrows). Plates were incubated at 30 °C for 2 d. CFW resistance was equally distributed in white color and green color ascopores, which indicated one mutation event happened in AXE49.

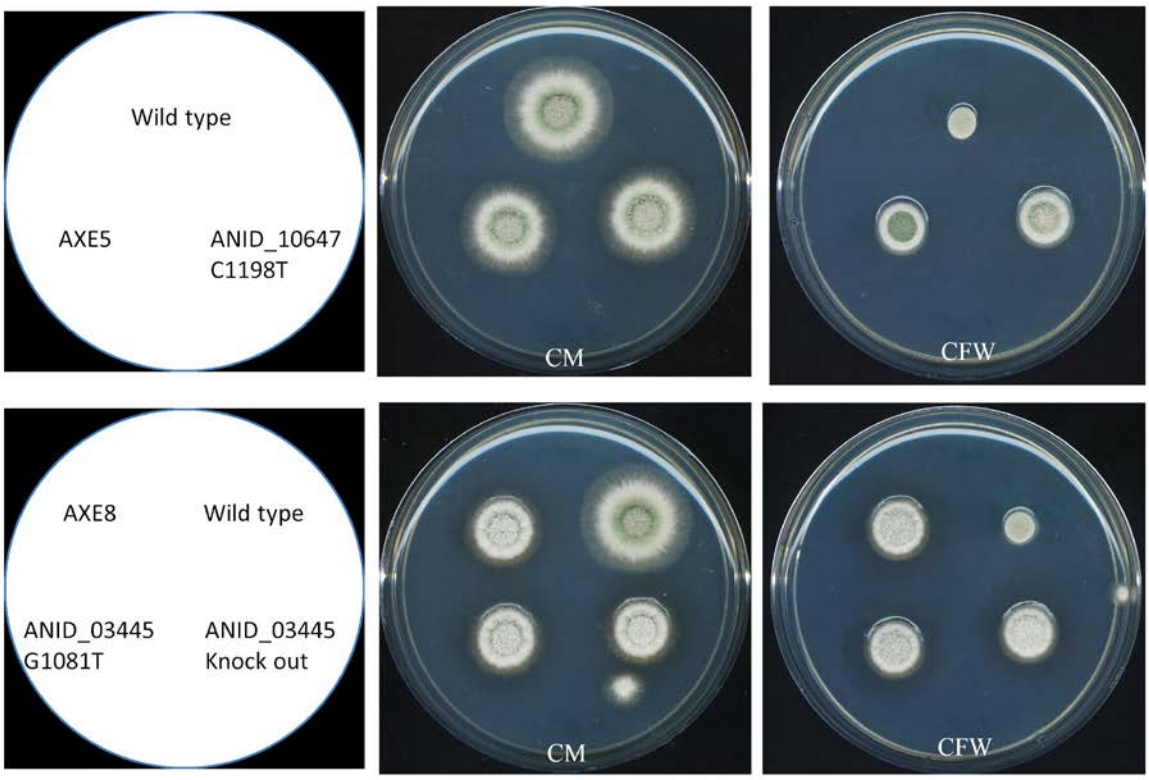

Fig. 5-4 Test of drug sensitivity for engineered strains

10^5 freshly harvested spores were inoculated on CM and CM+50 μg/mL CFW and plates were incubated at 30 °C for 2 d. Both site-mutagenesis strains showed the same drug resistance as parental strain. ANID_03445 knock out strain was also made and showed same phenotype as AXE8, which indicated mutation in AXE8 eliminate the function this gene.

5.9. Supplemental Materials

A

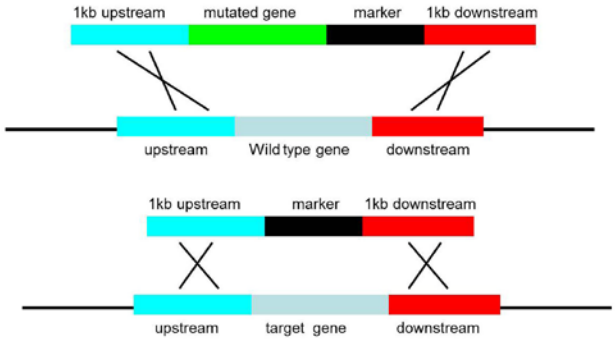

B

PCR construct of each strain and primer used in each reaction:

ANID_03445 gene replacement:

Mutated ANID_03445 with native promoter + Af pyroA with native promoter + 1kb ANID_03445 downstream — Fusion PCR:SE125+SE126
(SE121+SE271) (SE231+SE232) (SE272+SE124)

ANID_10647 gene replacement:

Mutated ANID_10647 with native promoter + Af pyroA with native promoter + 1kb ANID_10647 downstream — Fusion PCR:SE132+SE133
(SE139+SE269) (SE231+SE232) (SE270+SE131)

ANID_3445 gene deletion:

1kb ANID_03445 upstream + Af pyrG + 1kb ANID_03445 downstream — Fusion PCR:SE125+SE126
(SE121+SE122) (AME1+AME2) (SE123+SE124)

C

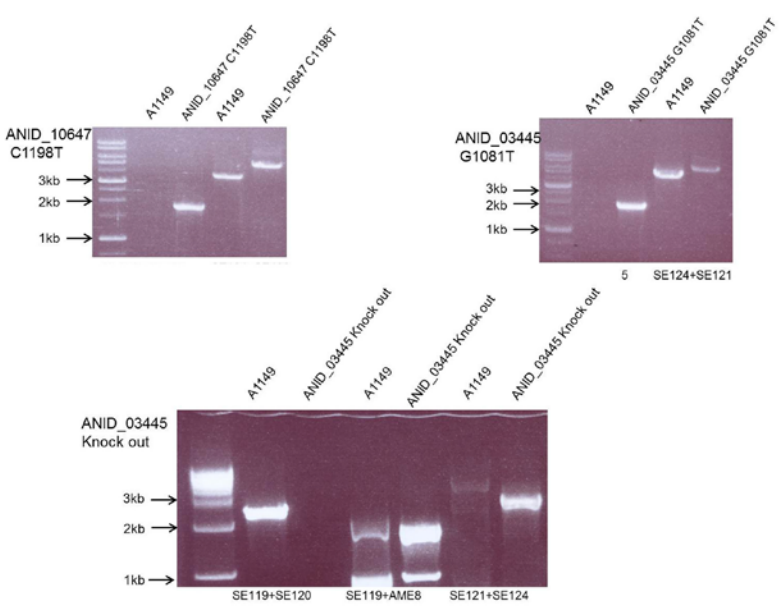

Fig. S5-1 Strategy and PCR confirmation for site-directed mutagenesis strains and gene knock out strain

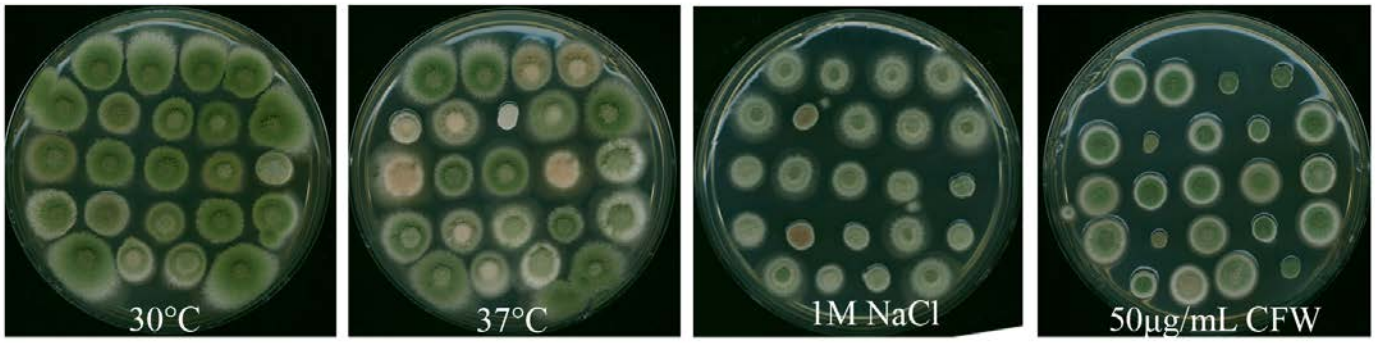

Fig. S5-2 Adaptive strains phenotype on different growth condition

10^5 freshly harvested spores of each strain were inoculated on medium and plates were incubated at 30 or 37 °C for 2 d. The order of strains is the same as Fig. 2B.

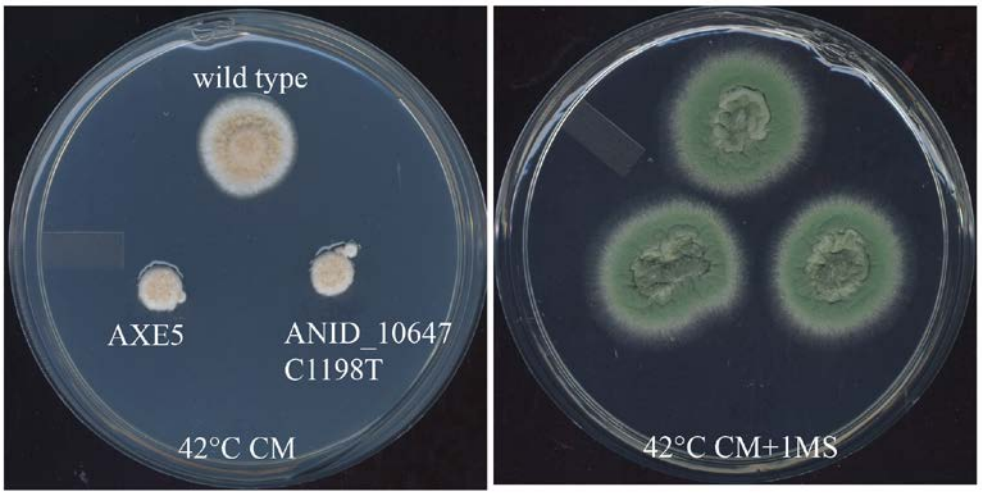

Fig. S5-3 AXE5 at high temperature, and remedial at high osmolarity plate.

10^5 freshly harvested spores were inoculated on medium and plates were incubated at 42 °C for 2 d. AXE5 and ANID_10647 C1198T were both temperature sensitive, but the defect was remedial by high osmolarity (1 M sucrose).

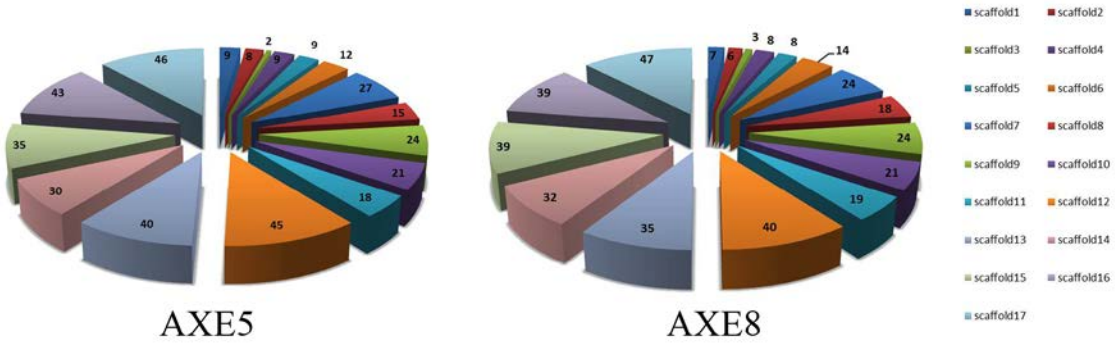

Fig. S5-4 Distribution of SNPs in AXE5 and AXE8 genome.

Genome was represented by 17 scaffolds. Total SNPs distributions were similar for AXE5 and AXE8, which indicates a similar genome background for these two strains.

Table S5-1 Strains, primer and plasmids used in this study

Strain		Genotype	Origin
A1149		*pyrG89*; *pyroA4*; *nkuA*::*argB*	FGSC
AXE5		*pyrG89*; *pyroA4*; *nkuA*::*argB*	this study
AXE8		*pyrG89*; *pyroA4*; *nkuA*::*argB*	this study
AXE20		*pyrG89*; *pyroA4*; *nkuA*::*argB*	this study
AXE22		*pyrG89*; *pyroA4*; *nkuA*::*argB*	this study
AXE29		*pyrG89*; *pyroA4*; *nkuA*::*argB*	this study
AXE30		*pyrG89*; *pyroA4*; *nkuA*::*argB*	this study
AXE33		*pyrG89*; *pyroA4*; *nkuA*::*argB*	this study
AXE35		*pyrG89*; *pyroA4*; *nkuA*::*argB*	this study
AXE37		*pyrG89*; *pyroA4*; *nkuA*::*argB*	this study
AXE41		*pyrG89*; *pyroA4*; *nkuA*::*argB*	this study
AXE43		*pyrG89*; *pyroA4*; *nkuA*::*argB*	this study
AXE44		*pyrG89*; *pyroA4*; *nkuA*::*argB*	this study
AXE46		*pyrG89*; *pyroA4*; *nkuA*::*argB*	this study
AXE49		*pyrG89*; *pyroA4*; *nkuA*::*argB*	this study
AXE51		*pyrG89*; *pyroA4*; *nkuA*::*argB*	this study
AXE52		*pyrG89*; *pyroA4*; *nkuA*::*argB*	this study
AXE54		*pyrG89*; *pyroA4*; *nkuA*::*argB*	this study
AXE58		*pyrG89*; *pyroA4*; *nkuA*::*argB*	this study
AXE62		*pyrG89*; *pyroA4*; *nkuA*::*argB*	this study
AXE63		*pyrG89*; *pyroA4*; *nkuA*::*argB*	this study
AXE64		*pyrG89*; *pyroA4*; *nkuA*::*argB*	this study
AXE65		*pyrG89*; *pyroA4*; *nkuA*::*argB*	this study
AXE66		*pyrG89*; *pyroA4*; *nkuA*::*argB*	this study
AXE69		*pyrG89*; *pyroA4*; *nkuA*::*argB*	this study
AXM5		*nicB, wA2(chaA)*	this study
AXM20		*nicB, wA2*	this study
ANID_10647 C1198T		*AN10647*::*AN10647*C1198T*: AfpyrG; pyrG89; pyroA4; nkuA::argB*	this study
ANID_03445 G1081T		*AN3445*::*AN3445*G1081T*: AfpyrG; pyrG89; pyroA4; nkuA::argB*	this study
ANID_03445 knock out		*AN3445*::*AfpyrG; pyrG89; pyroA4; nkuA::argB*	this study
Primers	**Alias**	**Sequence: 5’ to 3’**	**Description**
pyrG F	AME1	ATGTCGTCCAAGTCGCAATT	marker
pyrG R	AME2	TCATGACTTGCCGCATACTC	marker

pyroA F	SE231	GGACATCAGATGCTGGATTACTAAG	marker
pyroA R	SE232	TTACCATCCTCTCTTGGCCA	marker
10647 up F	SE139	GTCAAGCTCTCCGTGAGCTC	10647 replacement
10647 clone R	SE269	CTTAGTAATCCAGCATCTGATGTCCTGTCGGCACATCGTCAAT	10647 replacement
10647 down F	SE270	TGGCCAAGAGAGGATGGTAAGCAGGGTCCATATATTCAAGGT	10647 replacement
10647 down R	SE131	GGTTTCCACTTGCTGTTTGC	10647 replacement
10647 fusion F	SE132	TGACCGTCATGTGTTTGTCC	10647 replacement
10647 fusion R	SE133	CCATAACGCCGCATGTTC	10647 replacement
3445 up F	SE121	ACTTAGAACAAGACCCGGCA	3445 replacement
3445 clone R	SE271	CTTAGTAATCCAGCATCTGATGTCCTCACATGACGATCTGGTAAAGAG	3445 replacement
3445 down F	SE272	TGGCCAAGAGAGGATGGTAACGCGTCTATTTGTTTCGTGTAA	3445 replacement
3445 down R	SE124	TTTCTCGAGCTCCGTGATCT	3445 replacement
3445 fusion F	SE125	CTGGGGGCATACCTTGAAA	3445 replacement
3445 fusion R	SE126	GTTCTCCTTGAGACTGGAGAGTTG	3445 replacement
3445 up R	SE122	AATTGCGACTTGGACGACATTGTTCACGAGAATAGGCCG	3445 knock out
3445 down F(2)	SE123	GAGTATGCGGCAAGTCATGACGCGTCTATTTGTTTCGTGTAA	3445 knock out
3445 clone F	SE119	ATGAATCGACCACCACAAGG	strain confirmation
3445 clone R	SE120	TCACATGACGATCTGGTAAAGAG	strain confirmation
pyrG detect	AME8	CACATCCGACTGCACTTCC	strain confirmation
pyroA detect	AME15	ATTCCTGTCATGGCCAAAG	strain confirmation

Plasmids	Description	Origin
pAO81	S-TAG, *A. fumigatus pyrG*, kan ^{R}	FGSC
pHL85	GA5-mCherry, *A. fumigatus pyroA*, amp ^{R}, kan ^{R}	FGSC

Table S5-2 Details list of unique SNPs in AXE5 and AXE8

Gene ID	Mutation site	Confidence score	Codon change	Gene annotation#
AXE5				
ANID_8717	G1192A	88%	GAG→AAG	Uncharacterized; has domain(s) with predicted DNA binding, nucleic acid binding activity
ANID_8177	C1036G	33%	CGG→GGG	Uncharacterized; putative glucose responsive transcription factor
ANID_8179	C104A	45%	TCA→TAA	Uncharacterized; has domain(s) with predicted heat shock protein binding activity
ANID_7792	G1124A	99%	GGC→GGA	Uncharacterized; putative lysophospholipase A
ANID_6239	C1058A	29%	GGG→GTG	Uncharacterized; siderophore biosynthesis lipase/esterase
ANID_10647	C1198T	99%	CAA→TAA	Verified; putative cytochrome P450 protein
ANID_5254	A1164C	30%	GCA→GCC	Uncharacterized; has domain(s) with predicted RNA binding
ANID_5254	C679T	55%	CGT→TGT	Uncharacterized; has domain(s) with predicted RNA binding
ANID_5254	G659A	31%	CGG→CAG	Uncharacterized; has domain(s) with predicted RNA binding
ANID_5254	G515A	73%	CGT→CAT	Uncharacterized; has domain(s) with predicted RNA binding
ANID_5254	C90T	67%	TTC→TTT	Uncharacterized; has domain(s) with predicted RNA binding
ANID_2262	G333C	45%	GCG→GCC	Uncharacterized; ortholog(s) have role in cellular response to oxidative stress, response to osmotic stress
ANID_1453	C557T	30%	TCC→TTC	Uncharacterized
ANID_2154	G2186T	99%	GGT→GTT	pseudogene
ANID_0003	G1137A	57%	CTG→CTA	hypothetical protein
AXE8				
ANID_8541	T1223C	29%	GTC→GCC	Uncharacterized
ANID_8331	G1726C	20%	GGG→CGG	Hypothetical protein
ANID_7848	C60T	83%	CCC→CCT	Uncharacterized
ANID_7848	C37T	60%	CGC→TGC	Uncharacterized
ANID_6966	C108T	40%	CAC→CAT	Uncharacterized; putative transposon-encoded protein
ANID_6242	A193G	37%	AAT→GAT	Uncharacterized
ANID_5095	C399T	76%	GCC→GCT	Uncharacterized; predicted gypsy transposon-related ORF
ANID_5254	C941T	47%	TCA→TTA	Uncharacterized; has domain(s) with predicted RNA binding
ANID_5254	C254T	93%	GCA→GTA	Uncharacterized; has domain(s) with predicted RNA binding
ANID_4102	A2439G	99%	AAG→AAA	Uncharacterized; putative beta-glucosidase
ANID_3445	G1081T	99%	GGA→TGA	Uncharacterized; putative chitin synthase activator
ANID_2711	G1110C	99%	TCG→TCC	Uncharacterized; predicted LINE transposon-related ORF
ANID_1159	A1038C	71%	AAA→AAC	Uncharacterized; has domain(s) with predicted acid-amino acid ligase activity

#, annotation was based on information from online database (28,29).

CHAPTER 6

GENERAL DISCUSSION AND CONCLUSION

Systemic fungal infection is a fast growing problem in developed countries, in part due to the success of modern medicine. Fungi tend to infect immunocompromised patients, in which they can take advantage of the host's immunosuppressed condition. With the advances in medical technology, the number of surviving patients with immune deficiencies is growing fast (Steele and Wormley, 2012), thus providing many more opportunities for fungal infections. At the same time, fungal infections are causing an increasing danger for healthy people as well (Brown et al., 2010). The mortality due to systemic fungal infection may be as high as 50% (Netea and Brown, 2012) although other authors suggest even higher mortality levels. Thus, with respect to mortality rate, pathogenic fungi are very dangerous human pathogens.

Systemic fungal infections are difficult to treat by surgery, because fungi are seldom easily to be separated from the infected organ and any fungal residue will be able to grow again. Therefore anti-fungal drugs are the best clinical method to treat and cure systemic fungal infections. Polyenes and azoles are the most common anti-fungal drugs, which target the integrity or biosynthesis of ergosterol in the fungal membrane (Shapiro et al., 2011). However, due to the high chemical similarity between ergosterol in fungal cells and cholesterol in mammalian cells, polyenes and azoles are highly toxic to humans (Carrillo-Muñoz et al, 2006; Cowen, 2008). The newest class of anti-fungal drug—echinocandins, which target β-glucan synthase, have low toxicity, but also have a narrow activity spectrum (Denning, 2003). In

addition, all existing anti-fungal drugs are losing efficacy due to emerging drug resistance (Cowen, 2008). In particular, drugs that target biosynthetic enzymes are liable to resistance mutations. Substantial effort is still needed to protect us from fungal infections. I suggest that my work in the following two directions will be extremely helpful: 1) studying the metabolism of potential drug targets; 2) developing a strategy to identify the drug resistance mutations.

In my Ph.D. thesis research, I addressed these approaches using *A. nidulans*, which is a tractable model for experimental research. *Aspergillus nidulans* has been used in many fields of biological study for more than 70 years (Morris, 1975). Although *A. nidulans* is not a common human fungal pathogen, it is closely related to *A. fumigatus*, which is one of the most deadly human pathogens. Thus, *A. nidulans* can be used as a safe surrogate fungal model to understand the cell biology of related pathogenic fungi.

Recently, α-1,3-glucan was shown to have important roles for the virulence of several pathogenic fungi (Rappleye et al. 2007; Reese et al., 2007; Fujikawa et al., 2012; Beauvais et al., 2013), thus could be a potential drug target. To facilitate future drug development against this wall component, I explored the metabolism processes of α-1,3-glucan in *A. nidulans* (Chapter 2, 3 and 4). As introduced in chapter 1, the cell wall is an essential structure for fungi to survive in nature, and it is absent from human cells. Therefore, any drug developed against a cell wall component should have low toxicity to humans (Kingsbury et al., 2012). Echinocandins are just one successful example, which block the synthesis of β-glucan (Denning, 2003). Alpha-1,3-glucan is also a major cell wall component in many filamentous fungi and some yeast strains (Latgé, 2010). Unlike β-glucan, evidence showed α-1,3-glucan is not important for cell

morphology in many fungi (Damveld et al., 2005; Henry et al. 2012; Yoshimi et al., 2013; He et al., 2014a), but the presence of α-1,3-glucan appears to be critical for a maximum virulence (Rappleye et al. 2007; Reese et al., 2007; Fujikawa et al., 2012; Beauvais et al., 2013). Therefore, research on the metabolism process of α-1,3-glucan should reveal targets for drugs that are aimed at reducing virulence.

In order to identify anti-fungal resistance mutations, I developed a strategy by using *A. nidulans* and next generation sequencing to identify the drug resistance-causing mutations. The tractability of *A. nidulans* and the power of next generation sequencing enabled me to find the drug resistance mutations efficiently (He et al., 2014b). Finding out the causal mutations is a key step in understanding the molecular basis of resistance and the first step in assessing ways to overcome it. I suggest this strategy can be useful to study the drug resistance mechanisms for all current anti-fungal drugs and even the future ones while under development. In addition, the knowledge from these mutations will also contribute to our understanding of the fungal cell wall.

6.1. Alpha-1,3-glucan Affects Conidial Adhesion; Are There Other Functions?

Alpha-1,3-glucan is a major cell wall component in *Aspergillus* species. In my experiment, it comprised ~15 % of cell wall dry weight in a wild type *A. nidulans*, whereas in *A. fumigatus* it is estimated to be 30 % of cell wall carbohydrate (Latgé, 2007). However, using deletion analysis, α-1,3-glucan has been shown to be dispensable for cell morphology in several *Aspergillus* species (Damveld et al., 2005; Henry et al. 2012; Yoshimi et al., 2013; He et al., 2014a).

So far, the only characterized phenotypic changes associated with deletion of α-1,3-glucan are reduced conidial adhesion and increased sensitivity to calcofluor white (CFW) (Chapter 2). When α-1,3-glucan was removed by gene deletion or by α-1,3-glucanase treatment, conidia did not efficiently cluster together when grown in shaken liquid medium (Fontaine et al., 2010; Fig. 2-3). In contrast when grown on solid medium, the α-1,3-glucan deletion strain was phenotypically indistinguishable from the wild type strain, even under TEM examination (Fig. 2-4). Moreover, α-1,3-glucan is not always required in the wild type hyphae. When a wild type *A. nidulans* was grown in medium without glucose, the expression of AgsB, the major α-1,3-glucan synthase, was down-regulated and α-1,3-glucan was produced at a minimal level (*unpublished data from He and Kaminskyj*). This indicated that α-1,3-glucan is not critical for the cell wall formation and cell morphology of *A. nidulans*.

The CFW hypersensitivity upon α-1,3-glucan deletion suggested that chitin may be easier to access in this mutant, because CFW must physically bind to chitin in the cell wall to exert toxicity. Therefore, α-1,3-glucan may be playing a non-structural role in the cell wall, filling the spaces between the fibrillar skeleton, which is composed of β-glucan and chitin. This does not mean α-1,3-glucan is not cross-linked to other wall components or the cell membrane, because all existing evidence indicates that α-1,3-glucan is a very stable wall component. However, currently the linkages between α-1,3-glucan and other wall components are unknown.

In contrast to the α-1,3-glucan deletion strains, phenotypic defects on solid medium were seen for α-1,3-glucan overexpression strains. A 2-fold overexpression of α-1,3-glucan synthase (*actA*(p)-*agsB*) caused a moderate conidiation defect (Fig. 2-3), whereas a 14-fold

overexpression of α-1,3-glucan synthase (*H2A*(p)-*agsB*) led to a severe conidiation defect as well as a series of phenotypic changes (Fig. 3-1). However, none of the α-1,3-glucan overexpression strains showed increased conidial adhesion or CFW tolerance (Fig. 2-5 and 3-2). Therefore, when grown in complete medium, α-1,3-glucan content appears to be already optimal for the *A.nidulans* cell wall.

I did find the α-1,3-glucan overexpression strains have higher adhesion ability to hydrophobic materials (Fig. 3-2). And the 14-fold overexpression strain (*H2A*(p)-*agsB*) was even able to form a biofilm-like structure (Fig. 3-2). However, my results also showed this unnatural high amount of α-1,3-glucan caused cell wall defects and remodeling (Fig. 3-3), indicating the whole cell wall architecture was changed in the overexpression strain, probably due to the activation of CWI pathways. Therefore, the change of cellular adhesion to hydrophobic materials was triggered by overexpression of α-1,3-glucan, but not because of α-1,3-glucan itself (Chapter 3).

In conclusion, my studies showed α-1,3-glucan is only important for conidial adhesion and CFW sensitivity under the conditions that I tested. Though α-1,3-glucan content is apparently not necessary in structuring the cell wall of *A. nidulans*, abnormally high levels of α-1,3-glucan were harmful for cell morphology. The levels of α-1,3-glucan also correlate with the cell's ability to adhere to hydrophobic materials.

6.2. Alpha-1,3-glucan Produced by the AgsA and AgsB Are Not Equivalent

A. nidulans has two annotated α-1,3-glucan synthases (AgsA and AgsB), which were both functional proteins in my test (Chapter 2). When these proteins were overexpressed by the same promoter, a similar high level of α-1,3-glucan was found in the cell wall (Table 2-1), suggesting they have similar potency in synthesizing this wall component. However, these two synthases differ in expression profiles when regulated by their native promoters and even differ in their final products.

Under its native promoter, *agsB* had a constant high expression level throughout the asexual life cycle, whereas *agsA* was only highly expressed during conidiation stages (Fig. 2-7). Therefore, the *A. nidulans* hyphal cell wall α-1,3-glucan was mostly produced (up to 97%) through AgsB activity while in conidial cell wall the α-1,3-glucan was derived from the activities of both synthases (Chapter 2). Intriguingly, the α-1,3-glucan produced by two synthases is not even equivalent in respect to cellular function. To differentiate the source of α-1,3-glucan, one can speak of two subsets of polymers depending on the original enzyme used: AgsA-α-1,3-glucan and AgsB-α-1,3-glucan. The existing evidence suggests that AgsB-α-1,3-glucan was clearly more important: loss of AgsB-α-1,3-glucan substantially reduced conidial adhesion in liquid, but loss of AgsA-α-1,3-glucan did not change this phenotype (Fig. 2-3). As mentioned above the α-1,3-glucan in the conidial wall was composed of AgsA-α-1,3-glucan and AgsB-α-1,3-glucan, so AgsB-α-1,3-glucan was the only α-1,3-glucan responsible for the conidial adhesion ability. AgsB-α-1,3-glucan was also the only α-1,3-glucan responsible for the CFW sensitivity (Fig. 2-6). In addition, overexpression of AgsA-α-1,3-glucan

did not recover the conidial adhesion defect or the CFW sensitivity defect due to the loss of AgsB-α-1,3-glucan (Fig. 2-3 and 2-6). Consistent with these, using overexpression (by either the *actA* or the *H2A* promoter) analyses, only more AgsB-α-1,3-glucan led to phenotypic defects and cell wall defects (Fig. 3-1 and 3-3). Therefore, all the functions and phenotypic changes related to α-1,3-glucan content are due to AgsB-α-1,3-glucan. The function and role of AgsA-α-1,3-glucan is still a mystery.

I tried to explore the difference between AgsA-α-1,3-glucan and AgsB-α-1,3-glucan. But no difference was found in assays using an antibody that binds to α-1,3-glycosidic linked glucose, in chemical analysis using alkali extraction and the anthrone assay, and in TEM studies using immunogold technique (Fig. 2-8). Since α-1,3-glucan is suggested to have no side branches (Grün et al., 2005; Choma et al., 2013), other possible reasons for this difference could be the post-synthesis modification or the length of α-1,3-glucan, which warrants further research.

6.3. Alpha-1,3-glucan Synthesis Is Differentially Regulated by a Conserved Gene Cluster

Evidence showed the synthesis of α-1,3-glucan requires more than just α-1,3-glucan synthase (Grün et al., 2005). From my result, at least two amylase-like proteins (AmyD and AmyG) are involved in α-1,3-glucan synthesis regulation (Chapter 2 and 4). The encoding genes of these two amylase-like proteins (*amyD* and *amyG*) are adjacent to the major α-1,3-glucan synthase encoding gene (*agsB*) (Fig. 2-1), and these three genes together forms a small gene cluster [*agsB*←→*amyD amyG*]. Although a three-gene cluster is smaller than typical for gene cluster in filamentous fungi, as some of the cluster could have more than 20 genes (Keller et al.,

1997), I still think it is valid to claim these three genes as a gene cluster based on the following two reasons. First all these three genes are all involved in the same metabolic process, which is α-1,3-glucan synthesis. A similar use of 'gene cluster' has been used for the four galactose metabolism (Leloir pathway) genes by Slot and Rokas (2010). In addition, the localization relationship of these genes is conserved in almost all *Aspergillus* species except *A. fumigatus* (Chapter 2).

Among gene products from this gene cluster, α-1,3-glucan synthase (AgsB) is the key enzyme to synthesize α-1,3-glucan (as discussed above). My results showed the expression level of AgsB positively determines the amount of α-1,3-glucan in the cell wall (Chapter 2 and 3). In addition, the GFP-tagging results for AgsB-GFP strain strongly indicated the localization of AgsB is on the cell membrane (Fig. 2-7). Although due to the resolution of fluorescence microscope and the small size of *A. nidulans* cells, I could not generate very convincing evidence to conclude the localization of AgsB to date. Due to the lack of AgsB antibody, western blot and immunogold TEM technologies are also not available to further verify the localization of AgsB. But based on the sequence analysis of *agsB*, which has a 12 repeats transmembrane domain, and the GFP tagging result from *S. pombe* α-1,3-glucan synthase (Cortés et al., 2012), which also showed a cell membrane localization, I think it is still valid to say the localization of AgsB is on cell membrane. And the membrane localization of α-1,3-glucan synthase confirmed part of the protein model of α-1,3-glucan synthase presented by Grün et al. (2005) (Fig. 1-2), which suggested that α-1,3-glucan synthases localize on the cell membrane. This model also suggests that the transmembrane domain of α-1,3-glucan synthase forms a channel to transport the newly

synthesized α-1,3-glucan from the cytoplasm to the cell wall. In that case, the integrity of the transmembrane domain should be very important, which was also supported by my results. When GFP tagged at the C-terminal of AgsB (right after the transmembrane domain), AgsB completely lost its function (Chapter 2). In addition, a 6 amino acids deletion in transmembrane domain also totally abolished the function of the protein (Chapter 3). Altogether, I interpret this as showing the importance of the transmembrane domain in AgsB. The transmembrane domain in AgsB serves as more than just an element for localization, but also as a functional domain involved in the α-1,3-glucan synthesis process.

AmyG is another protein crucial for α-1,3-glucan synthesis. The function of this kind of protein was first reported in *H. capsulatum* (Marion et al., 2006). From results in this thesis, *A. nidulans* AmyG localized in the cytoplasm and its function was very important for α-1,3-glucan synthesis (Table 2-1 and Fig. 2-7). Unlike α-1,3-glucan synthase, overexpression of AmyG did not greatly increase wall α-1,3-glucan content (Table 2-1) suggesting it was not the limiting step in the synthesis process. Considering the localizations of AmyG and AgsB, AmyG should respond for an earlier step in α-1,3-glucan synthesis process, likely the synthesis of the α-1,4-glycosidic linked oligosaccharide primer structure (Grün et al., 2005; Marion et al., 2006) (Fig. 1-2). Since AmyG has an amylase-like domain, it may have a role in breaking down α-1,4-glycosidic linkage. Therefore, two possible working models could be hypothesized based on that enzymatic function. One model is AmyG may breakdown long chain α-1,4-glucan into small chains, which provides the primer structure for α-1,3-glucan synthesis. The second model

is AmyG may break down the α-1,4-glucan to provide glucose for α-1,3-glucan synthesis. But to test these models, a study on AmyG enzymatic function is needed first.

Interestingly, AmyD had a totally different impact on α-1,3-glucan content than AmyG. AmyD repressed α-1,3-glucan synthesis. In fungal cells, α-1,3-glucanase is expected to be the hydrolytic enzyme that degrades the α-1,3-glucan on cell wall. Although AmyD and α-1,3-glucanase both have repressive effects on α-1,3-glucan accumulation, their functions are independent from each other (Fig. 4-2 and 4-3). The dynamics of α-1,3-glucan accumulation study revealed different working mechanisms between AmyD and α-1,3-glucanase (Fig. 4-4) with AmyD impacting α-1,3-glucan accumulation much earlier than α-1,3-glucanase. Therefore, AmyD should not be involved in α-1,3-glucan degradation. As discussed in last paragraph for AmyG, if AmyD also served as a amylase to breakdown α-1,4-glycosidic linkage, the potential working model for AmyD would be to degrade the primer structure of α-1,3-glucan, which would prevent α-1,3-glucan from being synthesized.

Although AgsA is also a functional α-1,3-glucan synthase in *A. nidulans*, its activity only accounted for a small amount of α-1,3-glucan (mostly in conidia). Furthermore, AgsA-α-1,3-glucan had no characterized impact on cell wall formation and cell morphology. Therefore, AgsA activity does not appear to be important for functional α-1,3-glucan synthesis.

In summary, gene products from the conserved [*agsB*←→*amyD amyG*] gene cluster appear to control α-1,3-glucan synthesis in *A. nidulans* (Fig. 6-1). AgsB synthesizes α-1,3-glucan; AmyG works at an earlier step in the synthesis process, presumably the primer structure (Marion et al., 2006); and AmyD negatively regulates the production of α-1,3-glucan. Although these

three proteins have different roles, they all regulate the synthesis of the wall α-1,3-glucan content (Fig. 6-1).

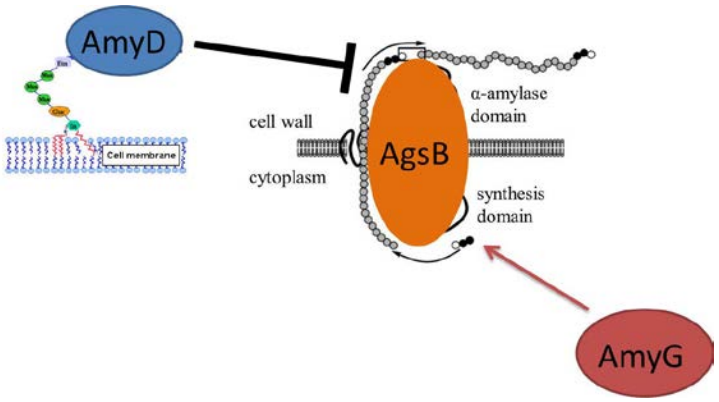

Fig. 6-1 Model of α-1,3-glucan synthesis regulation in *A. nidulans*

6.4. How Could These Data Help in Drug Development against α-1,3-glucan?

Is α-1,3-glucan a useful drug target? From the results presented here, α-1,3-glucan does not appear to be important for cell wall formation and cell morphology. With respect to the existing drug targets, which are mostly essential cell elements, α-1,3-glucan is not a suitable drug target. However, from other evidence, α-1,3-glucan was shown to be important for the virulence of three human pathogens and one plant pathogen (Rappleye et al. 2007; Reese et al., 2007; Fujikawa et al., 2012; Beauvais et al., 2013). Alpha-1,3-glucan is clearly a virulence factor in these pathogenic fungi. Discovering virulence factors is a new trend in antimicrobial drug development (Clatworthy et al. 2007; Allen et al., 2014), as few essential factors are left to explore. Therefore, α-1,3-glucan may be still a promising drug target to prevent fungal infections, at least for *H. capsulatum*, *C. neoformans*, *A. fumigatus* and *M. oryzae*. If α-1,3-glucan does turn

out to be a viable drug target, how could the results presented in this thesis contribute to this goal?

Since the presence of α-1,3-glucan is important for fungal virulence, the therapeutic strategy should be to eliminate α-1,3-glucan from the cell surface. If so, drugs that inhibit the function of α-1,3-glucan synthase will be the best choice. So far all α-1,3-glucan related studies showed α-1,3-glucan synthases are important for α-1,3-glucan synthesis process (Hochstenbach et al., 1998; Pereira et al., 2000; Rappeleye et al. 2004; Damveld et al., 2005; Henry et al. 2012; Yoshimi et al., 2013; He et al., 2014a). Alpha-1,3-glucan synthases are big (mostly ~2500 amino acids) and complex membrane proteins with at least three functional domains (Fig. 1-2) complicating the resolution of their protein structure. Maybe due to this reason, no anti-fungal drug that targets α-1,3-glucan synthase has so far been developed. A more realistic way to gather structural information on α-1,3-glucan synthases would be to resolve the structure of each individual functional domain. As discussed above, there is evidence showing that α-1,3-glucan synthase may initiate the synthesis from cytoplasmic side, suggesting that the cytoplasmic domain should be the primary target in an inhibitor screening. In addition, given that the transmembrane domain may work as a channel and is essential for the function (Grün et al. 2005; Cortés et al., 2012; Chapter 2), any compound that can specifically block this channel will likely also stop the α-1,3-glucan synthesis.

AmyG is also very important for α-1,3-glucan synthesis. The crucial function of this protein in α-1,3-glucan synthesis was also reported in *H. capsulatum* (Marion et al., 2006). Thus, AmyG is very likely a conserved protein involved in α-1,3-glucan synthesis in other fungi, (homologues

listed in Table 6-1). AmyG has an amylase-like domain and localizes in the cytoplasm of *A. nidulans* cell, which could facilitate the protein structure analysis. Therefore, AmyG could be an alternative target to block α-1,3-glucan synthesis process.

As an alternative to interrupting the synthesis of α-1,3-glucan, increasing its removal from the cell wall could theoretically lead to a similar decrease in virulence. Alpha-1,3-glucanase is the enzyme that degrades α-1,3-glucan. A transgenic rice plant expressing a bacterial α-1,3-glucanase has been shown to be resistant to *M. oryzae* infection (Fujikawa et al., 2012). In this thesis, AmyD activity, like α-1,3-glucanase, is shown to be important to suppress α-1,3-glucan accumulation (Chapter 2 and 4), suggesting AmyD may be a viable way to treat fungal infection. However, contrary to α-1,3-glucanase, AmyD activity is important to slow down the accumulation of α-1,3-glucan, but not to degrade already deposited α-1,3-glucan. In respect to that, I think AmyD will not be as useful as α-1,3-glucanase to treat fungal infection. In addition, digesting α-1,3-glucan from the fungal cell wall should be only valid to treat fungal infection in plants but not animals.

6.5. Can We Predict the Most Likely Drug Resistance Mutations?

Results from chapter 5 suggest the answer is YES. Using *A. nidulans* as a model to induce resistant mutants and using next generation sequencing to identify causal mutations may be a time-saving strategy to find out the genes and mutations involved in drug resistance.

Within two weeks under exposure to moderate levels of CFW, *A. nidulans* wild type strain developed resistant sectors. Because *A. nidulans* is haploid during its asexual life, we

hypothesized that the appearance of the accelerated growth sectors immediately follows the first beneficial mutation. By assessing the inheritance of resistance phenotypes from mating experiment between adaptive strain and wild type strain, we were able to support this hypothesis (Chapter 5). Isolation of single mutation strains is the first step towards the identification of the mutated genes that generated the resistance.

Data in Chapter 5 indicated that the dosage of the inducing drug was critical to isolate the mutants. For instance, while no resistant mutant was isolated on 15 μg/mL CFW medium, 24 individual mutants were isolated within 2 weeks on 30 μg/mL CFW medium. The higher CFW dosage (30 μg/mL) showed higher inhibition rate (70 %) on colonies growth and also induced Hülle cells at the edge of colonies (Fig. 5-1), which are a sign for cell fusion. Hyphal fusion and subsequent nuclear migration could lead to enhanced spread of nuclei bearing a beneficial mutation and a more efficient formation of a fast-growing sector. Therefore, higher drug dosage is more potent in inducing resistant mutants in this assay. However, high drug concentration will eventually lead to very weak growth rates that can also impact the ability to detect outgrowths of resistant mutants. In practice, the dosages of the inducing drug need to be tested individually. Based on the results from Chapter 5, a dose that inhibits the wild type *A. nidulans* growth to about 70 % or a dose that can enhance hyphal fusion (represented by appearance of the Hülle cells) are likely good starting points.

Eventually, the occurrence of resistant mutants in an inducing experiment will still be decided by the specific mechanism of the anti-fungal drug in question. For CFW, previous studies have reported many different mutations can cause resistance, explaining perhaps the fact

that so many different resistant mutants were isolated (Chapter 5). For polyenes, where the resistance rate has been suggested to be low (Kanafani and Perfect, 2008), fewer genes may be involved in the resistance mechanism(s). Irrespective of these differences, as long as single mutations lead to improved growth, and the size of inducing experiment is large enough, resistant mutants with single mutation should be able to be isolated within days. This is a convenient method to test the durability of anti-fungal drugs.

The isolation of drug resistant mutants could be the first step towards solving the drug resistance problem. Determining the identity of the mutated genes is the next important step. With the development of next generation sequencing, gene finding through single nucleotide polymorphism (SNP) mapping on a genome scale is much easier than before, especially for a small and haploid genome (30Mb for *A. nidulans*). In the inducing step, all mutants were induced from the same parental strain within a short time. Therefore genetic variabilities should be limited between different mutants. This was confirmed upon sequencing of two of the CFW resistant mutants (Chapter 5). Fewer than 20 unique SNPs per strain were identified (Table 5-2). Combining gene annotation data from two well established *Aspergillus* databases (AspGD and Broad Institute), the most probable genes bearing the mutations could be identified. As a final step to determine the exact gene involved, experiments to test the effects of mutations could be performed by re-introducing the mutated gene into a wild type genome.

These results suggest this strategy can be an efficient way to identify the causal mutations of most if not all drug resistance, perhaps as ways to predict their appearance in the clinic. By knowing such mutations, new drugs or new therapeutic strategies can be designed to promptly

respond to emerging resistance. This will enable us to stay ahead in the drug resistance arms race.

6.6. Future Directions

Given the fact that fungal systemic infection is on the rise and anti-fungal drug resistance is becoming more prevalent, we are facing the challenge of developing strategies to control the upwards trajectory of fungal infections. For that purpose, we need first to understand more about these organisms.

In this thesis, I used *A. nidulans* as a model to study the α-1,3-glucan synthesis process and also to develop a strategy for identifying the drug resistance mutations. For α-1,3-glucan synthesis, I systematically characterized the roles of two α-1,3-glucan synthases and two amylase-like proteins in the synthesis process. For the first time, I presented data that show the α-1,3-glucan polymers produced by two α-1,3-glucan synthases are not equivalent and that the α-1,3-glucan synthesis is differentially regulated by a conserved gene cluster [*agsB*←→*amyD amyG*]. But there are still many questions left to explore. Amongst these, four questions are particularly relavent.

1) Are the functions of AmyG and AmyD conserved in α-1,3-glucan containing fungi? Alpha-1,3-glucan synthase is the essential protein for α-1,3-glucan synthesis, and its function has been studied in several pathogenic fungi (Rappleye et al. 2007; Reese et al., 2007; Fujikawa et al., 2012; Beauvais et al., 2013), revealing a conserved working mechanism (Hochstenbach et al., 1998; Grün et al., 2005). In my study, I found that AmyD and AmyG also regulate α-1,3-glucan

synthesis, though in different ways. Homologues of AmyD and AmyG exist in α-1,3-glucan containing fungi, at least for *A. fumigatus*, *H. capsulatum*, *C. neoformans* and *M. oryzae* (Table 6-1). Therefore, it would be useful to know if the functions of AmyD and AmyG are conserved in these pathogenic fungal species.

	A. fumigatus	*H. capsulatum*	*C. neoformans*	*M. oryzae*
amyD	*Afu3g00910*	*HCBG_00468.2*	*CNAG_02189*	*MGG_09640.7*
		HCBG_03431.2	*CNAG_05264*	
amyG	*Afu1g15150*	*HCBG_01374.2**	*CNAG_03146*	*MGG_03287*
				MGG_09642

Table 6-1 Homologues of *amyD* and *amyG* in four pathogenic fungi

Data were gained by BLAST analysis using the protein sequence of AmyD and AmyG. Genome data were obtained from AspGD and Broad Institute. Genomes of following strains were used: *A. nidulans* A4, *A. fumigatus* AF293, *H. capsulatum* G186AR, *C. neoformans* H99 and *M. oryzae* 70-15. If multiple hits were found, the first two with highest similarity were listed in the table.

*: verified gene

2) What are the enzymatic functions of α-1,3-glucan synthase and AmyG? The critical roles of α-1,3-glucan synthase and AmyG in α-1,3-glucan synthesis have been confirmed in at least two different fungal species (Rappleye et al., 2004; Marion et al., 2006). However, no data from enzymatic studies are available so far. Without this information, we will not be able to reveal the details of α-1,3-glucan synthesis process. Therefore, understanding the enzymatic functions is a key step to move forward in the research of α-1,3-glucan synthesis.

3) What cell wall components enable *A. nidulans* to form the biofilm-like structure? It is very intriguing to see that *A. nidulans* can also form a biofilm-like structure as *A. fumigatus* (Fig. 3-2). The inability to form a biofilm is one of the reasons why *A. nidulans* is less virulent than *A.*

fumigatus. However, an *A. nidulans* AgsB overexpression strain [*H2A*(p)-*agsB*] showed the ability to form biofilm (Fig. 3-2). Data from one of our collaborators showed that overexpression of an adhesin in *A. nidulans* can also enable biofilm formation (*unpublished data from the D. Sheppard group, McGill University*). Together, these results revealed that *A. nidulans* may have a latent ability to form biofilm. This provides a useful tool to study the process of the biofilm formation itself, which is not very clear at the moment. *H2A(*p)-*agsB* had high α-1,3-glucan content and other changes in cell wall architecture (Fig. 2-3). A transcriptome comparison between *H2A(*p)-*agsB* and a wild type *A. nidulans* may reveal the key factors that regulate biofilm formation. The highly overexpressed wall components in *H2A(*p)-*agsB* are the most promising targets.

4) What are the resistance mechanisms for drugs of polyenes and echinocandins? As searching for new effective anti-fungal drugs is difficult and expensive, protecting our current anti-fungal drugs from emerging resistance is as important as developing new drugs. In this thesis, a strategy was developed to quickly identify drug resistance mutations by using *A. nidulans* and next generation sequencing. So far, the strategy has been successful in exploring CFW resistance. However, CFW is not a clinical anti-fungal drug, and all the CFW resistant mutants maintained the wild type drug sensitivity against caspofungin (Fig. 5-2), which belongs to the echinocandins. Therefore the mutations that we have identified have limited clinical relevance, though they have great potential for better understanding cell wall synthesis. To go forward, clinically used drugs should be used to induce resistant mutants. Polyenes and echinocandins are suitable candidates, since the resistance mechanism against these two kinds of

drug are not fully understood at the moment (Kanafani and Perfect, 2008). In addition, because of the predictive potential of this strategy, it would be reasonable to also test drugs currently under development. In this way, we may assess the drug durability and predict the likelihood and identities of resistance mutations before their occurence in the clinic.

In summary, the research conducted in this thesis systematically studied the synthesis process of α-1,3-glucan in *A. nidulans*. It showed that the α-1,3-glucan synthesis is regulated by two α-1,3-glucan synthases and two amylase-like proteins. The α-1,3-glucan polymers produced by two synthases were not equivalent; however none of them had an important impact on cell wall formation and cell morphology. These results shed light on therapeutic strategy development against α-1,3-glucan. In addition, a new strategy to quickly identify drug resistance mutations was presented. This may help us to predict the most likely mutations that can cause anti-fungal drug resistance. In the end, I hope this work will increase our general understanding about cell wall structure/function/composition and contribute to the existing arsenal against pathogenic fungi.

REFERENCES

Ait-Lahsen, H., Soler, A., Rey, M., de La Cruz, J., Monte, E., Llobell, A., 2001. An anti-fungal exo-alpha-1,3-glucanase (AGN13.1) from the biocontrol fungus *Trichoderma harzianum*. Appl. Environ. Microbiol. 67, 5833-9.

Alam, M.K., El-Ganiny, A.M., Afroz, S., Sanders, D.A.R., Liu, J., Kaminskyj, S.G., 2012. *Aspergillus nidulans* galactofuranose biosynthesis affects anti-fungal drug sensitivity. Fungal Genet. Biol. 49, 1033-43.

Alam, M.K., van Straaten, K.E., Sanders, D.A.R., Kaminskyj, S.G.W., 2014. *Aspergillus nidulans* cell wall composition and function change in response to hosting several *Aspergillus fumigatus* UDP-galactopyranose mutase activity mutants. PLoS One 9, e85735.

Alexander, B.D., Johnson, M.D., Pfeiffer, C.D., Jimenez-Ortigosa, C., Catania, J., Booker, R., Castanheira, M., Messer, S.A., Perlin, D.S., Pfaller, M.A., 2013. Increasing echinocandin resistance in *Candida glabrata*: clinical failure correlates with presence of *FKS* mutations and elevated minimum inhibitory concentrations. Clin. Infect. Dis. 56, 1724-32.

Allen, R.C., Popat, R., Diggle, S.P., Brown, S.P., 2014. Targeting virulence: can we make evolution-proof drugs? Nat. Rev. Microbiol. 12, 300-8.

Antinori, S., 2014. *Histoplasma capsulatum*: More Widespread than Previously Thought. Am. J. Trop. Med. Hyg.

Ashwell, G., 1957. Colorimetric analysis of sugars. Methods Enzymol II: 73–103.

Barr, D.P., Aust, S.D., 1994. Pollutant degradation by white rot fungi. Rev. Environ. Contam. Toxicol. 138, 49-72.

Bartnicki-Garcia, S., 2002. Molecular Biology of Fungal Development (book), Chapter 2: Hyphal tip growth: Outstanding questions. 29-50.

Bauchop, T., 1979. Rumen anaerobic fungi of cattle and sheep. Appl. Environ. Microbiol. 38, 148-58.

Beauvais, A., Bozza, S., Kniemeyer, O., Formosa, C., Balloy, V., Henry, C., Roberson, R.W., Dague, E., Chignard, M., Brakhage, A.A., Romani, L., Latgé, J.P., 2013. Deletion of the alpha-(1,3)-glucan synthase genes induces a restructuring of the conidial cell wall responsible for the avirulence of *Aspergillus fumigatus*. PLoS Pathog. 9, e1003716.

Beauvais, A., Maubon, D., Park, S., Morelle, W., Tanguy, M., Huerre, M., Perlin, D.S., Latgé, J.P., 2005. Two alpha-(1-3)-glucan synthases with different functions in *Aspergillus fumigatus*. Appl. Environ. Microbiol. 71, 1531-8.

Beauvais, A., Schmidt, C., Guadagnini, S., Roux, P., Perret, E., Henry, C., Paris, S., Mallet, A., Prevost, M.C., Latgé, J.P., 2007. An extracellular matrix glues together the aerial-grown hyphae of *Aspergillus fumigatus*. Cell. Microbiol. 9, 1588-600.

Bechman, A., Phillips, R.D., Chen, J., 2012. Changes in selected physical property and enzyme activity of rice and barley koji during fermentation and storage. J. Food Sci. 77, M318-22.

Bennett, J.W., 1998. Mycotechnology: the role of fungi in biotechnology. J. Biotechnol. 66, 101-7.

Blackwell, M., 2011. The fungi: 1, 2, 3 ... 5.1 million species? Am. J. Bot. 98, 426-38.

Brown, G.D., Denning, D.W., Levitz, S.M., 2012. Tackling human fungal infections. Science 336, 647.

Brown, J.K., Hovmoller, M.S., 2002. Aerial dispersal of pathogens on the global and continental scales and its impact on plant disease. Science 297, 537-41.

Camacho, E., Sepulveda, V.E., Goldman, W.E., San-Blas, G., Nino-Vega, G.A., 2012. Expression of *Paracoccidioides brasiliensis* AMY1 in a *Histoplasma capsulatum amy1* mutant, relates an alpha-(1,4)-amylase to cell wall alpha-(1,3)-glucan synthesis. PLoS One 7, e50201.

Carrillo-Munoz, A.J., Giusiano, G., Ezkurra, P.A., Quindos, G., 2006. Anti-fungal agents: mode of action in yeast cells. Rev. Esp. Quimioter. 19, 130-9.

Chen, S.C., Sorrell, T.C., 2007. Anti-fungal agents. Med. J. Aust. 187, 404-9.

Choma, A., Wiater, A., Komaniecka, I., Paduch, R., Pleszczynska, M., Szczodrak, J., 2013. Chemical characterization of a water insoluble (1-3)-alpha-D-glucan from an alkaline extract of *Aspergillus wentii*. Carbohydr. Polym. 91, 603-8.

Clatworthy, A.E., Pierson, E., Hung, D.T., 2007. Targeting virulence: a new paradigm for antimicrobial therapy. Nat. Chem. Biol. 3, 541-8.

Cortes, J.C., Sato, M., Munoz, J., Moreno, M.B., Clemente-Ramos, J.A., Ramos, M., Okada, H., Osumi, M., Duran, A., Ribas, J.C., 2012. Fission yeast Ags1 confers the essential septum strength needed for safe gradual cell abscission. J. Cell Biol. 198, 637-56.

Cosgrove, D.J., 2005. Growth of the plant cell wall. Nat. Rev. Mol. Cell Biol. 6, 850-61.

Cowen, L.E., 2008. The evolution of fungal drug resistance: modulating the trajectory from genotype to phenotype. Nat. Rev. Microbiol. 6, 187-98.

Crampin, H., Finley, K., Gerami-Nejad, M., Court, H., Gale, C., Berman, J., Sudbery, P., 2005. *Candida albicans* hyphae have a Spitzenkorper that is distinct from the polarisom found in yeast and pseudohyphae. J. Cell. Sci. 118, 2935-47.

Dagenais, T.R., Keller, N.P., 2009. Pathogenesis of *Aspergillus fumigatus* in Invasive Aspergillosis. Clin. Microbiol. Rev. 22, 447-65.

Damveld, R.A., Franken, A., Arentshorst, M., Punt, P.J., Klis, F.M., van den Hondel, C.A., Ram, A.F., 2008. A novel screening method for cell wall mutants in *Aspergillus niger* identifies UDP-galactopyranose mutase as an important protein in fungal cell wall biosynthesis. Genetics 178, 873-81.

Damveld, R.A., vanKuyk, P.A., Arentshorst, M., Klis, F.M., van den Hondel, C.A., Ram, A.F., 2005. Expression of *agsA*, one of five 1,3-alpha-D-glucan synthase-encoding genes in *Aspergillus niger*, is induced in response to cell wall stress. Fungal Genet. Biol. 42, 165-77.

Davies, G., Henrissat, B., 1995. Structures and mechanisms of glycosyl hydrolases. Structure 3, 853-9.

Davies, S., Guidry, C., Politano, A., Rosenberger, L., McLeod, M., Hranjec, T., Sawyer, R., 2014. *Aspergillus* Infections in Transplant and Non-Transplant Surgical Patients. Surg. Infect. (Larchmt) .

de Groot, P.W., Brandt, B.W., Horiuchi, H., Ram, A.F., de Koster, C.G., Klis, F.M., 2009. Comprehensive genomic analysis of cell wall genes in *Aspergillus nidulans*. Fungal Genet. Biol. 46 Suppl 1, S72-81.

Dekker, N., Speijer, D., Grun, C.H., van den Berg, M., de Haan, A., Hochstenbach, F., 2004. Role of the alpha-1,3-glucanase Agn1p in fission-yeast cell separation. Mol. Biol. Cell 15, 3903-14.

DeMarini, D.J., Adams, A.E., Fares, H., De Virgilio, C., Valle, G., Chuang, J.S., Pringle, J.R., 1997. A septin-based hierarchy of proteins required for localized deposition of chitin in the *Saccharomyces cerevisiae* cell wall. J. Cell Biol. 139, 75-93.

Denning, D.W., 2003. Echinocandin anti-fungal drugs. Lancet 362, 1142-51.

Douglas, C.M., D'Ippolito, J.A., Shei, G.J., Meinz, M., Onishi, J., Marrinan, J.A., Li, W., Abruzzo, G.K., Flattery, A., Bartizal, K., Mitchell, A., Kurtz, M.B., 1997. Identification of the *FKS1* gene of *Candida albicans* as the essential target of 1,3-beta-D-glucan synthase inhibitors. Antimicrob. Agents Chemother. 41, 2471-9.

El-Ganiny, A.M., Sanders, D.A.R., Kaminskyj, S.G.W., 2008. *Aspergillus nidulans* UDP-galactopyranose mutase, encoded by *ugmA* plays key roles in colony growth, hyphal morphogenesis, and conidiation. Fungal Genet. Biol. 45, 1533-42.

Elorza, M.V., Rico, H., Sentandreu, R., 1983. Calcofluor white alters the assembly of chitin fibrils in *Saccharomyces cerevisiae* and *Candida albicans* cells. J. Gen. Microbiol. 129, 1577-82.

Engel, J., Schmalhorst, P.S., Routier, F.H., 2012. Biosynthesis of the fungal cell wall polysaccharide galactomannan requires intraluminal GDP-mannose. J. Biol. Chem. 287, 44418-24.

Fekkar, A., Meyer, I., Brossas, J.Y., Dannaoui, E., Palous, M., Uzunov, M., Nguyen, S., Leblond, V., Mazier, D., Datry, A., 2013. Rapid emergence of echinocandin resistance during *Candida kefyr* fungemia treatment with caspofungin. Antimicrob. Agents Chemother. 57, 2380-2.

Firon, A., Beauvais, A., Latgé, J.P., Couve, E., Grosjean-Cournoyer, M.C., D'Enfert, C., 2002. Characterization of essential genes by parasexual genetics in the human fungal pathogen *Aspergillus fumigatus*: impact of genomic rearrangements associated with electroporation of DNA. Genetics 161, 1077-87.

Fisher, M.C., Henk, D.A., Briggs, C.J., Brownstein, J.S., Madoff, L.C., McCraw, S.L., Gurr, S.J., 2012. Emerging fungal threats to animal, plant and ecosystem health. Nature 484, 186-94.

Fontaine, T., Beauvais, A., Loussert, C., Thevenard, B., Fulgsang, C.C., Ohno, N., Clavaud, C., Prevost, M.C., Latgé, J.P., 2010. Cell wall alpha-1,3-glucans induce the aggregation of germinating conidia of *Aspergillus fumigatus*. Fungal Genet. Biol. 47, 707-12.

Fuchs, B.B., Mylonakis, E., 2009. Our paths might cross: the role of the fungal cell wall integrity pathway in stress response and cross talk with other stress response pathways. Eukaryot. Cell. 8, 1616-25.

Fujikawa, T., Kuga, Y., Yano, S., Yoshimi, A., Tachiki, T., Abe, K., Nishimura, M., 2009. Dynamics of cell wall components of *Magnaporthe grisea* during infectious structure development. Mol. Microbiol. 73, 553-70.

Fujikawa, T., Sakaguchi, A., Nishizawa, Y., Kouzai, Y., Minami, E., Yano, S., Koga, H., Meshi, T., Nishimura, M., 2012. Surface alpha-1,3-glucan facilitates fungal stealth infection by interfering with innate immunity in plants. PLoS Pathog. 8, e1002882.

Fujioka, T., Mizutani, O., Furukawa, K., Sato, N., Yoshimi, A., Yamagata, Y., Nakajima, T., Abe, K., 2007. MpkA-dependent and -independent cell wall integrity signaling in *Aspergillus nidulans*. Eukaryot. Cell. 6, 1497-510.

Furbino, L.E., Godinho, V.M., Santiago, I.F., Pellizari, F.M., Alves, T.M., Zani, C.L., Junior, P.A., Romanha, A.J., Carvalho, A.G., Gil, L.H., Rosa, C.A., Minnis, A.M., Rosa, L.H., 2014. Diversity patterns, ecology and biological activities of fungal communities associated with the endemic macroalgae across the Antarctic peninsula. Microb. Ecol. 67, 775-87.

Futagami, T., Nakao, S., Kido, Y., Oka, T., Kajiwara, Y., Takashita, H., Omori, T., Furukawa, K., Goto, M., 2011. Putative stress sensors WscA and WscB are involved in hypo-osmotic and acidic pH stress tolerance in *Aspergillus nidulans*. Eukaryot. Cell. 10, 1504-15.

Garcia-Rodriguez, L.J., Duran, A., Roncero, C., 2000. Calcofluor anti-fungal action depends on chitin and a functional high-osmolarity glycerol response (HOG) pathway: evidence for a physiological role of the *Saccharomyces cerevisiae* HOG pathway under noninducing conditions. J. Bacteriol. 182, 2428-37.

Gastebois, A., Clavaud, C., Aimanianda, V., Latgé, J.P., 2009. *Aspergillus fumigatus*: cell wall polysaccharides, their biosynthesis and organization. Future Microbiol. 4, 583-95.

Gifford, D.R., Schoustra, S.E., Kassen, R., 2011. The length of adaptive walks is insensitive to starting fitness in *Aspergillus nidulans*. Evolution 65, 3070-8.

Gordon, G.L., Phillips, M.W., 1998. The role of anaerobic gut fungi in ruminants. Nutr. Res. Rev. 11, 133-68.

Gravelat, F.N., Ejzykowicz, D.E., Chiang, L.Y., Chabot, J.C., Urb, M., Macdonald, K.D., al-Bader, N., Filler, S.G., Sheppard, D.C., 2010. *Aspergillus fumigatus* MedA governs adherence, host cell interactions and virulence. Cell. Microbiol. 12, 473-88.

Grun, C.H., Hochstenbach, F., Humbel, B.M., Verkleij, A.J., Sietsma, J.H., Klis, F.M., Kamerling, J.P., Vliegenthart, J.F., 2005. The structure of cell wall alpha-1,3-glucan from fission yeast. Glycobiology 15, 245-57.

Harris, S.D., 2011. Hyphal morphogenesis: an evolutionary perspective. Fungal Biol. 115, 475-84.

Harris, S.D., Hofmann, A.F., Tedford, H.W., Lee, M.P., 1999. Identification and characterization of genes required for hyphal morphogenesis in the filamentous fungus *Aspergillus nidulans*. Genetics 151, 1015-25.

Harris, S.D., Momany, M., 2004. Polarity in filamentous fungi: moving beyond the yeast paradigm. Fungal Genet. Biol. 41, 391-400.

Harris, S.D., Morrell, J.L., Hamer, J.E., 1994. Identification and characterization of *Aspergillus nidulans* mutants defective in cytokinesis. Genetics 136, 517-32.

Hattenschwiler, S., Fromin, N., Barantal, S., 2011. Functional diversity of terrestrial microbial decomposers and their substrates. C. R. Biol. 334, 393-402.

Hawkins, D.M., Smidt, A.C., 2014. Superficial fungal infections in children. Pediatr. Clin. North Am. 61, 443-55.

He, X., Li, S., Kaminskyj, S.G.W., 2014a. Characterization of *Aspergillus nidulans* alpha-1,3-glucan synthesis: roles for two synthases and two amylases. Mol. Microbiol. 91, 579-95.

He, X., Li, S., Kaminskyj, S.G.W., 2014b. Using *Aspergillus nidulans* to identify anti-fungal drug resistance mutations. Eukaryot. Cell., 13, 288-94

Hebecker, B., Naglik, J.R., Hube, B., Jacobsen, I.D., 2014. Pathogenicity mechanisms and host response during oral Candida albicans infections. Expert Rev. Anti Infect. Ther. 12, 867-79.

Hedayati, M.T., Pasqualotto, A.C., Warn, P.A., Bowyer, P., Denning, D.W., 2007. *Aspergillus flavus*: human pathogen, allergen and mycotoxin producer. Microbiology 153, 1677-92.

Henrissat, B., Bairoch, A., 1996. Updating the sequence-based classification of glycosyl hydrolases. Biochem. J. 316 (Pt 2), 695-6.

Henrissat, B., Callebaut, I., Fabrega, S., Lehn, P., Mornon, J.P., Davies, G., 1995. Conserved catalytic machinery and the prediction of a common fold for several families of glycosyl hydrolases. Proc. Natl. Acad. Sci. U. S. A. 92, 7090-4.

Henry, C., Latgé, J.P., Beauvais, A., 2012. Alpha-1,3-glucans are dispensable in *Aspergillus fumigatus*. Eukaryot. Cell. 11, 26-9.

Hill, T.W., Loprete, D.M., Momany, M., Ha, Y., Harsch, L.M., Livesay, J.A., Mirchandani, A., Murdock, J.J., Vaughan, M.J., Watt, M.B., 2006. Isolation of cell wall mutants in *Aspergillus nidulans* by screening for hypersensitivity to Calcofluor White. Mycologia 98, 399-409.

Hochstenbach, F., Klis, F.M., van den Ende, H., van Donselaar, E., Peters, P.J., Klausner, R.D., 1998. Identification of a putative alpha-1,3-glucan synthase essential for cell wall construction and morphogenesis in fission yeast. Proc. Natl. Acad. Sci. U. S. A. 95, 9161-6.

Hogan, L.H., Klein, B.S., 1994. Altered expression of surface alpha-1,3-glucan in genetically related strains of *Blastomyces dermatitidis* that differ in virulence. Infect. Immun. 62, 3543-6.

Jansen, G., Lee, A.Y., Epp, E., Fredette, A., Surprenant, J., Harcus, D., Scott, M., Tan, E., Nishimura, T., Whiteway, M., Hallett, M., Thomas, D.Y., 2009. Chemogenomic profiling predicts anti-fungal synergies. Mol. Syst. Biol. 5, 338.

Kanafani, Z.A., Perfect, J.R., 2008. Antimicrobial resistance: resistance to anti-fungal agents: mechanisms and clinical impact. Clin. Infect. Dis. 46, 120-8.

Kaminskyj, S.G.W., Heath, I.B. (1996). Studies on *Saprolegnia ferax* suggest the importance of the cytoplasm in determining hyphal morphology. Mycologia, 88, 20-37

Kaminskyj, S.G.W., 2000. Septum position is marked at the tip of *Aspergillus nidulans* hyphae. Fungal Genet Biol 31: 105–113

Kaminskyj, S.G.W., 2001. Fundamentals of growth, storage, genetics and microscopy of *Aspergillus nidulans*. Fungal Genet Newsl 48: 25–31.

Kaur, S., Singh, S., 2014. Biofilm formation by *Aspergillus fumigatus*. Med. Mycol. 52, 2-9.

Keller, N.P., Hohn, T.M., 1997. Metabolic Pathway Gene Clusters in Filamentous Fungi. Fungal Genet. Biol. 21, 17-29.

Kingsbury, J.M., Heitman, J., Pinnell, S.R., 2012. Calcofluor white combination anti-fungal treatments for *Trichophyton rubrum* and *Candida albicans*. PLoS One 7, e39405.

Klein, B.S., Aizenstein, B.D., Hogan, L.H., 1997. African strain of *Blastomyces dermatitidis* that do not express surface adhesin WI-1. Infect. Immun. 65, 1505-9.

Kovacs, Z., Szarka, M., Kovacs, S., Boczonadi, I., Emri, T., Abe, K., Pocsi, I., Pusztahelyi, T., 2013. Effect of cell wall integrity stress and RlmA transcription factor on asexual development and autolysis *in Aspergillus nidulans*. Fungal Genet. Biol. 54, 1-14.

Laitinen, R.A., Schneeberger, K., Jelly, N.S., Ossowski, S., Weigel, D., 2010. Identification of a spontaneous frame shift mutation in a nonreference *Arabidopsis* accession using whole genome sequencing. Plant Physiol. 153, 652-4.

Latgé, J.P., 2010. Tasting the fungal cell wall. Cell. Microbiol. 12, 863-72.

Latgé, J.P., 2007. The cell wall: a carbohydrate armour for the fungal cell. Mol. Microbiol. 66, 279-90.

Lee, E.H., Eo, J.K., Ka, K.H., Eom, A.H., 2013. Diversity of arbuscular mycorrhizal fungi and their roles in ecosystems. Mycobiology 41, 121-5.

Levin, D.E., 2005. Cell wall integrity signaling in *Saccharomyces cerevisiae*. Microbiol. Mol. Biol. Rev. 69, 262-91.

Li, Y.C., Korol, A.B., Fahima, T., Beiles, A., Nevo, E., 2002. Microsatellites: genomic distribution, putative functions and mutational mechanisms: a review. Mol. Ecol. 11, 2453-65.

Li, Y.C., Korol, A.B., Fahima, T., Nevo, E., 2004. Microsatellites within genes: structure, function, and evolution. Mol. Biol. Evol. 21, 991-1007.

Lilic, D., 2012. Unravelling fungal immunity through primary immune deficiencies. Curr. Opin. Microbiol. 15, 420-6.

Lin, X., Momany, M., 2004. Identification and complementation of abnormal hyphal branch mutants ahbA1 and ahbB1 in *Aspergillus nidulans*. Fungal Genet. Biol. 41, 998-1006.

Livak, K.J., Schmittgen, T.D., 2001. Analysis of relative gene expression data using real-time quantitative PCR and the 2(-Delta Delta C(T)) Method. Methods 25, 402-8.

Lovett, S.T., 2004. Encoded errors: mutations and rearrangements mediated by misalignment at repetitive DNA sequences. Mol. Microbiol. 52, 1243-53.

Lucas, G.M., Tucker, P., Merz, W.G., 1999. Primary cutaneous *Aspergillus nidulans* infection associated with a Hickman catheter in a patient with neutropenia. Clin. Infect. Dis. 29, 1594-6.

Lunghini, D., Granito, V.M., Di Lonardo, D.P., Maggi, O., Persiani, A.M., 2013. Fungal diversity of saprotrophic litter fungi in a Mediterranean maquis environment. Mycologia 105, 1499-515.

Lupetti, A., Danesi, R., Campa, M., Del Tacca, M., Kelly, S., 2002. Molecular basis of resistance to azole anti-fungals. Trends Mol. Med. 8, 76-81.

MacGregor, E.A., Janecek, S., Svensson, B., 2001. Relationship of sequence and structure to specificity in the alpha-amylase family of enzymes. Biochim. Biophys. Acta 1546, 1-20.

Mar Alba, M., Santibanez-Koref, M.F., Hancock, J.M., 1999. Amino acid reiterations in yeast are overrepresented in particular classes of proteins and show evidence of a slippage-like mutational process. J. Mol. Evol. 49, 789-97.

Mardis, E.R., 2008. Next-generation DNA sequencing methods. Annu. Rev. Genomics Hum. Genet. 9, 387-402.

Marichal, P., Koymans, L., Willemsens, S., Bellens, D., Verhasselt, P., Luyten, W., Borgers, M., Ramaekers, F.C., Odds, F.C., Bossche, H.V., 1999. Contribution of mutations in the cytochrome P450 14alpha-demethylase (Erg11p, Cyp51p) to azole resistance in *Candida albicans*. Microbiology 145 (Pt 10), 2701-13.

Marion, C.L., Rappleye, C.A., Engle, J.T., Goldman, W.E., 2006. An alpha-(1,4)-amylase is essential for alpha-(1,3)-glucan production and virulence in *Histoplasma capsulatum*. Mol. Microbiol. 62, 970-83.

Maubon, D., Park, S., Tanguy, M., Huerre, M., Schmitt, C., Prevost, M.C., Perlin, D.S., Latgé, J.P., Beauvais, A., 2006. AGS3, an alpha-(1,3)glucan synthase gene family member of *Aspergillus fumigatus*, modulates mycelium growth in the lung of experimentally infected mice. Fungal Genet. Biol. 43, 366-75.

Mavor, A.L., Thewes, S., Hube, B., 2005. Systemic fungal infections caused by *Candida* species: epidemiology, infection process and virulence attributes. Curr. Drug Targets 6, 863-74.

Metzker, M.L., 2010. Sequencing technologies − the next generation. Nature reviews 11, 31-46

Momany, M., Lindsey, R., Hill, T.W., Richardson, E.A., Momany, C., Pedreira, M., Guest, G.M., Fisher, J.F., Hessler, R.B., Roberts, K.A., 2004. The *Aspergillus fumigatus* cell wall is organized in domains that are remodelled during polarity establishment. Microbiology 150, 3261-8.

Momany, M., Westfall, P.J., Abramowsky, G., 1999. *Aspergillus nidulans* swo mutants show defects in polarity establishment, polarity maintenance and hyphal morphogenesis. Genetics 151, 557-67.

Montgomery, S.B., Goode, D.L., Kvikstad, E., Albers, C.A., Zhang, Z.D., Mu, X.J., Ananda, G., Howie, B., Karczewski, K.J., Smith, K.S., Anaya, V., Richardson, R., Davis, J., 1000 Genomes Project Consortium, MacArthur, D.G., Sidow, A., Duret, L., Gerstein, M., Makova, K.D., Marchini, J., McVean, G., Lunter, G., 2013. The origin, evolution, and functional impact of short insertion-deletion variants identified in 179 human genomes. Genome Res. 23, 749-61.

Morita, T., Tanaka, N., Hosomi, A., Giga-Hama, Y., Takegawa, K., 2006. An alpha-amylase homologue, aah3, encodes a GPI-anchored membrane protein required for cell wall integrity and morphogenesis in *Schizosaccharomyces pombe*. Biosci. Biotechnol. Biochem. 70, 1454-63.

Morris, N.R., 1975. Mitotic mutants of *Aspergillus nidulans*. Genet. Res. 26, 237-54.

Morris, N.R., Lai, M.H., Oakley, C.E., 1979. Identification of a gene for alpha-tubulin in *Aspergillus nidulans*. Cell 16, 437-42.

Munro, C.A., Selvaggini, S., de Bruijn, I., Walker, L., Lenardon, M.D., Gerssen, B., Milne, S., Brown, A.J., Gow, N.A.R., 2007. The PKC, HOG and Ca^{2+} signaling pathways co-ordinately regulate chitin synthesis *in Candida albicans*. Mol. Microbiol. 63, 1399-413.

Muszkieta, L., Beauvais, A., Pahtz, V., Gibbons, J.G., Anton Leberre, V., Beau, R., Shibuya, K., Rokas, A., Francois, J.M., Kniemeyer, O., Brakhage, A.A., Latgé, J.P., 2013. Investigation of *Aspergillus fumigatus* biofilm formation by various "omics" approaches. Front. Microbiol. 4, 13.

Nakamura, T., Maeda, Y., Tanoue, N., Makita, T., Kato, M., Kobayashi, T., 2006. Expression profile of amylolytic genes in *Aspergillus nidulans*. Biosci. Biotechnol. Biochem. 70, 2363-70.

Nather, K., Munro, C.A., 2008. Generating cell surface diversity in *Candida albicans* and other fungal pathogens. FEMS Microbiol. Lett. 285, 137-45.

Netea, M.G., Brown, G.D., 2012. Fungal infections: the next challenge. Curr. Opin. Microbiol. 15, 403-5.

Nevalainen, H., Peterson, R., 2014. Making recombinant proteins in filamentous fungi are we expecting too much? Front. Microbiol. 5, 75.

Oakley, B.R., Morris, N.R., 1980. Nuclear movement is beta-tubulin-dependent in *Aspergillus nidulans*. Cell 19, 255-62.

O'Brien, H.E., Parrent, J.L., Jackson, J.A., Moncalvo, J.M., Vilgalys, R., 2005. Fungal community analysis by large-scale sequencing of environmental samples. Appl. Environ. Microbiol. 71, 5544-50.

Osherov, N., Mathew, J., May, G.S., 2000. Polarity-defective mutants of *Aspergillus nidulans*. Fungal Genet. Biol. 31, 181-8.

Osmani, S.A., Mirabito, P.M., 2004. The early impact of genetics on our understanding of cell cycle regulation in *Aspergillus nidulans*. Fungal Genet. Biol. 41, 401-10.

Osono, T., 2006. Role of phyllosphere fungi of forest trees in the development of decomposer fungal communities and decomposition processes of leaf litter. Can. J. Microbiol. 52, 701-16.

Ostrosky-Zeichner, L., Casadevall, A., Galgiani, J.N., Odds, F.C., Rex, J.H., 2010. An insight into the anti-fungal pipeline: selected new molecules and beyond. Nat. Rev. Drug Discov. 9, 719-27.

Osumi, M., 2012. Visualization of yeast cells by electron microscopy. J. Electron. Microsc. (Tokyo) 61, 343-65.

Paul, B.C., El-Ganiny, A.M., Abbas, M., Kaminskyj, S.G.W., Dahms, T.E.S., 2011. Quantifying the importance of galactofuranose in *Aspergillus nidulans* hyphal wall surface organization by atomic force microscopy. Eukaryot. Cell. 10, 646-53.

Pereira, M., Felipe, M.S., Brigido, M.M., Soares, C.M., Azevedo, M.O., 2000. Molecular cloning and characterization of a glucan synthase gene from the human pathogenic fungus *Paracoccidioides brasiliensis*. Yeast 16, 451-62.

Perfect, J.R., 2014. Cryptococcosis: a model for the understanding of infectious diseases. J. Clin. Invest. 124, 1893-5.

Pfaller, M.A., Diekema, D.J., 2010. Epidemiology of invasive mycoses in North America. Crit. Rev. Microbiol. 36, 1-53.

Qin, Q.M., Luo, J., Lin, X., Pei, J., Li, L., Ficht, T.A., de Figueiredo, P., 2011. Functional analysis of host factors that mediate the intracellular lifestyle of *Cryptococcus neoformans*. PLoS Pathog. 7, e1002078.

Rappleye, C.A., Eissenberg, L.G., Goldman, W.E. 2007. *Histoplasma capsulatum* alpha-(1,3)-glucan blocks innate immune recognition by the beta-glucan receptor. Proc. Natl. Acad. Sci. U. S. A. 104, 1366-70.

Rappleye, C.A., Engle, J.T., Goldman, W.E., 2004. RNA interference in *Histoplasma capsulatum* demonstrates a role for alpha-(1,3)-glucan in virulence. Mol. Microbiol. 53, 153-65.

Read, N.D., 2011. Exocytosis and growth do not occur only at hyphal tips. Mol. Microbiol. 81, 4-7.

Reese, A.J., Doering, T.L., 2003. Cell wall alpha-1,3-glucan is required to anchor the *Cryptococcus neoformans* capsule. Mol. Microbiol. 50, 1401-9.

Reese, A.J., Yoneda, A., Breger, J.A., Beauvais, A., Liu, H., Griffith, C.L., Bose, I., Kim, M.J., Skau, C., Yang, S., Sefko, J.A., Osumi, M., Latgé, J.P., Mylonakis, E., Doering, T.L., 2007. Loss of cell wall alpha-(1,3)-glucan affects *Cryptococcus neoformans* from ultrastructure to virulence. Mol. Microbiol. 63, 1385-98.

Rodriguez, R., Redman, R., 2008. More than 400 million years of evolution and some plants still can't make it on their own: plant stress tolerance via fungal symbiosis. J. Exp. Bot. 59, 1109-14.

Roncero, C., Valdivieso, M.H., Ribas, J.C., Duran, A., 1988. Isolation and characterization of *Saccharomyces cerevisiae* mutants resistant to Calcofluor white. J. Bacteriol. 170, 1950-4.

Sanz, L., Montero, M., Redondo, J., Llobell, A., Monte, E., 2005. Expression of an alpha-1,3-glucanase during mycoparasitic interaction of *Trichoderma asperellum*. FEBS J. 272, 493-9.

Schmalhorst, P.S., Krappmann, S., Vervecken, W., Rohde, M., Muller, M., Braus, G.H., Contreras, R., Braun, A., Bakker, H., Routier, F.H., 2008. Contribution of galactofuranose to the virulence of the opportunistic pathogen *Aspergillus fumigatus*. Eukaryot. Cell. 7, 1268-77.

Schmitt, M.W., Kennedy, S.R., Salk, J.J., Fox, E.J., Hiatt, J.B., Loeb, L.A., 2012. Detection of ultra-rare mutations by next-generation sequencing. Proc. Natl. Acad. Sci. U. S. A. 109, 14508-13.

Schoustra, S.E., Bataillon, T., Gifford, D.R., Kassen, R., 2009. The properties of adaptive walks in evolving populations of fungus. PLoS Biol. 7, e1000250.

Schoustra, S.E., Debets, A.J., Slakhorst, M., Hoekstra, R.F., 2007. Mitotic recombination accelerates adaptation in the fungus *Aspergillus nidulans*. PLoS Genet. 3, e68.

Schoustra, S.E., Debets, A.J., Slakhorst, M., Hoekstra, R.F., 2006. Reducing the cost of resistance; experimental evolution in the filamentous fungus *Aspergillus nidulans*. J. Evol. Biol. 19, 1115-27.

Schuster, E., Dunn-Coleman, N., Frisvad, J.C., Van Dijck, P.W., 2002. On the safety of *Aspergillus niger*--a review. Appl. Microbiol. Biotechnol. 59, 426-35.

Shapiro, R.S., Robbins, N., Cowen, L.E., 2011. Regulatory circuitry governing fungal development, drug resistance, and disease. Microbiol. Mol. Biol. Rev. 75, 213-67.

Shaw, J.A., Mol, P.C., Bowers, B., Silverman, S.J., Valdivieso, M.H., Duran, A., Cabib, E., 1991. The function of chitin synthases 2 and 3 in the *Saccharomyces cerevisiae* cell cycle. J. Cell Biol. 114, 111-23.

Sheir-Neiss, G., Lai, M.H., Morris, N.R., 1978. Identification of a gene for beta-tubulin in *Aspergillus nidulans*. Cell 15, 639-47.

Shi, X., Sha, Y., Kaminskyj, S., 2004. *Aspergillus nidulans hypA* regulates morphogenesis through the secretion pathway. Fungal Genet. Biol. 41, 75-88.

Skepper, J.N., Powell, J.M., 2008. Immunogold Staining of London Resin (LR) White Sections for Transmission Electron Microscopy (TEM). CSH Protoc. 2008, pdb.prot5016.

Slot, J.C., Rokas, A., 2010. Multiple GAL pathway gene clusters evolved independently and by different mechanisms in fungi. Proc. Natl. Acad. Sci. U. S. A. 107, 10136-41.

Specht, C.A., Liu, Y., Robbins, P.W., Bulawa, C.E., Iartchouk, N., Winter, K.R., Riggle, P.J., Rhodes, J.C., Dodge, C.L., Culp, D.W., Borgia, P.T., 1996. The *chsD* and *chsE* genes of *Aspergillus nidulans* and their roles in chitin synthesis. Fungal Genet. Biol. 20, 153-67.

Srivatsan, A., Han, Y., Peng, J., Tehranchi, A.K., Gibbs, R., Wang, J.D., Chen, R., 2008. High-precision, whole-genome sequencing of laboratory strains facilitates genetic studies. PLoS Genet. 4, e1000139.

Stapley, J., Reger, J., Feulner, P.G., Smadja, C., Galindo, J., Ekblom, R., Bennison, C., Ball, A.D., Beckerman, A.P., Slate, J., 2010. Adaptation genomics: the next generation. Trends Ecol. Evol. 25, 705-12.

Steele, C., Wormley, F.L.Jr, 2012. Immunology of fungal infections: lessons learned from animal models. Curr. Opin. Microbiol. 15, 413-9.

Szewczyk, E., Nayak, T., Oakley, C.E., Edgerton, H., Xiong, Y., Taheri-Talesh, N., Osmani, S.A., Oakley, B.R., 2006. Fusion PCR and gene targeting in *Aspergillus nidulans*. Nat. Protoc. 1, 3111-20.

Takeshita, N., Yamashita, S., Ohta, A., Horiuchi, H., 2006. *Aspergillus nidulans* class V and VI chitin synthases CsmA and CsmB, each with a myosin motor-like domain, perform compensatory functions that are essential for hyphal tip growth. Mol. Microbiol. 59, 1380-94.

Taylor, J.W., Berbee, M.L., 2006. Dating divergences in the Fungal Tree of Life: review and new analyses. Mycologia 98, 838-49.

Teepe, A.G., Loprete, D.M., He, Z., Hoggard, T.A., Hill, T.W., 2007. The protein kinase C orthologue PkcA plays a role in cell wall integrity and polarized growth in *Aspergillus nidulans*. Fungal Genet. Biol. 44, 554-62.

Todd, R.B., Davis, M.A., Hynes, M.J., 2007. Genetic manipulation of *Aspergillus nidulans*: heterokaryons and diploids for dominance, complementation and haploidization analyses. Nat. Protoc. 2, 822-30.

van der Kaaij, R.M., Yuan, X.L., Franken, A., Ram, A.F., Punt, P.J., van der Maarel, M.J., Dijkhuizen, L., 2007. Two novel, putatively cell wall-associated and

glycosylphosphatidylinositol-anchored alpha-1,3-glucanotransferase enzymes of *Aspergillus niger*. Eukaryot. Cell. 6, 1178-88.

Vandecasteele, S.J., Boelaert, J.R., Verrelst, P., Graulus, E., Gordts, B.Z., 2002. Diagnosis and treatment of *Aspergillus flavus* sternal wound infections after cardiac surgery. Clin. Infect. Dis. 35, 887-90.

Verweij, P.E., Snelders, E., Kema, G.H., Mellado, E., Melchers, W.J., 2009. Azole resistance in *Aspergillus fumigatus*: a side-effect of environmental fungicide use? Lancet Infect. Dis. 9, 789-95.

Villalobos-Duno, H., San-Blas, G., Paulinkevicius, M., Sanchez-Martin, Y., Nino-Vega, G., 2013. Biochemical characterization of *Paracoccidioides brasiliensis* alpha-1,3-glucanase Agn1p, and its functionality by heterologous Expression in *Schizosaccharomyces pombe*. PLoS One 8, e66853.

Vos, A., Dekker, N., Distel, B., Leunissen, J.A., Hochstenbach, F., 2007. Role of the synthase domain of Ags1p in cell wall alpha-1,3-glucan biosynthesis in fission yeast. J. Biol. Chem. 282, 18969-79.

Walker, L.A., Gow, N.A., Munro, C.A., 2010. Fungal echinocandin resistance. Fungal Genet. Biol. 47, 117-26.

Walker, L.A., Munro, C.A., de Bruijn, I., Lenardon, M.D., McKinnon, A., Gow, N.A.R., 2008. Stimulation of chitin synthesis rescues *Candida albicans* from echinocandins. PLoS Pathog. 4, e1000040.

Wang, F., Tao, J., Qian, Z., You, S., Dong, H., Shen, H., Chen, X., Tang, S., Ren, S., 2009. A histidine kinase PmHHK1 regulates polar growth, sporulation and cell wall composition in the dimorphic fungus *Penicillium marneffei*. Mycol. Res. 113, 915-23.

Wei, H., Scherer, M., Singh, A., Liese, R., Fischer, R., 2001. *Aspergillus nidulans* alpha-1,3 glucanase (mutanase), mutA, is expressed during sexual development and mobilizes mutan. Fungal Genet. Biol. 34, 217-27.

Xiang, M.J., Liu, J.Y., Ni, P.H., Wang, S., Shi, C., Wei, B., Ni, Y.X., Ge, H.L., 2013. Erg11 mutations associated with azole resistance in clinical isolates of *Candida albicans*. FEMS Yeast Res. 13, 386-93.

Yoshijima, Y., Murakami, K., Kayama, S., Liu, D., Hirota, K., Ichikawa, T., Miyake, Y., 2010. Effect of substrate surface hydrophobicity on the adherence of yeast and hyphal *Candida*. Mycoses 53, 221-6.

Yoshimi, A., Sano, M., Inaba, A., Kokubun, Y., Fujioka, T., Mizutani, O., Hagiwara, D., Fujikawa, T., Nishimura, M., Yano, S., Kasahara, S., Shimizu, K., Yamaguchi, M., Kawakami, K., Abe, K., 2013. Functional analysis of the alpha-1,3-glucan synthase genes *agsA* and *agsB* in *Aspergillus nidulans*: *agsB* is the major alpha-1,3-glucan synthase in this fungus. PLoS One 8, e54893.

Yuan, X.L., van der Kaaij, R.M., van den Hondel, C.A., Punt, P.J., van der Maarel, M.J., Dijkhuizen, L., Ram, A.F., 2008. *Aspergillus niger* genome-wide analysis reveals a large number of novel alpha-1,3-glucan acting enzymes with unexpected expression profiles. Mol. Genet. Genomics 279, 545-61.

Ziman, M., Chuang, J.S., Schekman, R.W., 1996. Chs1p and Chs3p, two proteins involved in chitin synthesis, populate a compartment of the *Saccharomyces cerevisiae* endocytic pathway. Mol. Biol. Cell 7, 1909-19.